PUBLICATIONS AND PATENTS

A. Publications in peer-reviewed international journals/revised manuscripts communicated

1. **Dutta, S.**, Gogoi, D, Mukherjee, A. K. Anticoagulant mechanism and platelet deaggregation property of a non-cytotoxic, acidic phospholipase A_2 purified from Indian cobra (*Naja naja*) venom: Inhibition of anticoagulant activity by low molecular weight heparin. ***Biochimie 110***, 93-106 (2015).
2. **Dutta, S.**, Chanda, A., Kalita, B., Islam, T., Patra, A., Mukherjee, A. K. Proteomic analysis to unravel the complex venom proteome of eastern India *Naja naja*: Correlation of venom composition with its biochemical and pharmacological properties. ***Journal of Proteomics 156***, 29-39 (2017).
3. **Dutta, S.**, Sinha, A., Dasgupta, S., Mukherjee, A. K. Binding of a *Naja naja* venom acidic phospholipase A_2 cognate complex to membrane-bound vimentin of rat L6 cells: Implications in cobra venom-induced cytotoxicity. ***Biochimica et Biophysica Acta- Biomembranes 1861***, 958-977 (2019).
4. **Dutta, S.**, Chattopadhyay, P., Agarwal, M., Bose, B., Bidkar, A. P., Ghosh, S. S., Mukherjee, A. K. A novel synthetic peptide derived from Indian cobra *Naja naja* venom anticoagulant phospholipase A_2 demonstrates dual inhibition of thrombin and factor Xa. (*manuscript communicated*).

B. Patents filed

1. Indian Patent on **'Synthetic anticoagulant peptides derived from *Naja naja* snake venom'**, Patent Application No. 201831010001; Filling date: 19 March, 2018.
2. Indian Patent on **'Toxin epitope-based detection of species-specific snake envenomation'**, Patent Application No. 201831010002; Filling date: 19 September, 2018.

C. Publications in National Conferences/General Publications

1. **Dutta, S.,** Mukherjee, A. K. (2014) Biochemical and pharmacological characterization of an acidic, non-cytotoxic, phospholipase A_2 purified from Indian cobra (*Naja naja*) venom at the ***National Seminar on Recent Advances in***

Biotechnological Research in North East India: Challenges and Prospects, Tezpur University, Assam during November 27 – 29, 2014.

2. **Dutta, S.,** Mukherjee, A. K. (2014) Characterization of biochemical and pharmacological properties of a non-cytotoxic, acidic phospholipase A_2 purified from Indian cobra (*Naja naja*) venom at the ***83rd Annual Conference of Society of Biological Chemists of India***, KIIT University, Bhubaneswar during December 17 – 21, 2014.
3. **Dutta, S.,** Chanda, A., Islam, T., Kalita, B., Patra, A., Mukherjee, A.K. (2016) Proteomic, biochemical and pharmacological characterization of eastern India *Naja naja* venom and correlation of these properties with clinical manifestation of cobra bite at the ***National Seminar on Snake Venom Research and Snake Bite Therapy: National and International Perspectives (SnakSymp2016)***, Tezpur University, Assam during November 22 – 24, 2016.
4. **Dutta, S.,** Kalita, B., Mukherjee, A.K. (2017) Protein and peptide-based anticoagulant cardiovascular drug development from snake venom: Phospholipase A_2 is an example" at the ***3rd International Conference on Translational Research: Human Health and Agriculture,*** Amity University, Kolkata during December 23 – 25, 2017.

D. Other publications related to snake venom research (not from thesis work)

1. Mukherjee, A. K., Mackessy, S. P., **Dutta, S.** Characterization of a Kunitz-type protease inhibitor peptide (Rusvikunin) purified from *Daboia russelii russelii* venom. ***International Journal of Biological Macromolecules 67***, 154-162 (2014).
2. Mukherjee, A. K., **Dutta, S.**, Mackessy, S. P. (2014) A new C-type lectin (RVsnaclec) purified from venom of *Daboia russelii russelii* shows anticoagulant activity via inhibition of FXa and concentration-dependent differential response to platelets in a Ca^{2+}-independent manner. ***Thrombosis Research 134***, 1150-1156 (2014).
3. Majumdar, S., **Dutta, S.**, Das, T., Chattopadhyay, P., Mukherjee, A. K. Antiplatelet and antithrombotic activity of a fibrin(ogen)olytic protease from *Bacillus cereus* strain FF01. ***International Journal of Biological Macromolecules 79***, 477-489 (2015).

4. Mukherjee, A. K., **Dutta, S.,** Kalita, B., Jha, D. K., Deb, P., Mackessy, S. P. Structural and functional characterization of complex formation between two Kunitz-type serine protease inhibitors from Russell's Viper venom. ***Biochimie 128***, 138-147 (2016).
5. Kalita, B., **Dutta, S.**, Mukherjee, A. K. RGD-independent binding of Russell's Viper venom Kunitz-type protease inhibitors to platelet GPIIb/IIIa receptor. ***Scientific Reports 9***, 8316 (2019).

AWARDS RECEIVED IN NATIONAL CONFERENCES AND SEMINARS/OTHER AWARDS

1. Recipient of **Tezpur University Gold Medal** from honorable President of India **for securing first position** in M. Sc. in Molecular biology and Biotechnology examination, Tezpur University in 2013.
2. **Second Prize of ONGC-CPBT Best Poster Award** recipient in the 'National Seminar on Recent Advances in Biotechnological Research in North East India: Challenges and Prospects', 27th-29th November, 2014, Tezpur University, Assam.
3. Recipient of the prestigious **INSPIRE fellowship for University first rank holders** at post graduate-level, from the Department of Science and Technology, Government of India, **for pursuing full time PhD** since 2013-2018.

Biochimie 110 (2015) 93–106

Contents lists available at ScienceDirect

Biochimie

journal homepage: www.elsevier.com/locate/biochi

Research paper

Anticoagulant mechanism and platelet deaggregation property of a non-cytotoxic, acidic phospholipase A_2 purified from Indian cobra (*Naja naja*) venom: Inhibition of anticoagulant activity by low molecular weight heparin

Sumita Dutta, Debananda Gogoi, Ashis K. Mukherjee*

Microbial Biotechnology and Protein Research Laboratory, Department of Molecular Biology and Biotechnology, School of Science, Tezpur University, Tezpur 784028, Assam, India

ARTICLE INFO

Article history:
Received 12 April 2014
Accepted 31 December 2014
Available online 8 January 2015

Keywords:
Naja naja
Phospholipase A_2
Anticoagulant activity
Thrombin inhibition
Heparin neutralization
Platelet deaggregation

ABSTRACT

In the present study, anticoagulant and platelet modulating activities of an acidic phospholipase A_2 ($NnPLA_2$-I) purified from Indian cobra *Naja naja* venom was investigated. The $NnPLA_2$-I displayed a mass of 15.2 kDa and 14,186.0 Da when analyzed by SDS-PAGE and MALDI-TOF-MS, respectively. Peptide mass fingerprinting analysis of the $NnPLA_2$-I showed its significant similarity with phospholipase A_2 enzymes purified from cobra venom. BLAST analysis of one tryptic peptide sequence of $NnPLA_2$-I demonstrated putative conserved domains of the PLA_2-like superfamily. The *Km* and *Vmax* values of $NnPLA_2$-I toward hydrolysis of its most preferred substrate—phosphotidylcholine (PC)—were determined to be 0.72 mM and 29.3 μmol min^{-1} mg^{-1}, respectively. The anticoagulant activity of $NnPLA_2$-I was found to be higher than the anticoagulant activity of heparin/AT-III or warfarin. The histidine modifying reagent, monovalent and polyvalent antivenom differentially inhibited the catalytic and anticoagulant activities of $NnPLA_2$-I. Low molecular weight heparin did not inhibit the catalytic and platelet deaggregation activity of $NnPLA_2$-I, albeit its anticoagulant activity was significantly reduced. The $NnPLA_2$-I showed a non-enzymatic, mixed inhibition of thrombin with a *Ki* value of 9.3 nM. Heparin significantly decreased, with an IC_{50} value of 15.23 mIU, the thrombin inhibitory activity of $NnPLA_2$-I. The $NnPLA_2$-I uniquely increased the amidolytic activity of FXa without influencing its prothrombin activating property. $NnPLA_2$-I showed dose-dependent deaggregation of platelet rich plasma (PRP) and inhibited the collagen and thrombin-induced aggregation of PRP. However, deaggregation of washed platelets by $NnPLA_2$-I demonstrated in presence of PC or platelet poor plasma. Alkylation of histidine residue of $NnPLA_2$-I resulted in 95% and 21% reduction of its platelet deaggregation and platelet binding properties, respectively. $NnPLA_2$-I did not show cytotoxicity against human glioblastoma U87MG cells, bactericidal or hemolytic activity. The future therapeutic application of $NnPLA_2$-I for treatment and prevention of cardiovascular disorders is therefore suggested.

1. Introduction

The Indian cobra (*Naja naja*), also known as the *Spectacled cobra*, is a member of the "big four" venomous snakes in India. This snake is found throughout the Indian subcontinent including Pakistan, Bangladesh, Sri Lanka, and Nepal, and is responsible for a large number of snakebite fatalities and morbidity in this subcontinent. The primary function of snake venom is immobilization of bigger prey before being swallowed; secondarily, it is used by the snake as its lethal self-defense weapon. The interzonal and intrazonal variations in venom composition of the Indian cobra result in differences in pathobiological manifestations in victims [1,2]. Therefore, exploration of geographical variation in venom components has tremendous implications for improving production of effective antivenom to treat cobra bite patients [1,2]. Indian cobra venom is enriched in many toxins and enzymes such as neurotoxins, cardiotoxins, myotoxins, cytotoxins, and phospholipase A_2 enzymes

* Corresponding author. Tel.: +91 3712275405; fax: +91 3712 267005, +91 3712 267006.
E-mail address: akm@tezu.ernet.in (A.K. Mukherjee).

http://dx.doi.org/10.1016/j.biochi.2014.12.020
0300-9084/

[1,3,4]. The latter enzyme is one of the major constituents of most snake venoms including *N. naja* venom, which is reported to contain up to 14 isoenzymes of PLA_2 [5].

Phospholipase A_2 (EC: 3.1.1.4), due to its crucial role in inducing various pharmacological effects in victims and its puzzling structure–function relationships, is one of the most extensively studied snake venom enzymes [5–12]. Single venom may contain several isoenzymes of PLA_2, and depending on their overall charge, they may be classified as acidic, basic, or neutral PLA_2 enzymes. It has been well established that different PLA_2 isoenzymes of the same venom exhibit various pharmacological effects, viz. neurotoxicity, cardiotoxicity, myotoxicity, necrosis, anticoagulant, hypotensive, hemolysis, hemorrhage and edema by different mechanisms in experimental animals and victims [8]. Among the pharmacological effects, interfering with the blood coagulation system by injecting venom components is one of the important mechanisms to impede the hemostatic system of victim or prey [6,9–13]. Although most of the PLA_2 enzymes purified from snake venom have been demonstrated to possess anticoagulant activity [8,10–12], most of the PLA_2 enzymes purified from the Indian *N. naja* venom are devoid of anticoagulant activity [1,5,14,15], and only a few have been reported to show weak anticoagulant action [16]. In the present study, therefore, an effort has been made to purify a strong anticoagulant PLA_2 from the venom of the *N. naja* and characterize its anticoagulant mechanism as well as platelet modulating activity. To the best of our knowledge, this is the first report of a thrombin inhibitor PLA_2 isolated from *N. naja* venom.

2. Materials and methods

Crude *N. naja* venom was obtained from Calcutta Snake Park, Kolkata. Sephadex G-50 (fine grade) was obtained from Pharmacia Fine Chemicals, Sweden. Low molecular weight heparin (approximately 6 kDa) from porcine intestinal mucosa, chromogenic substrates, and other fine chemicals were purchased from Sigma Chemical Co., USA. Coagulation proteins were purchased from Calbiochem, Germany. Polyvalent antivenom (PAV), (effective against *Daboia russelii*, *N. naja*, *Echis carinatus* and *Bungarus caeruleus* venoms) was purchased from the Serum Institute of India Limited, Pune, India whereas *N. naja* monovalent antivenom (MAV) was obtained from VINS Bioproduct Limited, India. All kits used for serum analysis were purchased from Crest Biosystem, Goa. All other reagents were of analytical grade.

2.1. Purification of a phospholipase A_2 enzyme

Crude *N. naja* venom (dry weight 10 mg) was dissolved in 0.5 ml of 20 mM Tris–HCl buffer, pH 7.4 (buffer A), and centrifuged at 10,000 rpm. After filtration through 0.2 micron membrane, the clear supernatant was fractionated through a Hiprep CM FF 16/10 cation exchange column (pre-equilibrated with the buffer A) coupled with an FPLC system (AKTA purifier, Wipro GE Health Care, Sweden). After washing the column with two volumes of equilibration buffer, proteins bound to column were eluted with a linear gradient of 1.0 M NaCl dissolved in buffer A at a flow rate of 1.0 ml/min. The elution of protein was observed at 280 nm, and a 1.5 ml fraction was collected in each tube. Protein content and PLA_2 activity of each peak was screened (see below). The fractions showing the highest PLA_2 activity were pooled, desalted, concentrated, and then fractioned through a Sephadex G-50 gel-filtration column (1×64 cm^2) with a 20 mM Tris–HCl buffer, pH 7.4. The fraction volume was 1.0 ml, and each peak was screened for PLA_2 activity (see below), anticoagulant activity, and protein content [17].

The purity of the enzyme was determined by 12.5% SDS-PAGE with or without reduction of protein with β-mercaptoethanol [18]. The protein bands were fixed by incubating the gel in fixing solution (distilled water/methanol/glacial acetic acid, 50:40:10) for 30 min at room temperature. After extensive washing the gel with MilliQ water, the bands were visualized by silver staining the gel [19]. The molecular mass of the purified PLA_2 was also determined using a mass spectrometer (4800 plus, Applied Biosystems, USA). About 1.0 μg of purified protein in 0.1% TFA was spotted on 1 μl of an α-cyanosinapinic acid matrix (10 mg/ml) dissolved in 50% (v/v) acetonitrile containing 0.1% (v/v) TFA, and the mass of the protein was then determined.

2.2. Peptide mass fingerprinting analysis

The peptide band of interest was eluted from the gel, and after alkylation and reduction; it was subjected to trypsin digestion overnight at 37 °C [20]. The PMF analysis of the tryptic-digested peptides was done by MALDI-TOF-MS/MS analysis [12,21]. Spectra were collected over an m/z range of 600–2000 Da. The MS/MS spectra were searched against the NCBI data base of non-redundant protein sequences (NCBI nr) using the Mascot database search engine to find the significant hit. The tryptic sequences obtained by PMF analysis were subjected to a BLASTp search in NCBI database.

2.3. Phospholipase A_2 activity assay and enzyme kinetics

Phospholipase A_2 activity was assayed by the turbidometric method of Joubert and Tallijard [22] slightly modified as described previously [6,10]. Briefly, one egg yolk was suspended in 250 ml of 0.9% (w/v) NaCl containing 0.02% (w/v) sodium azide. Before PLA_2 assay, 1.0 ml of the suspension was mixed with 10.0 ml of 0.1 M Tris–HCl buffer, pH 8.0, and the absorbance of the resulting mixture was adjusted to 1.0 at 740 nm with the same buffer. For assaying the PLA_2 activity, different doses of enzyme were mixed with 2.0 ml of the above reaction mixture, and the decrease in turbidity after 10 min was monitored at 740 nm against a reagent blank. One unit of PLA_2 activity has been arbitrarily defined as a decrease in 0.01 absorbance at 740 nm after 10 min on incubation [6].

For determination of phospholipids substrate specificity, 25 nM of purified PLA_2 was incubated with different phospholipids such as PC, PS and PE (final concentration 1 mM) at 37 °C for the desired time periods. The PLA_2 activity was assayed by microtitration of liberated fatty acids (FA) with 0.01 N NaOH, and the amount of FA liberated was determined from a standard curve of palmitic acid [10]. The Lineweaver–Burk plot was used to determine kinetic parameters (K_m and V_{max}) of purified PLA_2 using different concentrations (1.0–300 mM) of substrate (PC), and then the values of 1/V were plotted as a function of 1/S.

2.4. Anticoagulation assay

To study the plasma clotting activity, goat blood obtained from a slaughter house was collected in 3.8% tri-sodium citrate. The platelet poor plasma (PPP) was prepared by centrifuging the blood twice at 5000 rpm for 20 min at 4 °C. Different concentrations of PLA_2 (in a total volume of 20 μl) were pre-incubated with 300 μl of PPP for 3 min at 37 °C, and clotting was initiated by adding 40 μl of 250 mM $CaCl_2$ [23]. For control, instead of PLA_2, the same volume of PBS was used. One unit of anticoagulant activity has been defined as crude venom/purified PLA_2-induced 1 s increase in clotting time of the control PPP [23].

To determine the correlation between the kinetics of plasma phospholipids hydrolysis and that of the anticoagulant activity, a fixed amount (100 nM) of purified PLA_2 was incubated with 300 μl of plasma from 3 to 20 min at 37 °C. Then, 40 μl of 250 mM $CaCl_2$

was added and the clotting time was recorded [10]. In another set of experiments, the PLA_2 was incubated with plasma under identical experimental conditions and the liberated fatty acids were titrated with 0.01 N NaOH. The amount of FA liberated was determined from a standard curve of palmitic acid [10]. The anticoagulant potency of *N. naja* acidic PLA_2 was compared with the commercial drugs heparin and warfarin. Briefly, different doses (40–200 nM) of PLA_2/warfarin/heparin were pre-incubated with PPP for 3 min, and then the Ca-clotting time was determined, as stated above.

Effect of *N. naja* PLA_2 (15–600 nM) on prothrombin time (PT) and partial thromboplastin time (APTT) of PPP was determined by using commercial diagnostic kits and following the instructions of the manufacturer (Tulip Diagnostics Pvt. Ltd., Mumbai, India).

2.5. Biochemical characterization

To study the effect of pH on enzyme activity, 25 nmol of PLA_2 was incubated with 2.0 ml of egg-yolk suspension (as stated above) prepared with different buffers having pH 5.0–10.0. The different buffers used were 0.1 M sodium acetate buffer (pH 5.0–6.5), 0.1 M potassium phosphate buffer (pH 7.0–7.5), and 0.1 M Tris–HCl buffer (pH 8.0–10.0). The PLA_2 activity was determined for each pH against a reagent blank. For determining the heat-denaturation of enzyme activity, 0.1 M PLA_2 solution (in 0.1 M Tris–HCl, pH 8.0) were incubated at 75 °C, and an appropriate volume of enzyme was withdrawn at different intervals (10–60 min) to assay the residual catalytic and anticoagulant activities. The activity of the control (unheated enzyme) was considered as 100% activity, with other values compared to that.

2.6. Effect of inhibitors, heparin, and antivenom

For determining the effect of different inhibitors on catalytic and anticoagulant activities of purified PLA_2 enzyme, 200 nM of PLA_2 enzyme was pre-incubated with different inhibitors, *viz*. tosyl phenylalanyl chloromethyl ketone (100 μM), N-α-p-tosyl-L-lysine chloromethyl ketone (100 μM), phenylmethanesulfonylfluoride (5 mM), *p*-bromophenacyl bromide (2 mM), ethylenediaminetetraacetic acid (5 and 10 mM), dithiothretol (5 mM), and iodoacetamide (2 mM) for 30 min at room temperature [7]. The purified $PLA_2$was also pre-incubated with 20 mIU of heparin for 30 min at 37 °C. The catalytic and anticoagulant activities of the modified enzyme were determined against appropriate controls in the corresponding assay systems. The activity of the unmodified enzyme (the control) was considered as 100% activity, with the other values compared to that.

The PLA_2 enzyme was pre-incubated for 30 min at 37 °C with antivenom (polyvalent or monovalent) at different protein to antivenom ratios ranging from 1:10 to 1:500 (protein: protein ratio). The mixtures were than assayed for their catalytic as well as plasma clotting activity against appropriate controls by following standard protocols. The percent inhibition of enzyme/anticoagulant activity was calculated by comparing the activity to that of untreated enzyme (100% activity).

2.7. Inhibition of thrombin and other coagulation factors

The inhibitory effect of PLA_2 on the amidolytic activity of thrombin was assayed using the chromogenic substrate of thrombin T1637 [N-(*p*-Tosyl)-Gly-Pro-Arg-*p*-nitroanilide acetate]. Graded concentrations of PLA_2 were incubated with a fixed amount of thrombin (5 nM) at 37 °C for 30 min. Then, the reaction was initiated by adding T1637 (0.2 mM final concentration). After incubation for 15 min at 37 °C, the amount of released p-nitroaniline was determined by measuring the change in absorbance at 405 nm [24]. The activity of thrombin in the absence of PLA_2 was considered to be 100%, and the other values were compared with that.

In another set of experiments, different concentrations of PLA_2 were pre-incubated with thrombin (3 μl, 10 NIH U/ml) for 30 min at 37 °C. A control was also set up in which thrombin was incubated with PBS under identical conditions. The reaction was started by adding 40.0 μl of fibrinogen (2.5 mg/ml), and the time of clot formation was recorded with a coagulometer. To measure fast or slow inhibition, 0.5 μM of the PLA_2 was pre-incubated with thrombin (3 μl, 10 NIH U/ml) from 5 to 30 min at 37 °C prior to the addition of human fibrinogen, and the clotting time was recorded as stated above.

To measure the inhibitory effect of PLA_2 on amidolytic activity of factor Xa, the procedures described by Saikia et al.[10] were followed. Briefly, 500 nmol of purified enzyme was pre-incubated with 0.1 μg of FXa isolated from human plasma (Calbiochem) for 60 min at 37 °C. Then, 1.0 μg of human prothrombin (Calbiochem) and chromogenic substrate (0.2 mM final concentration) for thrombin (T1637) were added to the reaction mixture. The release of *p*-nitroaniline was monitored for 30 min at intervals of 1 min at 405 nm in a plate reader (Multiskan GO, Thermo Scientific, USA). A control was run in parallel where FXa was pre-incubated with PBS instead of with PLA_2.

In another set of experiments, 3 μmol of PLA_2 was pre-incubated with 0.1 μg of Factor Xa for 60 min at 37 °C. Then, 15 μg of human prothrombin (PTH) was added, and the mixture was incubated at 37 °C for 60 min. Thereafter, PTH activation by FXa in presence or absence (control) of PLA_2 was determined by 12.5% SDS-PAGE analysis of the reaction products (PTH activated products) under reducing conditions. The proteins were stained with Coomassie Brilliant Blue R-250 and distained with methanol, acetic acid, and water. The peptides in gel were densitometrically scanned with the help of Image J Software. The formation of thrombin from prothrombin was reconfirmed by peptide mass fingerprinting analysis of the 36 kDa protein [21].

2.8. Kinetics of thrombin inhibition by PLA_2 in presence and absence of inhibitors

The effect of heparin, antithrombin-III, heparin/AT-III complex, and modification of histidine residue of PLA_2 with *p*BPB on the thrombin inhibition property of purified PLA_2 was also determined. A fixed dose of PLA_2 (500 nM) was pre-incubated with different doses of heparin (0.5 IU and 1.0 IU), AT-III (2.5 μM and 5.0 μM), and heparin/AT-III (0.5 IU heparin and 2.5 μM AT-III; and 1.0 IU heparin and 5.0 μM AT-III) for 30 min at 37 °C in a 96-well microplate. This was followed by the addition of thrombin (3 μl, 10 NIH IU/ml) and T1637 (0.2 mM). The kinetics of substrate hydrolysis was determined by measuring the release of p-nitroaniline at 405 nm for 10 min in a microplate reader (Thermo Scientific Multiskan GO, USA). A control was run in parallel where thrombin was pre-incubated with 1X PBS under identical conditions before assaying its amidolytic activity. The effect of histidine modification (done by treating purified PLA_2 with 2 mM *p*BPB, for 30 min at room temperature) on thrombin inhibitory activity of purified PLA_2 was also determined as above.

To study the effect of PLA_2-heparin on inhibition of the fibrinogen clotting activity of thrombin, 1 μmol of PLA_2 was pre-incubated with 20 mIU of heparin and 1X PBS (the control) for 30 min at 37 °C. Then, thrombin (3 μl of 10 NIH Unit/ml, ~167.0 nM) was added to this reaction mixture and re-incubated for an additional 30 min at 37 °C. In another set of experiments, only heparin (20 mIU) was incubated with thrombin under identical conditions. To these mixtures, 40 μl of fibrinogen (2.5 mg/ml) was added, and

the clotting time was recorded with a coagulometer. To determine the IC_{50} value of heparin on the thrombin inhibition activity of purified PLA_2, different doses of heparin (5–40 mIU) were pre-incubated with 1 μmol of PLA_2 for 30 min at 37 °C. The mixture was then re-incubated with thrombin (~167.0 nM) for 30 min at 37 °C, and then the fibrinogen clotting activity of thrombin was determined, as stated above. For each experiment, a control was run in parallel. The IC_{50} value of heparin on PLA_2 was also determined from the thrombin inhibition curve.

To determine the *Ki* value for the inhibition of amidolytic activity of thrombin from $NnPLA_2$-I, a fixed concentration of thrombin (3 μl of 10 NIH U/ml, ~167.0 nM) was pre-incubated with two different concentrations of PLA_2 (150.0 nM and 300.0 nM) at 37 °C for 30 min. A control was run in parallel where thrombin was incubated with a buffer instead of PLA_2 under identical experimental conditions. The reaction was initiated by adding graded concentrations (0.1–0.8 mM) of chromogenic substrate for thrombin (T1637). After incubation for 10 min, the release of *p*NA was determined, as stated above. For kinetic analysis, the reaction rate (V) was plotted against substrate concentration (S) at each concentration of inhibitor, and the data was fitted to a hyperbolic Michaelis–Menten model using GraphPad Prism 6.0 software. The inhibitory constant (*Ki*) was determined using the mixed model (shown below) for enzyme inhibition and using the same software.

$$V_{max(App)} = V_{max}/[1 + I/\alpha Ki] \quad (1)$$

$$K_{m(App)} = K_m[1 + I/Ki]/[1 + I/\alpha Ki] \quad (2)$$

$$Y = V_{max(App)}X\Big/\left[K_{m(App)} + X\right] \quad (3)$$

In the above equations (1) and (2), I indicate the inhibitor concentration, and *Vmax(App)* and *Vmax* represent maximum velocity in the presence and absence of the inhibitor (Nn-PLA_2), respectively. The *Km(App)* and *Km* in equation (2) denote the Michaelis constant in the presence and absence of inhibitor, respectively. The α is a constant.

2.9. Spectrofluorometric assay of interaction of PLA_2 with PC/thrombin/FXa

To determine the PLA_2-PC/thrombin/FXa interaction, in either the absence or presence of 2.0 mM Ca^{2+}, our previously described procedure was followed [10,25]. The excitation wavelength used was 280 nm with a slit width of 10 nm, while the emission spectrum was observed from 300 nm to 400 nm range [10,25]. All the spectrofluorometric binding assays were done in triplicate to ensure reproducibility.

2.10. Platelet modulating activity PLA_2

Platelet rich plasma (PRP) and subsequently washed platelets were prepared from citrated mammalian (human or goat) blood by following the procedures described by Bednar et al. [26]. The washed platelets were re-suspended in Tyrode's buffer (5 mM HEPES, 137 mM NaCl, 2.7 mM KCl, 12 mM $NaHCO_3$, 0.42 mM Na_2HPO_4, 1 mM $MgCl_2$, 0.1% glucose and 0.25% bovine serum albumin) and platelet count was adjusted with the same buffer to 1×10^6/ml.

Different concentrations (3–240 nM) of purified PLA_2 were added to 100 μl of pre-warmed (at 37 °C for 5 min) PRP or washed platelets suspension either in presence or absence of 2 mM Ca^{2+} in a 96-well microtiter plate and the contents were mixed for 5 s in a microplate reader (Multiskan GO, Thermo Scientific, Waltham, USA) [26]. The absorbance was then recorded continuously at 540 nm for 300 s at an interval of 15 s. As a control, the absorbance of PPP as well as PRP was also recorded under identical conditions. The absorbance value of PPP was subtracted from the experimental readings to determine the absorbance only due to platelets in PRP. Percent platelet aggregation after 300 s of incubation of platelets with different concentrations of PLA_2 was calculated by the following formula [27]:

Percent aggregation = (A_{540} of the platelet suspension/PRP before the addition of agonist − A_{540} of the platelet suspension/PRP after the addition of agonist) ÷ (A_{540} of the platelet suspension/PRP before the addition of agonist − A_{540} of the PPP/Tyrode's buffer) × 100. The A_{540} denotes absorbance value at 540 nm.

In other sets of experiments, washed platelets were pre-incubated with 0.1 μg/ml of phosphatidylcholine (PC) or phosphatidylserine (PS) or 10 μl of PPP for 5 min before addition of 60 nM of $NnPLA_2$-I and platelet modulating activity was determined as above.

2.11. Effect of heparin, pBPB, and antivenom on platelet modulating property of PLA_2

PLA_2 (60 nM) was pre-incubated with 20 mIU of low molecular weight (<8 kDa) heparin or 2 mM *p*BPB for 30 min at room temperature (~23 °C) and then excess of reagents were removed by dialysis. As a control, the PLA_2 was incubated with Tyrode's buffer under identical conditions. The platelet modulating activity of PLA_2 (native or modified) was assayed as above. The activity of unmodified (native) PLA_2 was considered as base value (100% activity) and other values were compared to that. The neutralization of platelet modulating activity of PLA_2 by polyvalent and monovalent antivenom was studied by pre-incubating a fixed concentration of PLA_2 (0.5 μM) with different concentrations of PVA or MVA for 30 min at room temperature (~23 °C) and then assayed for platelet modulating activity against appropriate controls.

2.12. Effect of $NnPLA_2$-I on collagen and thrombin-induced platelet aggregation

In another sets of experiments, PRP (100 μl, 1×10^6 cells/ml) was pre-incubated with different concentrations of PLA_2 (2–10 nM) for 5 min prior to addition of collagen type IV (1.0 μg/ml). The aggregation induced by the same dose of collagen was considered as 100% activity and other values were compared with that. The IC_{50} value of PLA_2 was calculated from the regression analysis of inhibition curve.

The thrombin-inhibitory activity was assayed on PRP prepared from human blood. The *in vitro* platelet aggregation inhibition property was investigated by pre-incubating different concentrations (0.5–5.0 μM) of purified PLA_2 with human thrombin (0.20 μg/ml) for 10 min. A control reaction was also set up where 1X PBS, instead of purified PLA_2, was used. The platelet aggregation was monitored in a Chrono-log dual channel aggregometer for 10 min.

2.13. Platelet binding assay

The ability of native or heparin/pBPB-modified *N. naja* PLA_2 to bind with washed platelet was studied by ELISA method. The 96-well microtitre plate coated with 1×10^6 platelets were washed for three times, each for 5 min duration, with 1X PBS containing 0.05% tween-20 (washing buffer) to remove the unbound platelets [28]. The wells were then blocked with 5% fat-free milk, washed for three times with washing buffer, and then incubated with 5 μg of purified PLA_2 (native or unmodified) for 30 min at room temperature. The unbound PLA_2 was removed by washing three times

with wash buffer followed by incubation with 1:500 dilutions of monovalent equine antivenom (1 mg/ml) against *N. naja* for 2 h at room temperature, and again washed with the wash buffer. Rabbit anti-horse IgG conjugated with horseradish peroxidase (HRP) (1: 2000) was used as the secondary antibody to detect the bound primary antibodies. After 2 h of incubation, the substrate (1X TMB/H_2O_2) was added and the plate was incubated at room temperature in dark. The color developed was measured at 492 nm against appropriate blanks in a microplate reader. The binding of native (unmodified) PLA_2 with platelets was considered as 100% binding and other values were compared to that.

2.14. Hemolytic activity, cell viability, and antibacterial activity assay

Hemolytic activity of PLA_2 against washed erythrocytes (5%) obtained from goat blood was measured, as stated previously [6,9]. Antibacterial activity of enzyme (50–500 nM) against gram positive *Bacillus subtilis* and gram negative *Escherichia coli* was assayed by our previously described procedure [9,25]. Human glioblastoma U87MG cells (1×10^4) obtained from NCCS, Pune, were cultured in 96-well culture plates in a DMEM medium containing 10% heat-inactivated fetal bovine serum. After allowing the cells to grow and adhere to the culture plates at 37 °C in a 5% CO_2 humidified incubator for 24 h, the medium was replaced with a fresh medium containing 50–500 nmol of purified PLA_2 enzyme or crude *N. naja* venom. After 48 h of incubation, the cytotoxicity of the PLA_2 enzyme, if any, was determined by an MTT-based assay [20,25]. Cytotoxicity (percent cell death) was determined by comparison with values obtained from a standard curve of control cells [20].

3. Results

3.1. Isolation and purification of a PLA_2

Fractionation of crude *N. naja* venom proteins through a cation exchange CM FF 16/10 column resulted in their separation into six peaks (Fig. 1a). Peak1 (NnCM1) eluted with the equilibration buffer containing either neutral or acidic proteins showed significant PLA_2 and anticoagulant activities. Gel-filtration of the NnCM1 peak separated the PLA_2 isoenzymes into several fractions (NnCM1GF5 to GF8) (data not shown). The peak NnCM1GF6 demonstrated significant PLA_2 as well as anticoagulant activities. A summary of purification of this PLA_2, labeled $NnPLA_2$-I, is shown in Table 1. The $NnPLA_2$-I represents 3.4% of total venom protein.

By SDS-PAGE analysis, 40 μg of reduced protein ($NnPLA_2$-I) showed a single band of ~15.2 kDa, whereas under non-reduction it displayed a diffused band of ~21 kDa (Fig. 1b). By MALDI-TOF-MS analysis, the $NnPLA_2$-I demonstrated a doubly charged [MH^{2+}], low intensity peak at *m*/*z* 7092.5, and an [MH^+] peak at *m*/*z* 14,186.0 (data not shown).

3.2. PMF identification of PLA_2

The MS/MS search of tryptic digested peptides of $NnPLA_2$-I showed significant similarity (rank 1, protein score 104, 18% sequence coverage) with phospholipase A_2 (M_r, 13468) from *N. naja* venom (gi|64104) as well as with chain A, crystal structure of cobra-venom phospholipase A_2 (M_r, 13135) from *Naja atra* venom (gi|443187). BLAST analysis of one tryptic peptide sequence (score 67) of $NnPLA_2$-I showed putative conserved domains of PLA_2-like superfamily. Another tryptic peptide sequence (score 37) of $NnPLA_2$-I also displayed significant similarity with PLA_2s from snake venom, more particularly with the acidic PLA_2s from cobra venom (Table 2).

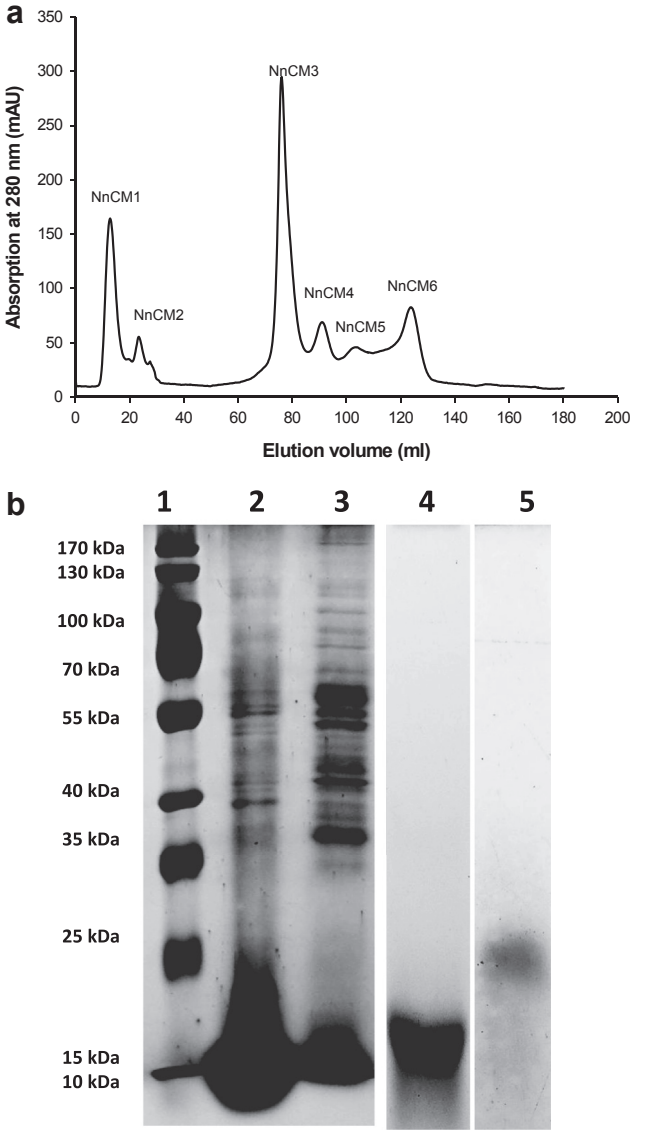

Fig. 1. a. Fractionation of crude *Naja naja* venom on cation exchange Hiprep CM FF 16/10 column (16 × 100 mm). The first peak corresponds to the elution of proteins showing phospholipid hydrolysis and anticoagulant activity. b. Determination of purity and molecular mass of $NnPLA_2$-I by 12.5% SDS-PAGE; Lane 1, protein molecular markers; lane 2, reduced crude *Naja naja* venom (30 μg); lane 3, reduced cation exchange fraction (30 μg); lanes 4 and 5, reduced and non-reduced $NnPLA_2$-I (40 μg), respectively.

3.3. Catalytic and anticoagulant activity

The $NnPLA_2$-I showed dose-dependent catalytic activity against egg-yolk phospholipids (Fig. 2a). Amongst the tested phospholipids substrate, it showed its highest activity in catalyzing the PC (7.4×10^4 Units mg^{-1}). The *Km* and *Vmax* values of $NnPLA_2$-I towards the PC were determined to be 0.72 mM and 29.3 μmol min^{-1} mg^{-1}, respectively. The $NnPLA_2$-I showed optimum activity at the alkaline range with its highest activity at pH 8.0 (data not shown). Heating this PLA_2 for a different time period at 75 °C did not result in any significant decrease in the catalytic activity of the heated enzyme as compared to that of the control (unheated) enzyme (data not shown). As shown in Fig. 2b, $NnPLA_2$-I dose-dependently enhanced the Ca-clotting time of PPP, suggesting that it is anticoagulant in nature. A comparison of the dose-

Table 1
A summary of purification of NnPLA$_2$-I from *N. naja* venom. Data represent a typical experiment.

Fraction	Total protein (mg)	% Yield of protein	PLA$_2$ activity		Anticoagulant activity		Purification fold	
			Unit (U)	Specific activity (U/mg)	Unit (U)	Specific activity (U/mg)	PLA$_2$ activity	Anticoagulant activity
Crude venom	5.6	100	91.7	1.83×10^3	115.8	2.3×10^4	1.0	1.0
Cation exchange fraction	3.0	53.6	91	3.03×10^4	134.6	4.5×10^4	16.6	1.9
Gel-filtration fraction	0.2	3.4	86.8	8.29×10^4	62.4	6.2×10^4	45.3	2.7

dependent anticoagulant activity of NnPLA$_2$-I with that of warfarin and heparin/AT-II is shown in Fig. 2c. It was observed that anticoagulant activity of NnPLA$_2$-I was significantly higher ($p < 0.05$) compared with that of heparin/AT-III or warfarin (Fig. 2c). Notably, heparin itself lacks anticoagulant activity; however, it binds with the antithrombin-III (AT-III) present in PPP to exert its anticoagulant effect. NnPLA$_2$-I increased the APTT of PPP in a dose-dependent manner (Fig. 2d); however, it did not affect the PT of PPP (Fig. 2d).

3.4. Effect of chemical modifications, heparin/antithrombin-III, and antivenom on catalytic and anticoagulant activities

The treatment of NnPLA$_2$-I with various chemical group modifying reagents resulted in a significant inhibition of catalytic and anticoagulant activities, although to a different extent (Table 3). Interestingly, heparin differentially modulated the catalytic and anticoagulant activities of NnPLA$_2$-I. Heparin failed to inhibit the catalytic activity of NnPLA$_2$-I; however, the anticoagulant activity of NnPLA$_2$-I was inhibited by heparin to 80% of its original activity (Table 3). A comparison of the neutralization potency of polyvalent (PVA) versus monovalent antivenom (MVA) shows that MVA was more efficient than PVA in neutralizing the catalytic as well as anticoagulant activities of NnPLA$_2$-I (Table 4). Both the antivenom up to a ratio of 1:100 differentially inhibited the catalytic as well as anticoagulant activities of NnPLA$_2$-I. With a further increase in the dose of antivenom, almost an equal inhibition of catalytic and anticoagulant activities of NnPLA$_2$-I was observed (Table 4).

3.5. Assessment of inhibition of thrombin, prothrombin and serine proteases

The NnPLA$_2$-I inhibited the amidolytic activity of thrombin (Fig. 3a). It was observed that heparin or AT-III did not have any effect on the amidolytic activity of thrombin; however, together heparin and AT-III can completely eliminate the amidolytic activity of thrombin (Fig. 3a). A comparison of thrombin inhibitory activity between NnPLA$_2$-I and heparin/AT-III showed that the latter was superior in showing the inhibition of amidolytic activity of thrombin (Fig. 3a). Pre-incubation of NnPLA$_2$-I with heparin resulted in a significant decrease in the thrombin inhibition property of the NnPLA$_2$-I (Fig. 3b), suggesting that heparin has some adverse effect on anticoagulant activity of NnPLA$_2$-I. Conversely, the NnPLA$_2$-I/AT-III complex has a greater thrombin inhibition activity than the amount of thrombin inhibition shown by NnPLA$_2$-I (Fig. 3b). Notably, the inhibition produced by heparin/AT-III/NnPLA$_2$-I complex on thrombin was superior to the same property exhibited by NnPLA$_2$-I/AT-III complex (Fig. 3b). Nevertheless, the thrombin inhibitory effect of heparin/AT-III was found to be the best (Fig. 3a).

The Michaelis–Menten plot to determine the amidolytic activity of thrombin in the absence or presence of NnPLA$_2$-I (inhibitor) is shown in Fig. 3c. The kinetic (*Km, Vmax and Kcat)* values of chromogenic substrate hydrolysis by thrombin in the absence or presence of the inhibitor (NnPLA$_2$-I) are shown in Table 5. It was observed that NnPLA$_2$-I produced a mixed inhibition of amidolytic activity of thrombin. The *Ki* value and α value for thrombin inhibition by NnPLA$_2$-I were determined at 9.3 ± 0.01 (mean ± SD) nM and 7.4 ± 0.7 (mean ± SD), respectively (Table 5).

The NnPLA$_2$-I dose-dependently inhibited the fibrinogen clotting activity of thrombin (Fig. 3d). Increasing the pre-incubation of thrombin with NnPLA$_2$-I from 5 to 30 min resulted in a decrease in fibrinogen clotting activity of thrombin; the optimum inhibition being observed at 30 min of pre-incubation of thrombin with NnPLA$_2$-I (Fig. 3e). Treatment of NnPLA$_2$-I with *p*BPB resulted in loss of its 58 ± 2% (mean ± SD) of thrombin inhibition property.

Table 6 shows that heparin does not have any effect on fibrinogen clotting activity of thrombin. In contrast, pre-incubation of NnPLA$_2$-I with heparin prior to the addition of thrombin

Table 2
BLAST analysis of tryptic digested *de novo* peptide sequences of NnPLA$_2$-I.

Peptide	Mr (expt)	Mr (calc)	Score	Sequences producing significant alignments	Accession no.
R.GGSGTPVDDXDR.C	1187.56	1187.54	67	Chain A, crystal structure of cobra-venom phospholipase A$_2$ in a complex with a transition-state analog from *N. atra*	1POB_A
				Chain B, X-ray crystal structure of a complex formed between two homologous isoforms of phospholipase A$_2$ From *N. naja*	1S6B_B
				Acidic phospholipase A$_2$ from *N. oxiana*	P25498
				Acidic phospholipase A$_2$ from *N. melanoleuca*	P00600
				Phospholipase A$_2$ from *N. kaouthia*	PSNJ3K
				Acidic phospholipase A$_2$ from *N. naja*	P15445
K.NMIXBCTVPSR.S + Carbamidomethyl (C)	1204.51	1204.61	37	Acidic phospholipase A$_2$ from *N.* oxiana	P25498
				Basic phospholipase A$_2$ from *Hemachatus haemachatus*	P00595
				Acidic phospholipase A$_2$ from *N. naja*	P15445
				Phospholipase A$_2$ from *N. naja sagittifera*	1LN8_A
				Acidic phospholipase A$_2$ natratoxin from *N. atra*	A4FS04
				Acidic phospholipase A$_2$ from *N. sagittifera*	P60045

Where, X = I/L, B = K/Q.

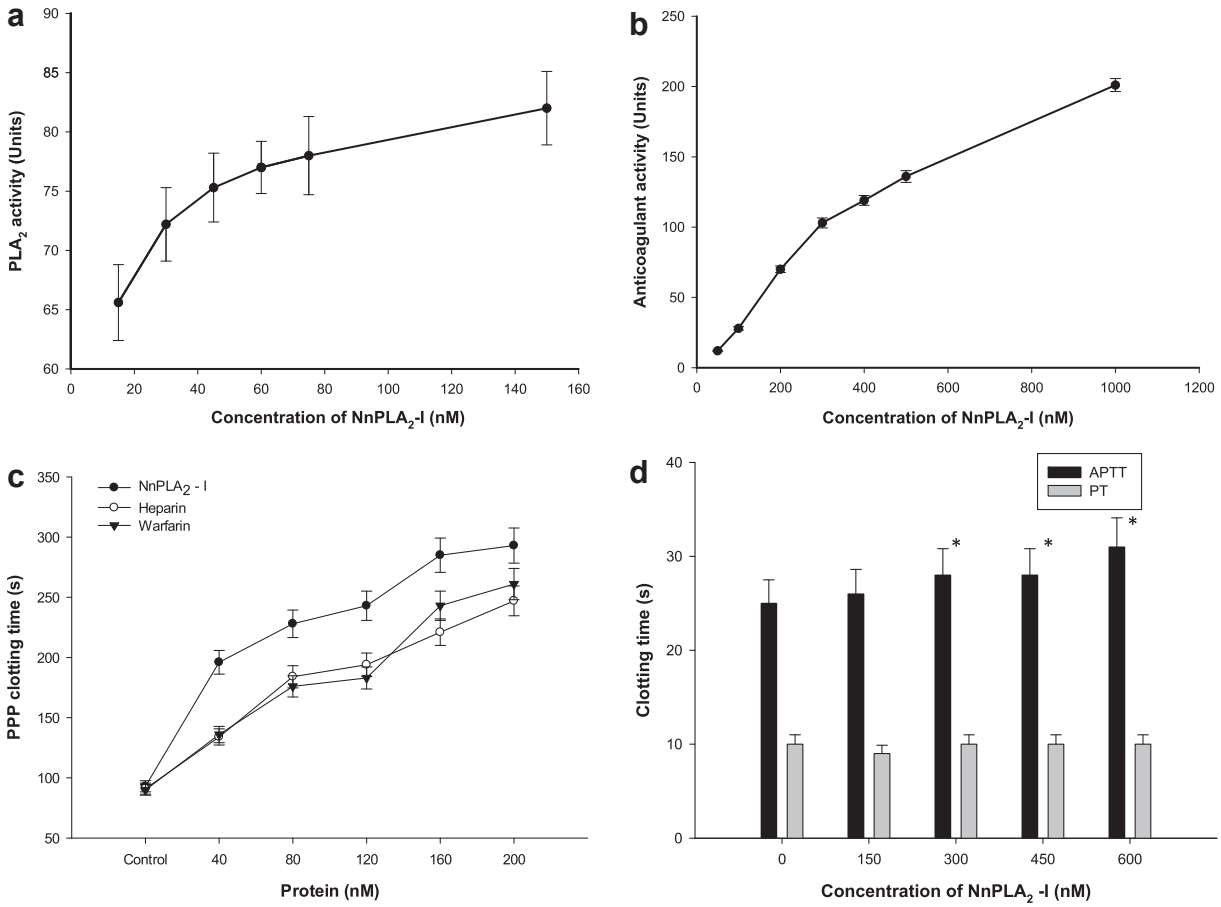

Fig. 2. a. Dose-dependent egg-yolk phospholipids hydrolytic activity of $NnPLA_2$-I. b. Dose dependent anticoagulant activity of $NnPLA_2$-I against PPP. c. Comparison of the dose-dependent anticoagulant activity (determined against PPP) of $NnPLA_2$-I (●), heparin (○) and warfarin (▼). d. Effect of different concentrations of $NnPLA_2$-I on APTT and PT of PPP. Values are mean ± S.D. of triplicate determinations.

significantly decreased the thrombin inhibitory activity of $NnPLA_2$-I (Table 6). The IC_{50} value of heparin to inhibit the $NnPLA_2$-I was determined to be 15.23 mIU (data not shown). However, neither pre-incubation of thrombin with heparin prior to the addition of $NnPLA_2$-I nor pre-incubation of thrombin with $NnPLA_2$-I prior to the addition of heparin resulted in any significant change ($p > 0.05$) in the thrombin inhibition potency of $NnPLA_2$-I (Table 6).

Pre-incubation of FXa with $NnPLA_2$-I for 5–15 min prior to the addition to its chromogenic substrate resulted in a significant (~8 fold) increase in amidolytic activity of FXa (Fig. 4a). However, SDS-PAGE analysis shows that $NnPLA_2$-I did not affect the prothrombin activation property of FXa (Fig. 4b). The $NnPLA_2$-I was also unable to inhibit some other tested serine proteases, viz. trypsin, chymotrypsin and plasmin (data not shown).

Table 3
Effect of chemical inhibitors and chelating agent on catalytic and anticoagulant activities of $NnPLA_2$-I. Values are mean ± SD of triplicate determinations. Significance of difference (Student's t test) with respect to catalytic activity $^*p < 0.01$.

Inhibitors (final concentration)	%Inhibition of activity	
	PLA_2 activity	Anticoagulant activity
p-BPB (2 mM)	96.5 ± 0.1	79.8 ± 2.1*
IAA (2 mM)	41.0 ± 0.9	55.3 ± 1.4*
EDTA (10 mM)	79.4 ± 6.2	98.1 ± 0.3*
DTT (5 mM)	97.3 ± 0.5	85.7 ± 1.2*
Heparin (20 mIU)	0	80.8 ± 4.1

3.6. Spectrofluorometric assay of interaction of $NnPLA_2$-I with PC/thrombin/FXa

The emission maximum of $NnPLA_2$-I observed at ~348 nm was significantly enhanced in the presence of PC (Fig. 5a). The fluorescence intensity of $NnPLA_2$-I/PC complex was further increased when 2.0 mM Ca^{2+} were added (data not shown). It was observed that there was no difference in emission maximum between native $NnPLA_2$-I/PC complex and *p*BPB-treated $NnPLA_2$-I/PC complex (Fig. 5a) implying both the native as well as histidine modified PLA_2 binds with PC to an equal extent.

Table 4
A comparison of neutralization potency of catalytic and anticoagulant activities of $NnPLA_2$-I by commercial polyvalent and monovalent antivenoms. Values are mean ± SD of triplicate determinations. Significance of difference (Student's t test) with respect to inhibition by monovalent antivenom $^*p < 0.01$. Significance of difference (Student's t test) with respect to inhibition of PLA_2 activity $^\dagger p < 0.001$; $^*p < 0.05$.

Ratio (PLA_2:AV)	%Inhibition of activity (Monovalent antivenom)		%Inhibition of activity (polyvalent antivenom)	
	PLA_2 activity	Anticoagulant activity	PLA_2 activity	Anticoagulant activity
1:50	7.98 ± 1.3	50.3 ± 3.1†	5.9 ± 1.2	41.7 ± 3.7†
1:100	77.02 ± 3.2	88.8 ± 0.0*	23.4 ± 3.1	53.1 ± 3.3†
1:200	95.1 ± 3.1	91.7 ± 7.9	72.9 ± 4.6	76.9 ± 4.6
1:500	100	100	98.4 ± 0.2	97.4 ± 2.2

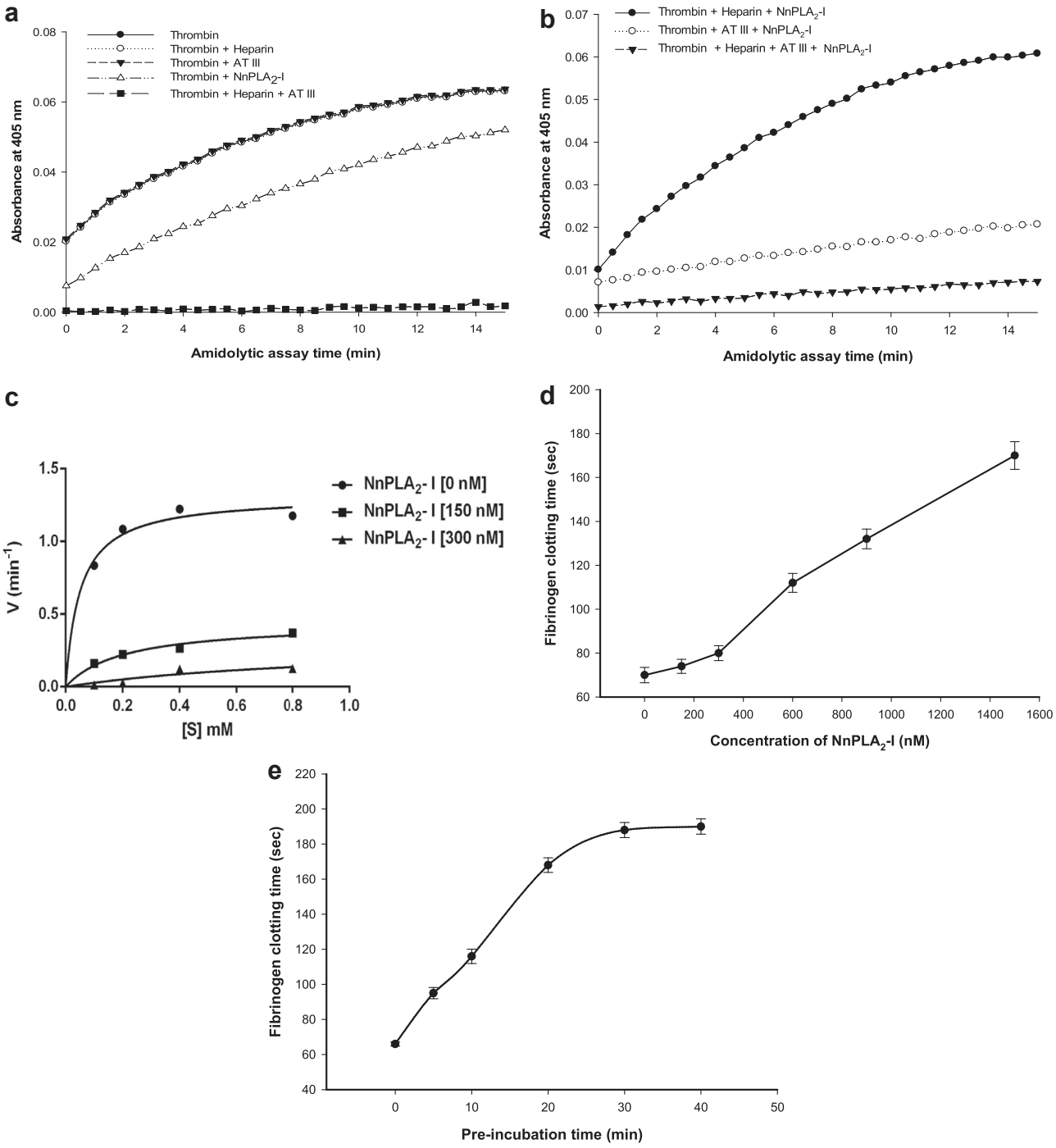

Fig. 3. a. A comparison of the amidolytic activity of thrombin (●) against its chromogenic substrate T1637 (0.2 mM in final volume); thrombin pre-incubated with 0.5 mIU of heparin (○), thrombin pre-incubated with 2.5 μM AT III (▼), thrombin pre-incubated with 500 nmol of $NnPLA_2$-I (Δ), thrombin pre-incubated with heparin/AT III (0.5 mIU/2.5 μM) complex (■); b. A comparison of the inhibition of amidolytic activity of thrombin against its substrate T1637 when 5 nm thrombin was pre-incubated with: heparin/$NnPLA_2$-I (0.5 mIU/500 nM) (●), AT III/$NnPLA_2$-I (2.5 μM/500 nM) (○) and heparin/AT III/$NnPLA_2$-I (0.5 mIU/2.5 μM/500 nM) (▼) complex; c. Michaelis–Menten plot for studying the kinetics of thrombin inhibition (by amidolytic activity assay) in two different inhibitor concentrations (150 nm and 300 nm) of $NnPLA_2$-I; d. Dose dependent thrombin inhibition by $NnPLA_2$-I (in terms of fibrinogen clotting assay). The control (fibrinogen and thrombin) showed a clotting time of 70 ± 3.6 s; e. Time dependent thrombin inhibition (determined by fibrinogen clotting activity assay) by a fixed dose of $NnPLA_2$-I (0.5 μM).

Interaction with PS and PE also enhanced the fluorescence intensity of $NnPLA_2$-I (data not shown). The interaction of $NnPLA_2$-I (50 nM) with FXa (0.1 μg) resulted in a significant increase in emission maximum at ~350 nm of $NnPLA_2$-I/FXa complex (Fig. 5b); the FXa did not show any emission at the concentration used. On the contrary, interaction of $NnPLA_2$-I (100 nM) with thrombin (1.0 μg) resulted in significant change (increase) in the fluorescence intensity of the $NnPLA_2$-I/thrombin complex (Fig. 5c). However, the fluorescence intensity of histidine alkylated $NnPLA_2$-I/thrombin complex was found to be much less as compared to the emission maxima of $NnPLA_2$-I (unmodified)/thrombin complex (Fig. 5c) suggesting histidine residue is essential for $NnPLA_2$-I binding to thrombin.

Table 5
Kinetics of thrombin inhibition by $NnPLA_2$-I. The kinetic parameters (*Km and Vmax*) were determined from Michaelis–Menten plot as described in the text. The values are mean ± SD of triplicate determinations.

Kinetic parameters	Concentration of $NnPLA_2$-I (nM)		
	0	150	300
Vmax (nmol pNA min^{-1})	1.31 ± 0.08	0.44 ± 0.05	0.31 ± 0.38
Km (nM)	0.05 ± 0.02	0.20 ± 0.07	1.03 ± 1.9
Kcat (min^{-1})	7.9 ± 0.6	2.7 ± 0.2	1.9 ± 0.1

3.7. Platelet modulating activity of $NnPLA_2$-I

$NnPLA_2$-I showed dose-dependent antiplatelet effect when tested against PRP (Fig. 6a); however, it did not demonstrate any effect against washed platelets (Fig. 6b). Addition of PPP or purified phospholipid PC or PS to washed platelets resulted in significant increase in platelet deaggregation property of $NnPLA_2$-I (Fig. 6b).

Incubation of PRP with *p*BPB modified $NnPLA_2$-I resulted in a significant ($p < 0.01$) reduction (~95%) of platelet deaggregation property of histidine-modified $NnPLA_2$-I compared to that shown by the native (unmodified) enzyme (Fig. 6c). In a sharp contrast, heparin did not interfere with the antiplatelet activity of $NnPLA_2$-I (Fig. 6c). Incubation of $NnPLA_2$-I with monovalent antivenom at 1:50 (protein:protein) did not inhibit its platelet deaggregation property; conversely, polyvalent antivenom under the identical experimental conditions enhanced the deaggregation property of $NnPLA_2$-I (data not shown).

$NnPLA_2$-I showed inhibition of collagen-induced aggregation of PRP in a dose-dependent manner; the IC_{50} value was calculated to be 4.9 nM (Fig. 6d). $NnPLA_2$-I dose-dependently inhibited the thrombin-induced aggregation of human platelets (Fig. 6e). It was observed that the extent of binding of both the native (unmodified) and heparin modified $NnPLA_2$-I to the washed platelets was equal; however, *p*BPB modification resulted in ~21% inhibition of platelet binding property of $NnPLA_2$-I (Fig. 7).

3.8. Hemolytic activity, cell cytotoxicity, and antibacterial activity

The $NnPLA_2$-I, at a dose of 500 nM, caused 0.9% hemolysis of mammalian erythrocytes. At the same dose, it did not show antibacterial activity against gram positive *B. subtilis* or gram negative *E. coli* cells. The cell viability study showed that $NnPLA_2$-I at a dose of 500 nM inhibited 5% growth of human glioblastoma U87MG cells (data not shown).

4. Discussion

During the past decades, significant progress has been made to explain the structure–function properties of both catalytically active and inactive snake venom PLA_2 enzymes [29–31]. It has been reported that this important class of venom molecules exerts pharmacological effects by distinctly different mechanisms, and apparently many controversial conclusions have been drawn [8]. The *N. naja* venom PLA_2 enzymes either did not show anticoagulant activity, or they were reported to possess weak anticoagulant action on PPP. In the present study, we report the purification and characterization of an acidic PLA_2 enzyme ($NnPLA_2$-I) possessing strong anticoagulant activity from venom of Indian cobra *N. naja*. Further, effort has also been given to explore the mechanism of anticoagulant action of $NnPLA_2$-I.

During the process of gel-filtration, the remaining anticoagulant proteins of *N. naja* venom were separated in peaks other than in an NnCM1GF6 fraction. Therefore, the NnCM1GF6 fraction showed a lower fold of purification of anticoagulant activity compared to that of the PLA_2 activity. The molecular weight of snake venom PLA_2 enzyme is generally reported in the range of 10–15 kDa [7–9,12]; therefore, the molecular mass of $NnPLA_2$-I is typical of the size of PLA_2 enzymes isolated from snake venom. The identity of $NnPLA_2$-I with classical PLA_2 enzymes from cobra venom was confirmed by PMF analysis, which may unambiguously be considered as a unique

Table 6
Fibrinogen clotting assay in the presence and absence of heparin. ND, not detected. The values are mean ± SD of triplicate determinations.

Conditions	Average clotting time (s)
Control (Thrombin)	60.0 ± 5.1
(Thrombin/Heparin)	61.0 ± 6.0
(Thrombin/$NnPLA_2$-I)	275.0 ± 12.3
($NnPLA_2$/Heparin) + Thrombin	119.0 ± 11.9
(Thrombin/Heparin) + $NnPLA_2$	268.0 ± 13.8
(Thrombin/$NnPLA_2$-I) + Heparin	266.0 ± 14.0
Heparin	ND
$NnPLA_2$-I	ND

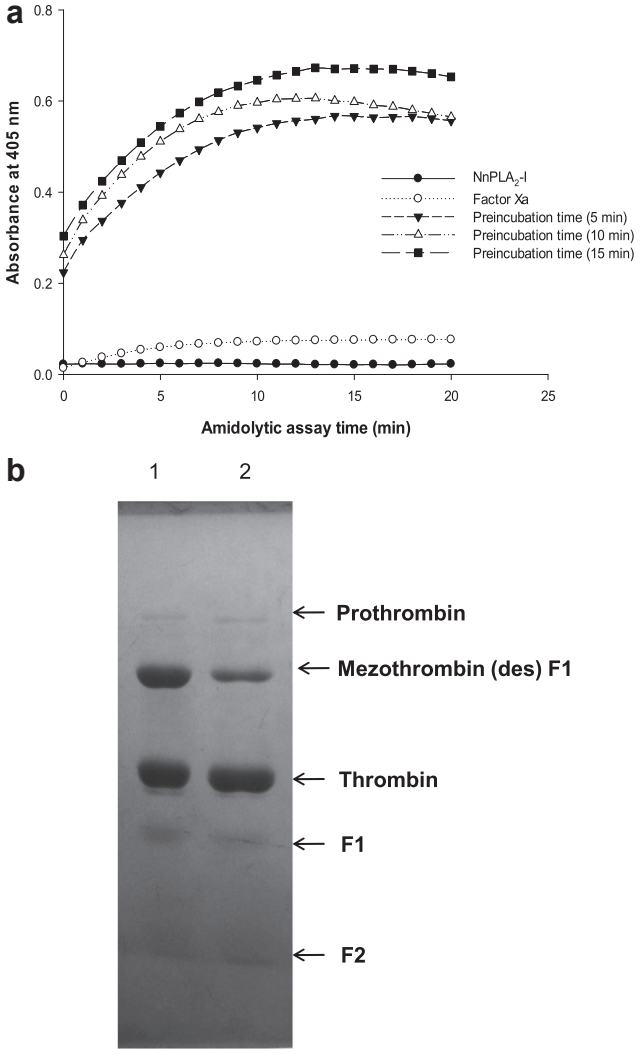

Fig. 4. a. Time-dependent activation of the amidolytic activity of Factor Xa (0.1 μg) by $NnPLA_2$-I (500 nM) against its chromogenic substrate F3301 (0.2 mM); b. The effect of $NnPLA_2$-I on the prothrombin activation as analyzed by 12.5% SDS-PAGE: lane 1, prothrombin (15 μg) incubated with factor Xa (0.1 μg), lane 2, prothrombin (15 μg) treated with factor Xa (0.1 μg) pre-incubated with $NnPLA_2$-I (3.0 μM).

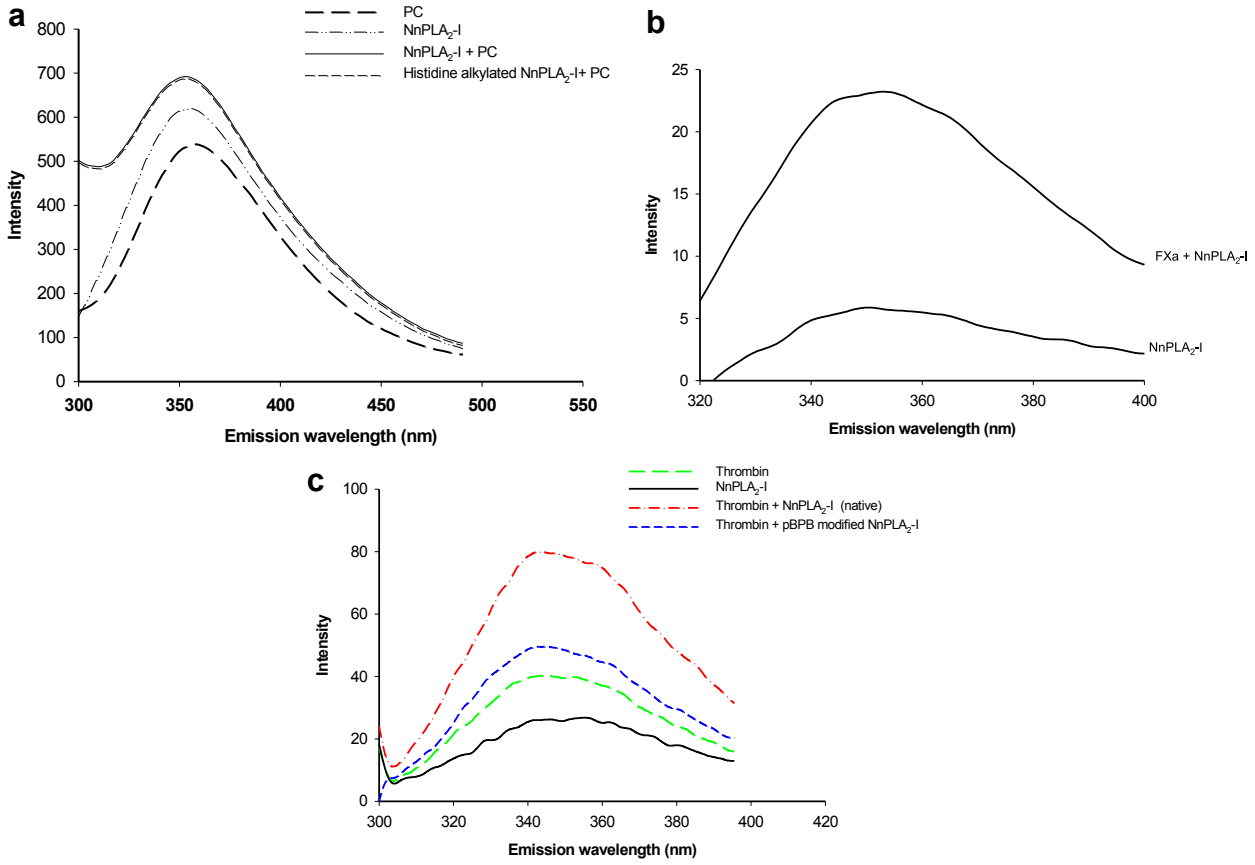

Fig. 5. Fluorescence spectra showing interaction of (a) native and histidine-modified $NnPLA_2$-I (500 nM) with phosphatidylcholine (2.0 μM), (b) $NnPLA_2$-I (50 nM) with Factor Xa (0.1 μg), and (c). Native and *p*BPB-treated $NnPLA_2$-I (100 nM) with human thrombin (1.0 μg). Experiments were repeated to three times to assure the reproducibility.

approach to identify unknown protein/peptide. The presence of putative conserved domains of the PLA_2—like superfamily reinforces the conclusion that $NnPLA_2$-I is a PLA_2 enzyme purified from *N. naja* venom. Moreover, like classical PLA_2 enzymes from snake venom, the catalytic activity of $NnPLA_2$-I was also inhibited by histidine inhibitor *p*-BPB suggesting the presence of histidine in the active site of $NnPLA_2$-I [6,7,9,10,12].

The PLA_2 enzymes, on the basis of their strengths to prolong the re-calcification time of PPP, are classified into groups of weak or strong anticoagulant enzymes [8,32]. The $NnPLA_2$-I can show an anticoagulant effect at a dose of 20 nM, thus suggesting that it is a strong anticoagulant enzyme [10,12]. This is in a close agreement to the previous reports showing that it is not the overall positive or negative charge on the venom PLA_2 molecule but rather the nature of charge in the anticoagulant site of this group of enzyme that is the sole determinant of its anticoagulant potency [8,10,11]. The anticoagulant region is positively charged in strong anticoagulant PLA_2 enzymes, but negatively charged in weak and non-anticoagulant enzymes [8].

The anticoagulant action of snake venom PLA_2 enzymes is either fully or partially dependent on their catalytic (phospholipids hydrolysis) activity such that no uniform mechanism could be proposed [6–12]. Our study suggests that, similar to our previous reports on PLA_2 enzymes purified from Russell's viper venom [10–12], the anticoagulant mechanism of $NnPLA_2$-I is partially dependent on its catalytic activity (~20% of the total anticoagulant activity shown by $NnPLA_2$-I), and to a major extent is executed through a non-catalytic mechanism via thrombin inhibition. It is well known that plasma phospholipids play a crucial role in the formation of several coagulation complexes. Very low but specific hydrolysis of plasma phospholipids through the catalytic mechanism of $NnPLA_2$-I might lead to the destruction of the specific phospholipid surface that accounts for the anticoagulant effect of this enzyme [8,11,12]. It is noteworthy that hydrolysis of very low but specific plasma phospholipids is the characteristic feature of strong anticoagulant PLA_2s, whereas non-specific, non-anticoagulant PLA_2 enzymes hydrolyze the plasma phospholipids at random [8,12,25].

One of the most important factors influencing the anticoagulant potency is the penetrating property of PLA_2 enzymes [8,10,11,33]. Intrinsic fluorescence distinguishes the phospholipases according to their affinity for phospholipids, and a significant increase in fluorescence signal post binding of $NnPLA_2$-I with PC vesicles, even in absence of Ca^{2+}, suggests its high penetrating ability that in turn reflects its strong anticoagulant activity [10,12,25]. This enhanced fluorescence signal may be correlated with Trp quenching in $NnPLA_2$-I, and Ca^{2+} might promote a better interaction of this PLA_2 with PC resulting in an increase in the fluorescence signal in the presence of this ion [10,25].

The non-catalytic mechanism for the anticoagulant action of snake venom PLA_2 is executed by competing with blood clotting factors such as Xa, Va, or prothrombinase complex in the lipid surface [8,10]. $NnPLA_2$-I shows a unique example of activation of amidolytic activity of FXa without influencing its prothrombin activating property. This is further evidenced by the fact that $NnPLA_2$-I does not increase the PT of PPP suggesting it does not impede the extrinsic pathways possible due to non-binding of $NnPLA_2$-I to coagulation factors such as V, VII, and X. Conversely, an

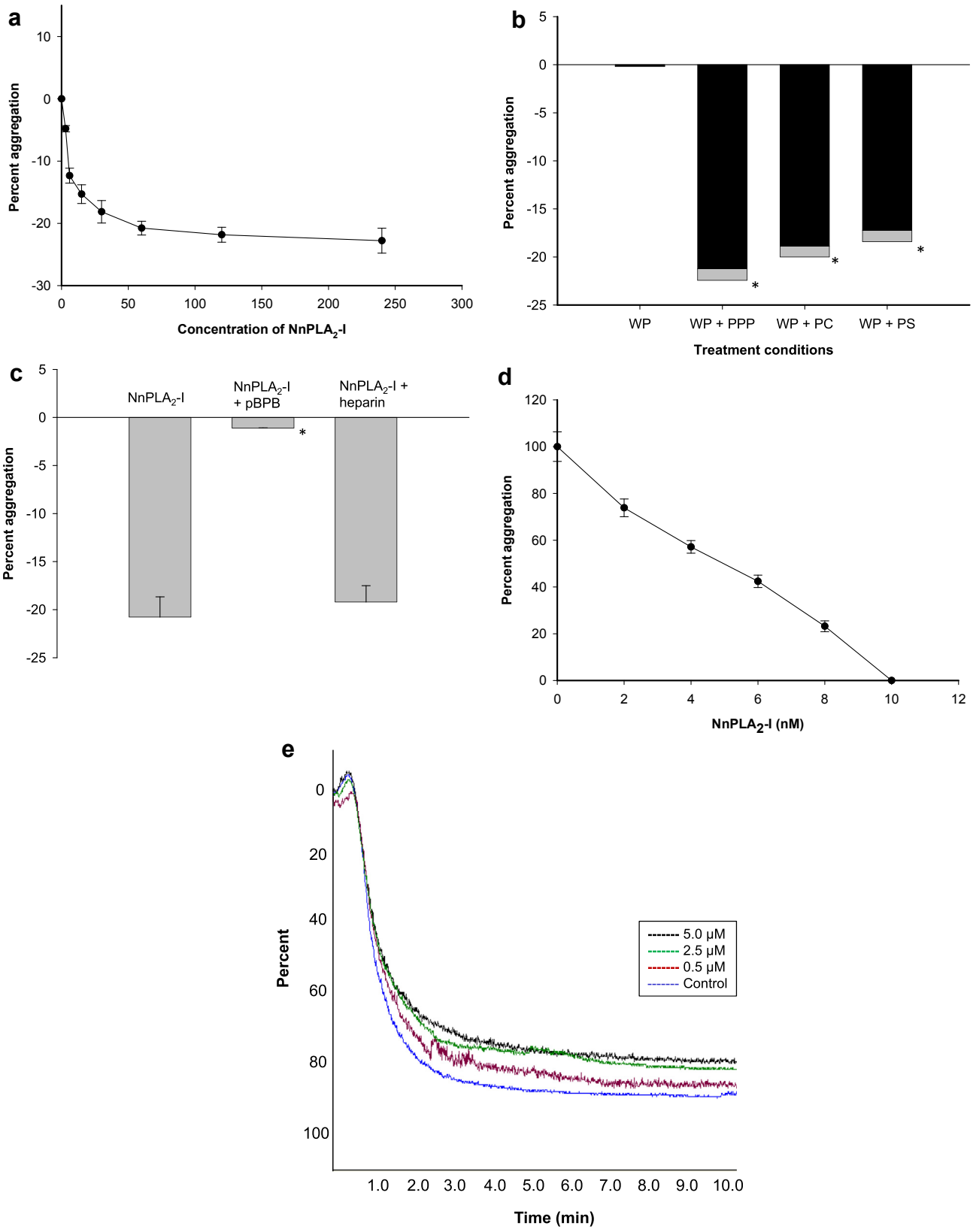

Fig. 6. (a) Dose-dependent platelet deaggregation property of $NnPLA_2$-I. (b) Effect of $NnPLA_2$-I (60 nM) on washed platelets in absence and presence of PPP/PC/PS. (c) A comparison of platelet modulating activity between native and heparin (20 mIU) or *p*BPB (2 mM)-treated $NnPLA_2$-I (60 nM). (d) Inhibition of collagen (1.0 μg/ml) – induced aggregation of PRP by different concentrations (2–10 nM) of$NnPLA_2$-I. (e) Dose-dependent inhibition of thrombin-induced platelet aggregation by $NnPLA_2$-I. A range of concentrations of $NnPLA_2$-I (0.5–5.0 μM) was pre-incubated with human thrombin (0.20 μg/ml) for 10 min at 37 °C prior to the addition of washed platelets. Values are mean ± S.D. of three independent experiments. Significance of difference with respect to control, *$p < 0.01$.

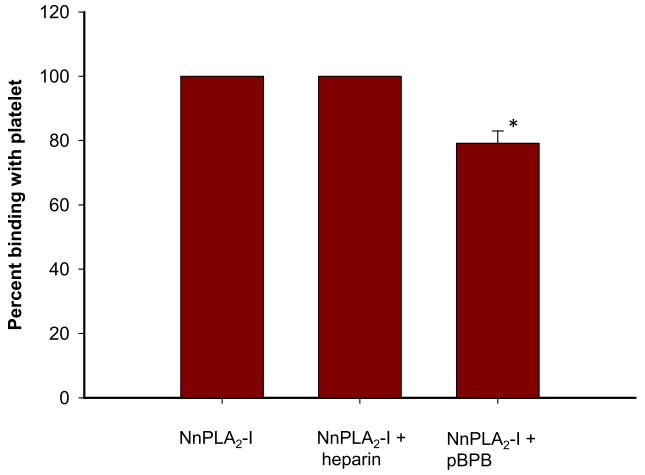

Fig. 7. A comparison of platelet binding property between native $NnPLA_2$-I (250 nM) and heparin (20 mIU) or pBPB (2 mM)-treated $NnPLA_2$-I. Values are mean ± S.D. of three independent experiments.

increase in APTT of PPP by $NnPLA_2$-I indicates that this enzyme inhibits intrinsic and common pathways of coagulation cascade to exert its anticoagulant activity. The interaction of $NnPLA_2$-I with FXa probably allosterically activates the catalytic activity of the latter towards its small chromogenic substrate; however, this activation might not be sufficient to enhance the catalytic activity of FXa towards its large physiological substrate prothrombin.

To date only two thrombin inhibitor PLA_2 enzymes have been purified and characterized from snake venoms [12,13]. Since thrombin catalyzes the key step of blood coagulation cascade; therefore, thrombin is a key pharmaceutical target for the management and/or prevention of thrombotic associated disorders [34]. Sadly, classical anticoagulant drugs such as heparin and warfarin demonstrate several side effects including bleeding complications that suggest the search for new anticoagulants [35]. Notably, potent anticoagulants derived from snake venom have shown the potential to be developed as better antithrombotic agents [24,27,36]. The non-cytotoxic PLA_2 molecules showing thrombin inhibitory activity may therefore hold great promise for pharmaceutical application in the treatment or prevention of various cardiovascular disorders such as thrombosis [34]. The present study suggests that, like anticoagulant PLA_2s from *Naja haje* and *D. russelii* venoms [12,13], $NnPLA_2$-I partially exerts its anticoagulant activity by non-covalent binding to thrombin at a site other than its heparin binding exosite-II [34]. Besides, $NnPLA_2$-I, similar to heparin, also induces a conformational change in the AT-III to activate it, which in turn inhibits the binding of thrombin with fibrinogen. This effect leads to a greater anticoagulant effect of the $NnPLA_2$-I/AT-III complex [34]. Furthermore, similar to PLA_2 from *N. haje* venom, $NnPLA_2$-I is also found to be a mixed inhibitor of thrombin, although the strength of thrombin inhibition by $NnPLA_2$-I is superior to PLA_2 purified from *N. haje* venom [13], or $RVAPLA_2$ from *D. ruselii* venom [12].

Previous studies have shown that heparin, which is a sulfated glycosaminoglycan, binds to snake venom PLA_2 enzymes to neutralize their various pharmacological properties such as cytotoxicity, myonecrosis, anticoagulant activity, and edema-induction [37–40]. These studies suggest the advantage of applying a low concentration of heparin as a complementary treatment against various snake envenomation [37,39]. Notably, heparin does not neutralize the phospholipids hydrolysis activity of $NnPLA_2$-I. Therefore, this indicates that heparin does not bind to the catalytic site of this enzyme or interfere with the phospholipids or membrane binding property of $NnPLA_2$-I. In 1994, Lomonte et al. [37] also reported that the interaction of myotoxin III with heparin significantly eliminated its myotoxicity without inhibiting its enzymatic activity. Therefore, partial neutralization of antithrombin activity of $NnPLA_2$-I without affecting its enzymatic activity in the presence of low molecular weight heparin supports the dissociation of catalytic and anticoagulant (pharmacological) regions in most of the snake venom PLA_2 molecules [6,8,9,11,12]. It has been shown that residues 105–118 possessing strongly cationic sites in the C-terminal loop of Lys49 myotoxin II purified from the venom of *Bothrops asper* are responsible for binding with negatively charged heparin and subsequent blocking of its myotoxicity [37]. Nevertheless, unlike the C-terminal region of myotoxic PLA_2s, the site containing residues 54–77 in snake venom PLA_2 molecule is responsible for showing anticoagulant activity [8]. In strongly anticoagulant PLA_2 molecules, such as $NnPLA_2$-I, this region is positively charged, located on the surface of the enzyme, and is accessible for interaction with the pharmacological target [8]. Therefore, it may be concluded that the positive residues in the anticoagulant region of $NnPLA_2$-I bind with the negatively charged heparin through electrostatic interaction resulting in neutralization of the thrombin inhibiting property of $NnPLA_2$-I [40].

Platelet aggregation is an important hemostatic mechanism; therefore, modulation of platelet functioning by a snake venom toxin may have an adverse effect on envenomed prey/victims. Large numbers of snake venom PLA_2 enzymes are known to influence the platelet aggregation property [5,41,42]. Based on their platelet modulating activity, venom PLA_2 enzymes can be categorized in three groups: group I PLA_2s show aggregation of platelets, group II PLA_2s inhibit the platelet aggregation induced by several physiological agents, whereas group III PLA_2s show dose-dependent platelet aggregation and deaggregation properties [42]. Therefore, $NnPLA_2$-I may be classified as a member of the group II snake venom PLA_2 enzymes.

The role of catalytic activity in platelet modulating property of $NnPLA_2$-I is evidenced by the fact that washed platelet is unaffected by this PLA_2 enzyme; nevertheless, supplementation of PPP (a source of phospholipids) or purified PC/PS to the platelets suspension resulted in formation of lysophospholipids from the hydrolysis of phospholipids by added $NnPLA_2$-I which in turn shows platelet deaggregation and inhibition of collagen-induced platelet aggregation [43]. Moreover, complete loss of platelet deaggregating property of $NnPLA_2$-I following alkylation of histidine residue indicates that the catalytic activity of $NnPLA_2$-I is involved in its platelet deaggregation [5]. Heparin, on the other hand, did not influence the antiplatelet activity of $NnPLA_2$-I owing to the fact that it does not influence the catalytic activity of this PLA_2. Moreover, the concentration of low molecular mass heparin used in this study does not show any adverse effect on platelet function may be due to formation of an antithrombin-heparin complex [44]; therefore, therapeutic application of low dose heparin besides antivenom therapy for hospital management of snakebite may be suggested. Notably, in terms of platelet binding property, $NnPLA_2$-I shows similarity to a PLA_2 purified from *N. nigricollis* venom which also demonstrates lower affinity for membrane phospholipids after histidine modification [45]. Conversely, histidine modification does not interfere with the membrane binding property of *Naja kaouthia* PLA_2s [7].

Many PLA_2s from snake venom have been shown to possess cytotoxicity [28,46] albeit the absence of *in vitro* hemolytic activity, cell cytotoxicity, and antibacterial activity of $NnPLA_2$-I may correlate with our previous observations regarding PLA_2 enzymes purified from Indian cobra and Russell's viper venom [9,12,25]. It has been suggested that the biochemical properties of PLA_2 enzymes, the availability of PC in a PLA_2-sensitive membrane and/or various

physicochemical properties of a cell membrane are the major factors that show the venom PLA_2-induced membrane damage [7,9,25,47].

5. Conclusion

The anticoagulant activity of a 15 kDa PLA_2 enzyme ($NnPLA_2$-I) purified from *N. naja* venom is partially dependent on its catalytic activity and is also influenced by the non-catalytic inhibition of thrombin. Conversely, antiplatelet activity of $NnPLA_2$-I is dependent on catalytic hydrolysis of plasma phospholipids. Heparin inhibits the anticoagulant activity of $NnPLA_2$-I, but does not interfere with the catalytic or antiplatelet activity of this enzyme suggesting that therapeutic application of a low dose of low molecular weight heparin in treating cobra bite patients. Further studies on thrombin-$NnPLA_2$-I interaction may advance our understanding of protein–protein interaction. Acquiring this progressive knowledge of the molecular basis of PLA_2-thrombin interaction offers promise for identifying new drug molecules to treat or prevent various cardiovascular diseases such as thrombosis.

Conflict of interest

None declared.

Acknowledgments

Authors thank Prof. S. S. Ghosh, IIT Guwahati for helping in cell toxicity analysis; Dr. D. Panda, IIT, Mumbai for mass spectroscopic analysis, Dr. D. Dash, IMS, BHU for platelet aggregation inhibition study, and Mr. P. Mudoi, TU for spectrofluorometric interaction study. SD is a recipient of DST-INSPIRE JRF fellowship. The present work is supported partially by financial assistance to AKM from the National Bioscience Award for Career Development-2013 (BT/HRD/NBA/34/01/2012-13) grant from the Department of Biotechnology, Ministry of science and Technology, Govt. of India. The instrumental facility provided under UGC-SAP (DRS-I) and DST-FIST programmes to the Department is duly acknowledged.

References

[1] A.K. Mukherjee, C.R. Maity, Composition of *Naja naja* venom sample from three district of West Bengal, Eastern India, Comp. Biochem. Physiol. 119 (A) (1998) 621–627.
[2] R. Shashidharamurthy, Y.H. Mahadeswaraswamy, L. Ragupathic, B.S. Vishwanath, K. Kemparaju, Systemic pathological effects induced by cobra (*Naja naja*) venom from geographically distinct origins of Indian peninsula, Exp. Toxicol. Pathol. 62 (2010) 587–592.
[3] A.K. Mukherjee, C.R. Maity, Biochemical composition, lethality and pathophysiology of venom from two cobras: *Naja naja* and *N. kaouthia*, Comp. Biochem. Physiol. 131 (B) (2002) 125–132.
[4] L.M.S. Rudrammaji, T.V. Gowda, Purification and characterization of three acidic cytotoxic phospholipase A_2 from Indian Cobra (*Naja naja naja*) venom, Toxicon 36 (1998) 921–932.
[5] S. Satisha, J. Tejaswinia, T.P. Krishnakanthab, T.V. Gowda, Purification of a class B1 platelet aggregation inhibitor phospholipase A_2 from Indian cobra (*Naja naja*) venom, Biochim 86 (2004) 203–210.
[6] R. Doley, A.K. Mukherjee, Purification and characterization of an anticoagulant phospholipase A_2 from Indian monocled cobra (*Naja kaouthia*) venom, Toxicon 41 (2003) 81–91.
[7] R. Doley, G.F. King, A.K. Mukherjee, Differential hydrolysis of erythrocyte and mitochondrial membrane phospholipids by two phospholipase A_2 isoenzymes ($NK\text{-}PLA_2$-I and $NK\text{-}PLA_2$-II) from the venom of the Indian monocled cobra *Naja kaouthia*, Arch. Biochem. Biophys. 425 (2004) 1–13.
[8] R.M. Kini, Anticoagulant proteins from snake venoms: structure, function and mechanism, Biochem. J. 397 (2006) 377–387.
[9] A.K. Mukherjee, Correlation between the phospholipids domains of the target cell membrane and the extent of *Naja kaouthia* PLA_2-induced membrane damage: evidence of distinct catalytic and cytotoxic sites in PLA_2 molecules, Biochem. Biophys. Acta 1770 (2007) 187–195.
[10] D. Saikia, R. Thakur, A.K. Mukherjee, An acidic phospholipase A_2 (RVVA-PLA_2-I) purified from *Daboia russelli* venom exerts its anticoagulant activity by enzymatic hydrolysis of plasma phospholipids and by non-enzymatic inhibition of factor Xa in a phospholipids/Ca^{2+} independent manner, Toxicon 57 (2011) 841–850.
[11] D. Saikia, S. Majumdar, A.K. Mukherjee, Mechanism of in vivo anticoagulant and haemolytic activity by a neutral phospholipase A_2 purified from *Daboia russelii russelii* venom: correlation with clinical manifestations in Russell's Viper envenomed patients, Toxicon 76 (2013) 291–300.
[12] A.K. Mukherjee, A major phospholipase A_2 from *Daboia russelli russelii* venom shows potent anticoagulant action via thrombin inhibition and binding with plasma phospholipids, Biochim 99 (2014) 153–161.
[13] A.V. Osipov, S.Y. Filkin, Y.V. Makarova, V.I. Tsetlin, Y.N. Utkin, A new type of thrombin inhibitor, noncytotoxic phospholipase A_2, from the *Naja haje* cobra venom, Toxicon 55 (2) (2010) 186–194.
[14] M.K. Bhat, B.N. Prasad, T.V. Gowda, Purification and characterization of neurotoxic phospholipase A_2 from Indian cobra (*Naja naja*) venom, Toxicon 29 (1991) 1345–1349.
[15] D.K. Machiaha, T.V. Gowda, Purification of a post-synaptic neurotoxic phospholipase A_2 from *Naja naja* venom and its inhibition by a glycoprotein from *Withania somnifera*, Biochim 88 (2006) 701–710.
[16] R. Shashidharamurthy, K. Kemparaju, A neurotoxic phospholipase A_2 variant: isolation and characterization from eastern regional Indian cobra (*Naja naja*) venom, Toxicon 47 (2006) 727–733.
[17] O.H. Lowry, N.J. Rosebrough, A.L. Farr, R.J. Randall, Protein measurement with Folin–phenol reagent, J. Biol. Chem. 193 (1951) 265–275.
[18] U.K. Laemmli, Cleavage of structural protein during the assembly of the head of bacteriophage T4, Nature 227 (1970) 680–685.
[19] J.H. Morrissey, Silver stain for proteins in polyacrylamide gels: a modified procedure with enhanced uniform sensitivity, Anal. Biochem. 117 (1981) 307–310.
[20] B. Thiede, W. Höhenwarter, A. Krah, J. Mattow, M. Schmid, F. Schmidt, P.R. Jungblut, Peptide mass fingerprinting, Methods 35 (2005) 237–247.
[21] A.K. Mukherjee, S.P. Mackessy, Biochemical and pharmacological properties of a new thrombin-like serine protease (Russelobin) from the venom of Russell's viper (*Daboia russelii russelii*) and assessment of its therapeutic potential, Biochem. Biophys. Acta – Gen. Sub. 1830 (2013) 3476–3488.
[22] J. Joubert, N. Taljaard, Purification, some properties and amino acid sequences of two phospholipase A_2 (CM-II and CM-III) from *Naja naja kaouthia*, J. Biochem. 112 (1980) 493–499.
[23] A.K. Mukherjee, S.K. Ghosal, C.R. Maity, Some biochemical properties of Russell's viper (*Daboia russelli*) venom from Eastern India: correlation with clinical pathological manifestation in Russell's viper bite, Toxicon 38 (2000) 163–175.
[24] A.K. Mukherjee, S.K. Rai, R. Thakur, P. Chattopadhyay, S. Kar, Bafibrinase: a non-toxic, non-hemorrhagic, direct-acting fibrinolytic serine protease from *Bacillus* sp. strain AS – S20-I exhibits in vivo anticoagulant activity and thrombolytic potency, Biochim 94 (2012) 1300–1308.
[25] D. Saikia, N.B. Bordoloi, P. Chattopadhyay, S. Chocklingam, S.S. Ghosh, A.K. Mukherjee, Differential mode of attack on membrane phospholipids by an acidic phospholipase A_2 (RVVA-PLA_2-I) from *Daboia russelli* venom, Biochim. Biophys. Acta. – Biomembr 1818 (2012) 3149–3157.
[26] B. Bednar, C. Condra, R.J. Gould, T.M. Connolly, Platelet aggregation monitored in a 96 well microplate reader is useful for evaluation of platelet agonists and antagonists, Thromb. Res. 77 (1995) 453–463.
[27] A.K. Mukherjee, S. Dutta, S. Mackessy, A new C-type lectin (RVsnaclec) purified from venom of *Daboia russelii russelii* shows anticoagulant activity via inhibition of FXa and concentration-dependent differential response to platelets in a Ca^{2+}–independent manner, Thromb. Res. 134 (2014) 1150–1156.
[28] C. Chanda, A. Sarkar, S. Sistla, D. Chakrabarty, Anti-platelet activity of a three-finger toxin (3FTx) from Indian monocled cobra (*Naja kaouthia*) venom, Biochem. Biophys. Res. Comm. 441 (2013) 550–554.
[29] Q. Liu, Q. Huang, M. Teng, C.M. Weeks, C. Jelsch, R. Zhang, L. Niu, The crystal structure of a novel, inactive, lysine 49 PLA_2 from *Agkistrodon acutus* venom an ultrahigh resolution, ab initio structure determination, J. Bio. Chem. 278 (2003) 41400–41408.
[30] I. Tsai, Y. Wang, A.C. Cheng, V. Starkov, A. Osipov, I. Nikitin, Y. Makarova, R. Ziganshin, Y. Utkin, cDNA cloning, structural, and functional analyses of venom phospholipases A_2 and a Kunitz-type protease inhibitor from steppe viper *Vipera ursinii renardi*, Toxicon 57 (2011) 332–341.
[31] Z.-M. Yang, Q. Guo, Z.R. Ma, Y. Chen, Z.Z. Wang, X.M. Yang, Y.M. Yang, I.H. Tsai, Structures and functions of crotoxin-like heterodimers and acidic phospholipases A_2 from *Gloydius intermedius* venom: insights into the origin of neurotoxic-type rattlesnakes, J. Proteomics 112 (2014) 210–223.
[32] H.M. Verheij, M.C. Boffa, C. Rothen, M.C. Bryckaert, R. Verger, G.H. De Haas, Correlation of enzymatic activity and anticoagulant properties of phospholipase A_2, Eur. J. Biochem. 112 (1980) 25–32.
[33] E. Condrea, J.E. Feltcher, J.E. Rapuano, C.C. Yang, P. Rosenberg, Effect of modification of one histidine residue on the enzymatic and pharmacological properties of a toxic phospholipase A_2 from *Naja nigricollis* snake venom and less toxic phospholipase A_2 from *Hemachatus haemachatus* and *Naja naja atra* venoms, Toxicon 19 (1981) 61–71.
[34] W. Bode, Structure and interaction modes of thrombin, Blood Cells Mol. Dis. 36 (2006) 122–130.
[35] S. Schulman, R.J. Beyth, C. Kearon, M.N. Levine, Hemorrhagic complications of anticoagulant and thrombolytic treatment: in American College of Chest

Physicians evidence-based clinical Practice Guidelines (8th Edition), Chest 133 (2008) 257S–298S.
[36] R. Thakur, A. Kumar, B. Bose, D. Panda, D. Saikia, P. Chattopadhyay, A.K. Mukherjee, A new peptide (Ruviprase) purified from the venom of *Daboia russelii russelii* shows potent anticoagulant activity via non-enzymatic inhibition of thrombin and factor Xa, Biochim 105 (2014) 149–158.
[37] B. Lomonte, A. Tarkowski, U. Bagge, L.A. Hanson, Neutralization of the cytolytic and myotoxic activities of phospholipases A_2 from *Bothrops asper* snake venom by glycosaminoglycans of the heparin/heparan sulfate family, Biochem. Pharmacol. 47 (1994) 1509–1518.
[38] E.C.T. Landucci, M. Toyama, S. Marangoni, B. Oliveira, G. Cirino, E. Antunes, G. de Nucci, Effect of crotapotin and heparin on the rat paw oedema induced by different secretory phospholipases A_2, Toxicon 38 (2000) 199–208.
[39] S. Rostelato-Ferreira, G.B. Leite, A.D.O. Cintra, M.A. da Cruz-Höfling, L. Rodrigues-Simioni, Y. Oshima-Franco, Heparin at low concentration acts as antivenom against *Bothrops jararacussu* venom and bothrops toxin-I neurotoxic and myotoxic actions, J. Venom. Res. 1 (2010) 54–56.
[40] A.M. Perchuc, L. Menin, P. Favreau, B. Bühler, P. Bulet, R. Schöni, M. Wilmer, E. Beat, R. Stöcklin, Isolation and characterization of two new Lys49 PLA_2s with heparin neutralizing properties from *Bothrops moojeni* snake venom, Toxicon 55 (6) (2010) 1080–1092.
[41] L.B. Silveira, D.P. Marchi-Salvador, N.A. Santos-Filho, F.P. Silva Jr., S. Marcussi, A.L. Fuly, A. Nomizo, S.L. da Silvag, R.G. Stábelih, E.C. Arantesa, A.M. Soares, Isolation and expression of a hypotensive and anti-platelet acidic phospholipase A_2 from *Bothrops moojeni* snake venom, J. Pharm. Biomed. Anal. 73 (2013) 35–43.
[42] F. Chérifi, A. Namane, F. Laraba-Djebari, Isolation, functional characterization and proteomic identification of CC2-PLA_2 from *Cerastes cerastes* venom: a basic platelet-aggregation-inhibiting factor, Protein J. 33 (2014) 61–74.
[43] Y. Yuan, S.P. Jackson, H.H. Newnham, C.A. Mitchell, H.H. Salem, An essential role for lysophosphatidylcholine in the inhibition of platelet aggregation by secretory phospholipase A_2, Blood 86 (1995) 4166–4174.
[44] E.W. Salzman, R.D. Rosenberg, M.H. Smith, J.N. Lindon, L. Favreau, Effect of heparin and heparin fractions on platelet aggregation, J. Clin. Investig 65 (1980) 64.
[45] J.P. Dachary, M.C. Boffa, M.R. Boisseau, J. Dufourcq, Snake venom phospholipases A_2. A fluorescence study of their binding to phospholipid vesicles correlation with their anticoagulant activities, J. Biol. Chem. 255 (1980) 7734–7739.
[46] S. Khunsap, N. Pakmanee, O. Khow, L. Chanhome, V. Sitprija, M. Suntravat, S.E. Lucena, J.C. Perez, E.E. Sánchez, Purification of a phospholipase A_2 from *Daboia russelii siamensis* venom with anticancer effects, J. Venom. Res. 2 (2011) 42–45.
[47] A.K. Mukherjee, S.K. Ghosal, C.R. Maity, Lysosomal membrane stabilization by α-tocopherol against the damaging action of *Vipera russelli* venom phospholipase A_2, Cell. Mol. Life Sci. CMLS 53 (2) (1997) 152–155.

Journal of Proteomics 156 (2017) 29–39

Contents lists available at ScienceDirect

Journal of Proteomics

journal homepage: www.elsevier.com/locate/jprot

Proteomic analysis to unravel the complex venom proteome of eastern India *Naja naja*: Correlation of venom composition with its biochemical and pharmacological properties

Sumita Dutta, Abhishek Chanda, Bhargab Kalita, Taufikul Islam, Aparup Patra, Ashis K. Mukherjee *

Microbial Biotechnology and Protein Research Laboratory, Department of Molecular Biology and Biotechnology, Tezpur University, Tezpur 784028, Assam, India

ARTICLE INFO

Article history:
Received 18 August 2016
Received in revised form 27 December 2016
Accepted 29 December 2016
Available online 4 January 2017

Keywords:
Acetylcholinesterase
LC-MS/MS
Phospholipase A_2
Three-finger toxins
Tandem mass spectrometry
Venomics
Pathophysiology

ABSTRACT

The complex venom proteome of the eastern India (EI) spectacled cobra (*Naja naja*) was analyzed using tandem mass spectrometry of cation-exchange venom fractions. About 75% of EI *N. naja* venom proteins were <18 kDa and cationic at physiological pH of blood. SDS-PAGE (non-reduced) analysis indicated that in the native state venom proteins either interacted with each-other or self-aggregated resulting in the formation of higher molecular mass complexes. Proteomic analysis revealed that 43 enzymatic and non-enzymatic proteins in EI *N. naja* venom with a percent composition of about 28.4% and 71.6% respectively were distributed over 15 venom protein families. The three finger toxins (63.8%) and phospholipase A_2s (11.4%) were the most abundant families of non-enzymatic and enzymatic proteins, respectively. nanoLC-ESI-MS/MS analysis demonstrated the occurrence of acetylcholinesterase, phosphodiesterase, cholinesterase and snake venom serine proteases in *N. naja* venom previously not detected by proteomic analysis. ATPase, ADPase, hyaluronidase, TAME, and BAEE-esterase activities were detected by biochemical analysis; however, due to a limitation in the protein database depository they were not identified in EI *N. naja* venom by proteomic analysis. The proteome composition of EI *N. naja* venom was well correlated with its *in vitro* and *in vivo* pharmacological properties in experimental animals and envenomed human.

Biological significance: Proteomic analysis reveals the complex and diverse protein profile of EI *N. naja* venom which collectively contributes to the severe pathophysiological manifestation upon cobra envenomation. The study has also aided in comprehending the compositional variation in venom proteins of *N. naja* within the Indian sub-continent. In addition, this study has also identified several enzymes in EI *N. naja* venom which were previously uncharacterized by proteomic analysis of *Naja* venom.

1. Introduction

Snakebite is a neglected tropical disease and the Indian scenario is a bit of a concern. Statistical data suggests that snake bite mortality ranges from about 1300 to 50,000 in this region [1]. Envenoming by Indian spectacled cobra (*Naja naja*) is responsible for the mortality and morbidity of snakebite in India [2,3]; therefore, *N. naja* is included in category 1 of medically important snakes in India, the envenomation of which requires immediate medical attention [4]. Common clinical features of cobra envenomation follow a definite pattern. Drowsiness is the first symptom immediately after a bite that hints at the onset of the systemic effect of envenomation. Ptosis, frothy saliva, slurred speech, respiratory failure, and skeletal muscle paralysis are outcomes of the neuromuscular effect of venom proteins within 8–19 h of a cobra bite [5–7]. The *N. naja* venom is predominantly rich in low molecular weight protein(s)/peptides (6–15 kDa) which mainly comprises of phospholipase A_2s (PLA_2s) and three finger toxins (3FTxs), some of which show specific binding to postsynaptic nAChRs at the skeletal muscle neuromuscular junction to block the neuromuscular transmission [8,9]. The other toxic proteins of cobra venom such as snake venom metalloproteases (SVMPs), cobra venom factors (CVFs) and phospholipase A_2s (PLA_2) contribute to local tissue damage and necrosis [10–14]. However, regional variation in venom composition plays a significant role in pathogenesis developed after snakebite [2,15]; henceforth, in depth studies on composition of venom from snakes in a particular locality are of utmost important. Noteworthy, a detailed analysis of venom composition of eastern India (EI) *N. naja* and correlation of this complex venom proteome profile with clinical manifestations in a cobra bite have yet to be established.

The traditional methods of identification of venom components by chromatographic separation of crude venom followed by its biochemical and/or pharmacological characterization seem to be incompetent

* Corresponding author: Department of Molecular Biology and Biotechnology, Tezpur University, Tezpur 784028, Assam, India.
E-mail address: akm@tezu.ernet.in (A.K. Mukherjee).

http://dx.doi.org/10.1016/j.jprot.2016.12.018
1874-3919/

for global analysis of snake venoms. During the last decade, the field of proteomics has vastly expanded due to the availability of large sets of proteomic and genomic databases that resulted in elucidation of the detailed composition of snake venom [16,17]. The proteomic analysis led to identification of 124 proteins and peptides in the venom of the Asiatic non-spitting cobra *N. naja atra* [18]. Recently, by proteomic approach Ali et al. [19] demonstrated the presence of 28 proteins in Pakistan *N. naja* venom, whereas 26 and 25 proteins were reported to be present in *N. naja* venom from north-western India and Sri Lanka, respectively [20].

Although the EI *N. naja* venom or some of its purified components were subjected to biochemical analysis and/or pharmacological characterization [2,3,15,21]; however, a detailed toxin profile of this venom for a better insight into the pathophysiology of envenomation is still warranted. Henceforth, in the present study an attempt was made to identify the components of EI *N. naja* venom through a proteomic approach and this data was correlated with the biochemical properties as well as pharmacological activities of this venom. Remarkably, we have identified few enzymatic proteins in EI *N. naja* venom which were previously unrevealed by proteomic analysis from the venom of the same species of the snake.

2. Materials and methods

Pooled *N. naja* venom from four snakes of EI origin (Nadia district, West Bengal) was procured from Calcutta Snake Park. Diagnostic kits for thromboplastin time (APTT) and prothrombin time (PT) assays were purchased from Tulip Diagnostics Pvt. Ltd., Mumbai, India. All other chemicals used were of analytical grade and procured from Sigma-Aldrich, USA.

2.1. Fractionation of crude Naja naja venom through ion-exchange chromatography

Crude *N. naja* venom (dry weight 25 mg) was dissolved in 0.5 ml of 20 mM Tris–HCl buffer, pH 7.4 (buffer A), centrifuged at 10,000 rpm for 10 min and then filtered through a 0.2 μm nylon membrane syringe filter (Genetix, Biotech Asia Pvt. Ltd.). The filtrate was subjected to fractionation through a cation-exchanger HiPrep CM FF 16/10 (Wipro GE Health Care, Sweden) pre-equilibrated with the buffer A and coupled to an AKTA purifier 10 FPLC system (Wipro GE Health Care, Sweden) [21]. After washing the column with buffer A to remove the unbound proteins, the bound proteins were eluted with a gradient (0–100%) of 1 M NaCl dissolved in buffer A (buffer B). The elution of protein at a flow rate of 1 ml/min at 4 °C was monitored at 280 nm, and a 1.5 ml fraction was collected in each tube [21]. Protein content of crude venom and fractions was determined by the method of Lowry et al. [22]. From a standard curve of BSA, the concentration of unknown protein was determined at 660 nm. Each cation-exchange fraction was subjected to LC-MS/MS analysis and the crude venom was assayed for enzyme activities and *in vitro* pharmacological properties (see below).

2.2. Determination of molecular masses of EI N. naja venom proteins through sodium dodecyl sulfate polyacrylamide gel electrophoresis (SDS-PAGE)

Crude EI *N. naja* venom was subjected to 12.5% SDS-PAGE analysis under reduced and non-reduced conditions. Proteins were visualized by staining the gels with 0.1% Coomassie Brilliant Blue R-250 and destaining with methanol/acetic acid/water (40:10:50). Approximate molecular masses of the venom proteins were determined from a plot of log MW of standards *vs. Rf* values. The relative abundance of each band was determined by densitometry scanning of SDS-PAGE bands using Image J Software.

2.3. LC-MS/MS analysis of cation-exchange fractions of N. naja venom

The trypsin digested fragments of the cation-exchange fractions (50 μg protein) of EI *N. naja* venom were subjected to LC-MS/MS analysis as described previously [23–25]. Briefly, 1 μl of trypsin-digested sample was desalted and concentrated by ZipTip C_{18} (Merck, USA) and then subjected to nano-UHPLC-MS/MS analysis. ESI (nano-spray) was used as the ion source, fragmentation mode used was collision-induced dissociation (only y and b ions were considered), FT-ICR/Orbitrap was used as MS scan mode and MS/MS scan in the range from 500 to 2000 *m/z* was acquired in linear ion trap mode [23–25]. For collision-induced dissociation (CID)-MS/MS analysis doubly or triply-charged ions were selected [23–25]. The signal:noise ratio was kept >2 for selecting the precursors for MS/MS data acquisition and keratin as well as trypsin autolysis peak signals were excluded from analysis.

For variable modifications carbamidomethylation of cysteine residues, oxidation of methionine residues, pyro-glu from glutamine, and deamidation of asparagine and glutamine were selected [26]. The percent mass error tolerance and fragment mass error tolerance were set to 12 ppm and 0.8 Da, respectively and up to two missed cleavages and three maximum variable modifications per peptide were allowed [23–25]. The data were searched in the UniProt Swiss-Prot database (non-redundant database with reviewed proteins) and NCBI against Elapidae venom (taxid: 8602) and the data were analyzed using PEAKS 7.0 search engine. Further, to improve the sequence coverage of identification of venom proteins, the semi-tryptic and non-tryptic peptide sequences with an average local confidence (ALC) score of ≥55% were also derived directly from the MS/MS spectrum (*de novo* sequencing) using PEAKS 7.0 software. Only matching proteins and peptides showing a −10logP value ≥30 and 20, respectively were considered for identification purposes and the false discovery rate (FDR) was kept very stringent (1.0%) [25]. In addition, redundant peptides were removed from the data set to make identification based only on the presence of overlapping homologous distinct peptides. The spectral count method was followed to determine the relative abundance of *N. naja* venom proteins [27,28]. Mean spectral count of a protein was normalized by dividing the summed spectra of the identified protein by its number of peptides generated Eq. (1) [27]. The relative abundance of a protein in a particular chromatographic fraction was determined as described previously [25,29] Eq. (2).

$$\text{Mean spectral count of a protein } X \text{ in chromatographic fraction } Y = \frac{\text{Total spectral count of } X \text{ in fraction } Y}{\text{Total number of peptides of } X \text{ in } Y} \quad (1)$$

$$\text{Relative abundance of a protein or peptide } X \text{ in chromatographic fraction } Y = \frac{\text{Mean spectral count of } X \text{ in fraction } Y}{\text{Total mean spectral counts of all proteins/peptides in } Y} \times \text{Percent protein content of } Y\ (\%) \quad (2)$$

2.4. Assay of enzyme activities

The proteolytic activity of the crude venom was assayed against human fibrinogen or fibrin. The reaction mixture containing 20 μg/ml of venom protein and substrate (2.5 mg/ml) dissolved in 1× phosphate buffered saline (PBS), pH 7.4 was incubated for 3 h at 37 °C [30]. One unit (U) of protease activity was defined as 1.0 μg of tyrosine equivalent liberated per min per ml of enzyme [30].

The PLA_2 activity of crude *N. naja* venom (20 μg/ml) was assayed by our previously described procedure [31]. One unit of PLA_2 activity was defined as the amount of protein which produced a decrease in 0.01 absorbance in 10 min at 740 nm [31]. For the assay of L-amino acid oxidase (LAAO) activity L-kynurenine was used as a substrate [32]. One unit of LAAO activity was defined as nmol kynurenic acid produced/min

under the assay conditions and specific LAAO activity was expressed as units/mg protein.

The phosphohydrolase activity against adenosine tri-phosphate (ATP), adenosine di-phosphate (ADP) and adenosine mono-phosphate (AMP)/5′-nucleotide was assayed by adding crude venom (20 μg/ml) to the reaction mixture (500 μl) containing 0.5 mM ATP/ADP/AMP in 20 mM Tris-HCl, pH 7.4 [33]. After incubation for 30 min at 37 °C, the reaction was stopped by the addition of 10 μl of ice cold 10% TCA and liberated P_i was determined spectrophotometrically at 695 nm [34]. One unit of ATPase/ADPase/AMPase activity was defined as μM P_i released per min.

The hyaluronidase activity was assayed by measuring the relative decrease in turbidity of hyaluronic acid substrate (1.0 mg/ml) [35]. Crude EI *N. naja* venom (20 μg/ml) was added to 10 μl of substrate and reaction volume was adjusted to 100 μl with the assay buffer (0.2 M sodium acetate buffer, pH 6.0 containing 150 mM NaCl). After incubation for 30 min at 37 °C, the reaction was stopped by adding 200 μl of 2.5% CTAB in 2% NaOH. Absorbance was noted at 405 nm in a 96-well microplate reader (Multiskan GO, Thermo Scientific, USA). Considering the control as 100% turbid, the unit of enzyme activity was expressed as turbidity reduction unit (TRU) per min per mg of venom [35].

2.5. Assay of esterase activities

Esterase activity was assessed by measuring the rates of hydrolysis of *p*-Tosyl-L-arginine methyl ester hydrochloride (TAME) or Nα-Benzoyl-L-arginine ethyl ester hydrochloride (BAEE) as a substrate (1 mM) [36]. One unit of BAEE-esterase and TAME-esterase activity was defined as an increase of 0.01 absorbance unit at 244 nm and 254 nm, respectively during the first 5 min of the reaction at 37 °C. A control having an equal volume of the assay buffer instead of enzyme was run in parallel. Specific activity was calculated as units of TAME or BAEE activity per mg venom protein. Acetylcholinesterase (AChE) activity was determined colorimetrically using 1 mM acetylthiocholine iodide as a substrate [37]. Enzyme activity was defined as the amount of protein which hydrolyzed 0.01 M of acetylcholine iodide per min under the assay conditions [37]. The phosphodiesterase (PDE) activity was assayed by slightly modifying the method described of Sulkowoski and Laskowoski [38]. The assay mixture (100 μl) contained 10 μM $MgCl_2$, 200 μM Tris-HCl (pH 9.0) and 10 μM bis-*p*-nitrophenyl phosphate as a substrate. The reaction was initiated by adding crude venom (20 μg/ml) to the reaction mixture and was incubated at 37 °C for 10 min. The increase in absorbance was read at 400 nm in a plate reader (MultiSkan GO, Thermo Scientific, USA) and the activity was expressed in μmol of *p*-nitrophenol released per min (using 17,600 as molar extinction coefficient of bis-*p*-nitrophenyl phosphate).

2.6. Assay of pharmacological properties

The dose-dependent (5 to 40 μg/ml) anticoagulant activity of EI *N. naja* venom was assayed against goat (mammalian) platelet poor plasma (PPP) [21,25]. One unit of anticoagulant activity was defined as crude venom induced 1 s increase in clotting time of the control PPP (incubated with buffer) [33]. Dose-dependent effect of crude *N. naja* venom (5 to 40 μg/ml) on prothrombin time (PT) and activated partial thromboplastin time (APTT) of PPP was determined by using commercial diagnostic kits following the instructions of the manufacturer. In another set of experiment, the effect of the crude *N. naja* venom on whole blood was studied by incubating 40 μg/ml of crude venom/buffer (control) with 300 μl of whole blood at 37 °C for 3 min, and then 40 μl of 250 mM $CaCl_2$ was added for initiation of the blood clotting. The clotting time was measured as described above.

Effect of EI *N. naja* venom or buffer (control) on Factor Xa was determined by pre-incubating two different doses of crude venom (20 μg/ml and 40 μg/ml) with FXa (1 μg/ml) for 60 min at 37 °C. Then prothrombin (15 μg) was added to the reaction mixture and it was incubated at 37 °C for 60 min. The thrombin formation (an indicator of prothrombin activation) was determined by 12.5% SDS-PAGE analysis of the reaction mixture [39]. Formation of thrombin from prothrombin by FXa (control) was considered as 100% activity and FXa inhibition (reduction in thrombin formation) by crude *N. naja* venom, if any, was calculated from the densitometry scanning of the gel and analysis of this data by Image J software.

Inhibition of fibrinogen clotting activity of thrombin was determined by pre-incubating thrombin (3 μl, 10 NIH U/ml) with crude venom (5 to 40 μg/ml) or buffer (control) for 30 min at 37 °C [36]. The reaction was initiated by adding 40 μl of fibrinogen (2.5 mg/ml) and the time for clot formation by thrombin was determined. The fibrinogen clotting time (s) of thrombin was considered as control activity and other values were compared to that.

Platelet rich plasma (PRP) was prepared from citrated goat blood by following the procedures described by Bednar et al. [40] and modified by Dutta et al. [21]. Concentration-dependent platelet modulating activity (% platelet aggregation) of EI *N. naja* venom (5 to 40 μg/ml) as compared to control (PRP incubated with buffer under identical conditions) was determined as described previously [21].

3. Results and discussion

3.1. Fractionation and SDS-PAGE analysis of EI N. naja venom

Cation-exchange fractionation of crude *N. naja* venom from EI resulted in its separation into 6 peaks (Fig. 1). The percent protein yield of different fractions (as determined by Lowry method) was observed in the following order: NnCM3 (29.0%) > NnCM4 (25.1%) > NnCM1 (23.2%) > NnCM6 (14.0%) > NnCM5 (6.5%) > NnCM2 (2.2%). Approximately 75% venom proteins were bound to the cation-exchange column under the experimental conditions (Fig. 1) indicating that majority of EI *N. naja* venom proteins were cationic at physiological pH (7.4) thus supporting our previous observation [2].

SDS-PAGE analysis of crude *N. naja* venom under reduced conditions showed 11 protein bands (Fig. 2A). Densitometry analysis suggested that venom proteins (~5 to 11 kDa) of band 11 were the most abundant components (~60%) of EI *N. naja* venom (Fig. 2A, Supplementary Table S1A).

Separation of EI *N. naja* venom by non-reduced SDS-PAGE showed clustering of venom proteins into three major regions (Fig. 2B, Supplementary Table S1B). The proteins of cluster 3 (molecular mass 5 to 22 kDa) were found to be the most abundant and collectively account for 69.7% of EI *N. naja* venom proteome (Fig. 2B, Supplementary Table S1B). Cluster 2 comprised of a protein band of ~45 kDa which accounts for 20.4% of the whole venom (Fig. 2B, Supplementary Table S1B). Very high molecular mass proteins (~110 to 180 kDa) were observed in cluster 1, and they contribute 9.9% of EI *N. naja* venom proteins (Fig. 2B, Supplementary Table S1B). Therefore, the SDS-PAGE analysis is suggestive of the predominance of low molecular weight proteins in EI *N. naja* venom, which is in accordance with the earlier reports [19,20]

3.2. LC-MS/MS analysis of cation- exchange fractions of EI N. naja venom

The vast array of pharmacological activities exhibited by Indian cobra envenomation is correlated to the occurrence of enormous proteins in its venom [2,3,41]. Although the shotgun proteomic approach has evolved as an efficient technique in proteomic studies nevertheless, small peptide coverage by considering only the tryptic peptides may not be adequate for analysis of a complex venom proteome. Therefore, in this study the accuracy of protein identification as well as sequence coverage of identified venom proteins was enhanced by allowing the semi-tryptic (one trypsin cleavage site at one of the terminals of the peptide) and *de novo* peptide sequences [25,42].

The LC-MS/MS analysis of the cation-exchange fractions of EI *N. naja* venom identified 43 proteins distributed across 15 venom protein

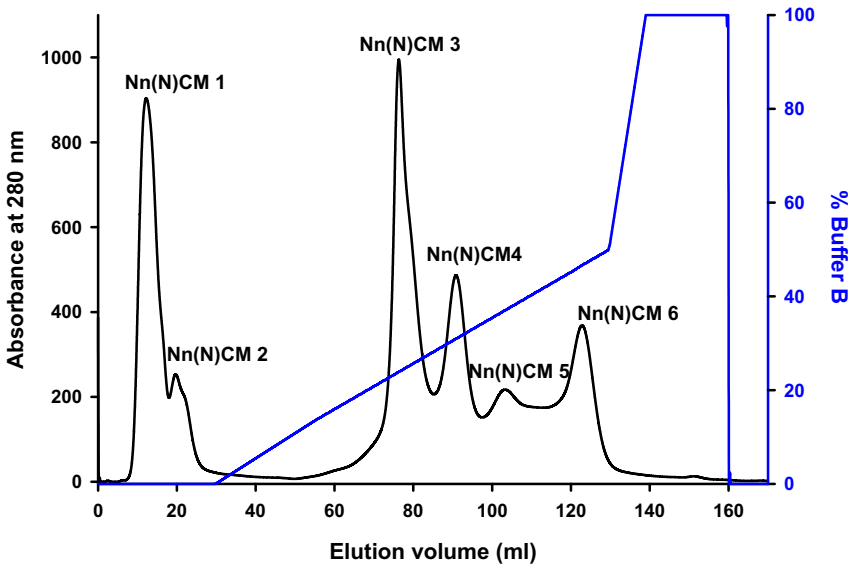

Fig. 1. Fractionation of EI *N. naja* venom (25 mg dry weight) on a HiPrep CM FF 16/10 cation exchange column coupled to an FPLC system. The flow rate was maintained at 1 ml/min at 4 °C and fraction volume was 1.5 ml.

families (Table 1, Supplementary Table S1). The alignment of MS/MS-derived peptide sequences with the homologous proteins from the Elapidae snake venom protein databases is shown in Supplementary Fig. S1. The proteomic analysis indicated that EI *N. naja* venom contains a mixture of enzymatic (28.4%) and non-enzymatic (71.6%) proteins/toxins; the three finger toxin (3FTx) (63.8%) alone is the most predominant class of toxin found in this venom sample (Fig. 3). This result is in accordance to the previous reports on *N. naja* venomic studies, wherein the 3FTxs constitute the majority of the *N. naja* venom proteome [19,20,43]. A brief description of the different classes of proteins identified in EI *N. naja* venom follows below.

3.3. Enzymatic proteins of EI N. naja venom

LC-MS/MS analysis showed that PLA_2 is the most predominant enzyme (11.4%) of EI *N. naja* venom followed by cholinesterase AChE (6.3%), (ChE) (6.0%), PDE (2.1%) and SVMP (1.0%). Interestingly, LAAO (0.8%), 5′-nucleotidase (NT) (0.4%) and SVSP (0.3%) comprise only a small fraction of EI *N. naja* venom proteome (Fig. 3).

PLA_2s (13–15 kDa molecular mass) are a class of snake venom enzymes known to exhibit a wide array of pharmacological activities [21,23,31,44–47]. LC-MS/MS analysis demonstrated the presence of 3 acidic PLA_2 isoenzymes corresponding to a relative abundance of

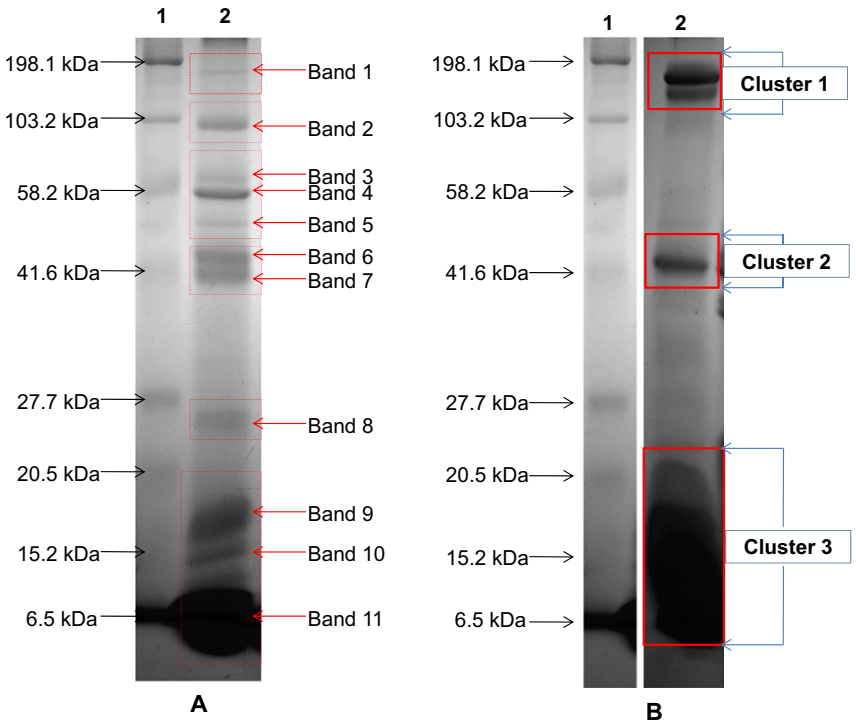

Fig. 2. 12.5% SDS-PAGE analysis of EI *N. naja* venom under reduced and non-reduced conditions. Lane 1, protein molecular markers; lane 2, crude *N. naja* venom (75 μg protein) under (A) reduced, and (B) non-reduced conditions.

Table 1
List of proteins identified by ESI-LC-MS/MS analysis of the cation exchange fractions of EI *N. naja* venom.

S. No.	Protein	Accession no.	−10logP	% Coverage	Molecular weight (kDa)	Unique peptide(s)	Homology with protein from	CM fraction
Enzymatic proteins								
Phospholipase A_2 (PLA_2)								
1	Acidic phospholipase A_2 2	gi|129514	258.4	91.0	13,346	2	*Naja naja*	1,2,3,4,5,6
2	Acidic phospholipase A_2 2	gi|24638099	242.2	74.0	15,949	2	*Naja atra*	1,2
3	Acidic phospholipase A_2 1	gi|24638468	244.0	80.0	16,271	2	*Naja kaouthia*	1,2,3,4,5,6
Acetylcholinesterase (AChE)								
4	Acetylcholinesterase	gi|1389604	78.8	8.0	64,723	14	*Bungarus fasciatus*	1,2,3,4,6
5	Acetylcholinesterase, partial	gi|565297659	30.6	5.0	48,355	1	*Ophiophagus hannah*	1,3,4,5
Cholinesterase (ChE)								
6	Cholinesterase, partial	gi|565319474	78.6	11.0	153,465	27	*Ophiophagus hannah*	1,2,3,4,5,6
Snake venom metallo-protease (SVMP)								
7	Hemorrhagic metalloproteinase-disintegrin-like kaouthiagin	gi|32469675	136.3	15.0	44,493	0	*Naja kaouthia*	3,4,6
8	Metalloproteinase atrase A	gi|294845712	96.9	8.0	68,254	3	*Naja atra*	3,4,6
9	Zinc metalloproteinase-disintegrin-like cobrin	gi|82223366	222.9	20.0	67,662	0	*Naja kaouthia*	3,4,6
Phosphodiesterase (PDE)								
10	cGMP-specific 3′,5′-cyclic phosphodiesterase, partial	gi|565318232	54.5	5.0	97,127	9	*Ophiophagus hannah*	2,3,4,5,6
Nucleotidase (NT)								
11	Soluble calcium-activated nucleotidase 1	gi|565292399	120.9	34.0	18,083	3	*Ophiophagus hannah*	5,6
L-Amino acid oxidase (LAAO)								
12	L-Amino-acid oxidase	gi|347602454	198.5	24.0	51,439	8	*Naja atra*	3,4
Snake venom serine-protease (SVSP)								
13	Alpha- and beta-fibrinogenase OhS1	gi|387935404	52.7	5.0	28,656	1	*Ophiophagus hannah*	3
Non-enzymatic proteins								
Three finger toxins (3FTx)								
14	Cytotoxin 2; Toxin V(II)2	gi|117681	75.5	53.0	6871	1	*Naja nivea*	2,3,4,6
15	Vc-1 = cytotoxin	gi|117667	128.3	75.0	6791	1	*Naja naja*	3,4,5,6
16	Cytotoxin 2a	gi|298351637	115.1	79.0	3230	3	*Naja naja*	3,4,6
17	Cytotoxin 2; Cobramine-B	gi|117680	153.3	90.0	6763	2	*Naja naja*	4,5,6
18	Cytotoxin 9; Toxin CM-2e	gi|117725	109.9	60.0	6669	2	*Naja annulifera*	5,6
19	Cytotoxin-like basic protein	gi|85687562	100.6	34.0	7014	4	*Naja naja*	5,6
20	Cardiotoxin 8	gi|4388776	112.3	47.0	8923	0	*Naja atra*	2,6
21	Cardiotoxin isoform 1	gi|299268	180.2	58.3	6700	0	*Naja naja atra*	6
22	Long neurotoxin 1	gi|128932	172.0	66.0	7847	2	*Naja naja*	2,3,4,6
23	Chain A of α-Cobratoxin	gi|157834776	7334.0	97.2	7833	2	*Naja naja siamensis*	2,3,4,5,6
24	Cobrotoxin	gi|46397633	206.7	52.0	9262	11	*Naja kaouthia*	2,3,4,5,6
25	Cobrotoxin-C	gi|28380029	149.6	84.0	6859	8	*Naja kaouthia*	2,3,4,5,6
26	κ-cobrotoxin	gi|3334611	69.5	26.0	9815	1	*Naja atra*	5
27	Cobrotoxin-C	gi|28380028	50.5	43.0	6944	1	*Naja kaouthia*	2
28	Post synaptic alpha neurotoxin precursor	gi|2688936	51.4	33.0	9289	0	*Naja sputatrix*	2,4
29	Tryptophan-containing weak neurotoxin	gi|311033516	185.0	59.0	9915	9	*Naja kaouthia*	3,4,5,6
30	Unnamed protein product	gi|4165568	99.6	30.0	9743	0	*Naja atra*	3,4,5,6
31	Miscellaneous type neurotoxin	gi|232522	43.3	14.0	7637	1	*Naja naja*	6
32	Weak toxin CM-2	gi|136560	61.3	39.0	7033	1	*Naja haje haje*	2
33	Muscarinic toxin-like protein 3	gi|12230756	144.1	83.0	7624	0	*Naja kaouthia*	2,3,4,6
34	Muscarinic toxin-like protein 2	gi|12230755	150.5	80.0	7298	6	*Naja kaouthia*	2,3,4,5,6
35	Muscarinic toxin-like protein 1	gi|12230754	152.7	72.0	7366	3	*Naja kaouthia*	2,3,6
36	Siamenotoxin I precursor, partial	gi|164605303	114.2	47.0	9263	1	*Naja siamensis*	6
Cysteine-rich secretory proteins (CRISP)								
37	Cysteine-rich venom protein kaouthin-2	gi|485956112	201.8	40.0	26,216	7	*Naja kaouthia*	5,6
38	Chain B, crystal structure of Natrin, a snake venom crisp from Taiwan cobra	gi|85543949	1200.7	70.1	24,900	0	*Naja atra*	2,3,4,6
Nerve growth factor (NGF)								
39	Venom nerve growth factor 2	gi|82080590	171.0	39.0	27,030	1	*Naja sputatrix*	2,3,6
Kunitz-type serine protease (KSPI)								
40	Kunitz-type serine protease inhibitor	gi|125050	31.6	40.0	6371	2	*Naja naja*	2,3
Natriuretic peptides (NP)								
41	Natriuretic peptide	gi|374253733	30.6	18.0	12,915	2	*Micrurus altirostris*	1,6
Ohanin like proteins (OLP)								
42	Thaicobrin	gi|32363235	158.2	62.0	12,038	0	*Naja kaouthia*	2,3,4
Cobra venom factor (CVF)								
43	Chain D, Structure of complement C5 in complex with Cvf and Ssl7	gi|319443756	256.5	17.0	184,517	26	*Naja kaouthia*	2,3,4,6

The −10logP score, % coverage, molecular weight and homology were calculated using PEAKS 7.0 software.

11.4% in an EI *N. naja* venom sample (Table 1, Fig. 3, Supplementary Fig. S1). Notably, 1 and 6 PLA_2 isoenzymes were identified in *N. naja* venom from north-western India as well as from Sri Lanka [20], and from Pakistan [19], respectively indicating geographical variation in venom composition that may result in differences in severity and/or clinical manifestations following cobra envenomation. Notably, many of the venom toxins, for example PLA_2 isoenzymes, were found to be present in more than one cation-exchange fractions of EI *N. naja* venom (Table 1). This may be attributed to a non-specific or specific interaction of venom proteins [24–25].

AChE (~65 kDa) belongs to the ChE family of venom proteins which shows substrate specificity by hydrolyzing acetylcholine ester [48] and

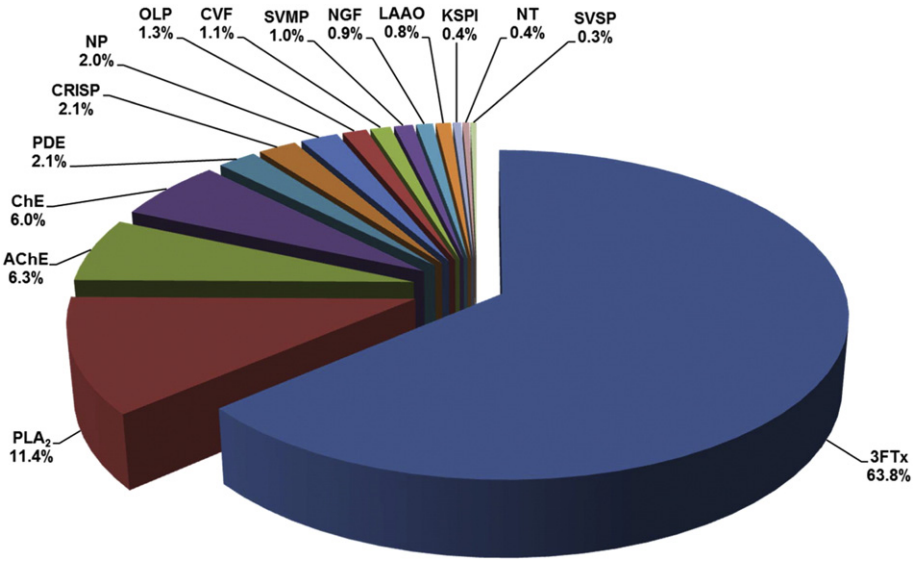

Fig. 3. Percentage composition of enzymatic and non-enzymatic protein families of EI *N. naja* venom proteome. The relative abundance of enzymatic and non-enzymatic protein families of *N. naja* venom is expressed as percent relative abundance of the total identified proteins by LC-MS/MS analysis.

maybe responsible for showing neurotoxicity [49]. By LC-MS/MS analysis, relative abundance of 2 AChE and 1 ChE enzymes in EI *N. naja* venom was found to be 6.3% and 6.0%, respectively (Fig. 3). Interestingly, proteomic studies did not reveal the presence of AChE and ChE in the venom of *N. naja* from Pakistan, north-western India or Sri Lanka [19,20,43].

Snake venom proteases (15–380 kDa) are broadly classified into two major groups—metalloproteases (SVMPs) and serine proteases (SVSPs) [50]. However, unlike viperid and crotalid venoms the proteolytic activity of elapid venoms has not been studied extensively. By biochemical analysis only a few SVMPs from the venoms of elapids such as *N. nigricollis* [51], *O. hannah* [52], *N. mocambique mocambique* [53], *N. kaouthia* [54] and *N. naja* [55] were characterized. LC-MS/MS analysis showed the occurrence of 3 SVMPs and only one SVSP (Table 1, Supplementary Fig. S1) accounting for a relative abundance of 1.0% and 0.3%, respectively of EI *N. naja* venom (Fig. 3) thus indicating that protease is a minor component of *N. naja* venom. However, to date, the presence of SVSP in *N. naja* venom has not been demonstrated by proteomic analysis and only one SVMP (NN-PF3) with a yield of 0.7% was purified and characterized from the EI *N. naja* venom [55].

LC-MS/MS analysis revealed that only one PDE enzyme accounted for 2.1% of the EI *N. naja* venom (Table 1, Fig. 3); although, there is no report on the presence of PDE in *N. naja* venom of other regions of the Indian sub-continent [19,20]. Nevertheless, the exact role of PDE enzymes in the pathophysiology of snakebite is not well understood and further studies should be directed to determine the role of this class of protein in cobra bite inflicted toxicity.

Snake venom LAAOs are high molecular weight (110–150 kDa) thermolabile flavoenzymes [56,57]. LAAOs are widely distributed in all snake venoms and proteomic analysis demonstrated the existence of LAAOs in venom of *N. sumatrana* [58], *N. haje legionis* [59], *N. kaouthia* [29] and *N. atra* [60]. The present study established the occurrence of only one LAAO isoenzyme representing 0.8% of the EI *N. naja* venom (Table 1, Fig. 3). By proteomic analysis Ali et al. [19] have also reported the presence of two LAAO isoenzymes in Pakistan *N. naja* venom. However, proteomic analysis did not reveal the presence of LAAO in the venom of *N. naja* from the north-western region of India [20].

NTs are known to be present ubiquitously in all snake venoms [61,62], suggesting that they may have some contribution in venom induced toxicity presumably by causing hemostatic dysfunction [62]. By LC-MS/MS analysis, one NT enzyme (Table 1, Supplementary Fig. S1) representing only a minor fraction (0.4%) of EI *N. naja* venom was identified (Fig. 3). Nevertheless, proteomic analyses of the *N. naja* venom samples obtained from north-western India, Sri Lanka [20] and Pakistan [19] did not report the presence of NT in cobra venom, reinstating the geographical variation in venom composition in the same species of snake.

Enzyme assay demonstrated the presence of hyaluronidase, also referred to as the 'spreading factor', in EI *N. naja* venom. However, LC-MS/MS analysis did not demonstrate the presence of a hyaluronidase enzyme in *N. naja* venom from EI (present study), north-western India, Sri Lanka [20] as well as in Pakistan [19].

3.4. Non-enzymatic proteins of EI N. naja venom

The 3FTx are the most predominant low molecular weight (6–9 kDa) components in venom of almost all elapids, the genus *Naja* included [20,29,59,63]. Despite of their structural similarity, this group of proteins exhibits diverse pharmacological effects upon envenomation [63]. Broadly, 3FTxs can be classified as—(i) neurotoxins (NTx), (ii) cytotoxins (CTx), cardiotoxins (CdTx), (iii) AChE inhibitors, (iv) non-conventional 3FTxs, and (v) platelet aggregation inhibitors [63,64]. A total of 23 3FTxs with a relative abundance of 63.8% in EI *N. naja* venom were identified by proteomic analysis (Table 1, Fig. 3, Supplementary Fig. S1). Previous proteomic studies have identified only 12, 13 and 15 3FTxs in *N. naja* venom samples from north-western India, Sri Lanka [20], and Pakistan [19], respectively.

Characterization of snake venom neurotoxins has contributed significantly to the advancement of our understanding of their biological activity and toxic manifestations of envenomation. Considering the tremendous geographical variation in neurotoxic symptoms after a cobra bite, qualitative and quantitative identification of neurotoxins present in the venom of a cobra from a particular locality will undoubtedly help in improving management of neurotoxic envenoming [65]. On the basis of their receptor selectivity, NTxs are further divided into—(i) α-neurotoxins (curaremimetic NTx) (abbreviated as αNTx), that bind to muscle (α1) nicotinic receptors and inhibit the acetylcholine from binding to the receptor, resulting in impaired neuromuscular transmission [66]; (ii) κ-neurotoxins (κNTx), that specifically bind to neuronal (α3β4) nicotinic receptors [67] thereby inhibiting transmission of nerve impulses; and (iii) muscarinic toxins (MTLP) that target muscular nicotinic receptors [68,69]. On the basis of their structure, NTxs are classified into long-chain (LNTx) and short-chain (SNTx) neurotoxins [64]. By proteomic analysis 1 LNTx, 5 cobrotoxins (CbTx), 1 αNTx, 3 weak NTx (WNTx), 1 weak toxin (WTx) and 3 MTLPs showing sequence

similarity across the genus *Naja* were identified in the EI *N. naja* venom sample (Table 1, Supplementary Fig. S1). Sintiprugnat et al. [20] have identified 1 LNTx, 3 SNTx, 1 WNTx and 1 MTLP from the venom of *N. naja* from north-western India, and 2 LNTx, 3 SNTx and 1 WNTx from the venom of *N. naja* from Sri Lanka.

CdTxs, another member of 3FTxs identified only in cobra venom, structurally resemble SNTx [70,71]. CdTxs show concentration dependent pharmacological activity; at lower concentrations they increase the heart rate, albeit at higher concentrations they kill the prey by cardiac arrest [70]. However, some of the toxins of this group exhibiting cytolysis are referred to as CTx [70]. In this study, 4 CTx and 2 CdTx were identified (Table 1, Supplementary Fig. S2). Nevertheless, *N. naja* venom from north-western India and Sri Lanka were found to contain only 6 CTx [20].

NPs are low molecular weight peptides (4–20 kDa) of snake venom [39]. Although NPs have been isolated from the venom of *Pseudonaja textilis*, *Pseudechis australis* [72], *Bungarus flaviceps* [73] and *N. atra* [74]; nevertheless, there is no report on the isolation and characterization of NP from *N. naja* venom. By proteomics analysis only one NP (Table 1, Supplementary Fig. S1), with a relative abundance of 2.0% was identified in EI *N. naja* venom (Fig. 3). However, proteomic analysis could not identify NPs in *N. naja* venom samples from Pakistan, north-western India and Sri Lanka [19,20].

Cysteine-rich secretory proteins (CRISP) having molecular weights in the range of 20–30 kDa are single chain polypeptides showing a conserved protein sequence [75]. Snake venom CRISPs exert their pharmacological effect by blocking ion channels [76,77] albeit their pathophysiology in snakebite is unknown [78]. In the present study 2 CRISPs (Table 1, Supplementary Fig. S1) with a relative abundance of 2.1% (Fig. 3) were identified in EI *N. naja* venom. However, CRISPs constitute 7.14%, 2.53% and 3.71% of *N. naja* venom from Pakistan [19], north-western India, and Sri Lanka [20], respectively.

CVF, also known as the anti-complement factor, is a high molecular weight (~150 kDa), complement-activating, multimeric protein found in venoms of elapids including *Naja* sp. [79,80]. Although CVF is non-toxic in nature; however, it interacts with the components of the complement system in the victim, thereby leading to complement activation which results in consumption of complement activity [10]. By LC-MS/MS analysis only one CVF (Table 1, Supplementary Fig. S1), with a relative abundance of 1.1% (Fig. 3) was identified in the EI *N. naja* venom proteome.

NGFs are low molecular weight monomeric (12–14 kDa) or dimeric proteins (25–28 kDa) of snake venom that are known to support neuronal maintenance and survival [81]. Occurrence of a single isoform of NGF in venoms of *N. naja* from north-western India, Sri Lanka [20] and Pakistan [19] was demonstrated by proteomic analyses. By LC-MS/MS study, only one NGF (Table 1, Supplementary Fig. S1) with a relative abundance of 0.9%, was identified in EI *N. naja* venom (Fig. 3).

The KSPIs are an important class of low molecular mass (6–7 kDa) venom peptides reported to occur in Viperidae and Elapidae venoms [23,82–85]. KSPIs are responsible for the inhibition of one or more specific serine proteases such as trypsin, chymotrypsin, elastase, thrombin, and activated factor X and they exhibit a wide array of pharmacological effects [23,24,83–86]. In this study, only 1 KSPI (Table 1, Supplementary Fig. S1) constituting 0.4% of total venom was identified in EI *N. naja* venom (Fig. 3). Our result corroborates well with previous findings showing occurrence of low percentage of KSPI in *N. naja* venom from north-western India (0.08%) as well as in Sri Lanka (0.33%) [20].

Vespryn or OLP is a relatively new class of low molecular weight (~12 kDa) snake venom protein first identified in *O. hannah* venom [87]. By proteomics analysis OLP could not be identified in Pakistan, north-western India and Sri Lankan *N. naja* venom samples [19,20]. By LC-MS/MS analysis only one OLP showing 62% sequence coverage to Ohanin from *N. kaouthia* venom was identified in EI *N. naja* venom (Table 1, Supplementary Fig. S1). The relative abundance of OLP was found to be 1.3% suggesting that it is also a very minor component of EI *N. naja* venom (Fig. 3).

3.5. Correlation of venom composition with biochemical and pharmacological properties of EI N. naja venom

Crude *N. naja* venom from Nadia district of West Bengal, EI showed profound phospholipid hydrolytic (PLA_2) activity (Table 2) which substantiates the LC-MS/MS data (Table 1, Fig. 3) and our previous observations on membrane phospholipid hydrolysis [2,45,88,89]. Elapid venoms in general exhibit low proteolytic activity; however, the exceptions are *O. hannah* and *Pseudechis collettii* venom samples [90]. Proteomic analysis indicated that proteases comprise only a small proportion of EI *N. naja* venom (Fig. 3) which was also evident from a biochemical assay of protease enzyme (Table 2). Crude venom demonstrated weak proteolytic activity against fibrin and fibrinogen (Table 2) advocating that *N. naja* venom from EI is devoid of appreciable proteolytic activity against the above protein substrates [2,15].

EI *N. naja* venom also demonstrated feeble LAAO enzyme activity (Table 2) which is in close agreement with proteomic identification of a relatively low proportion (0.8%) of this class of enzyme in crude venom (Fig. 3). Nonetheless, the pathophysiological significance of a low quantity of LAAO in EI *N. naja* venom may not be ignored [56]. Crude EI *N. naja* venom showed ATPase, ADPase and AMPase activities; nevertheless, the latter enzyme activity was found to be the highest (Table 2) which is according to our previous observation [3]. EI *N. naja* venom also demonstrated hyaluronidase activity (Table 2); however, LC-MS/MS analysis did not identify ADPase, and ATPase enzymes in EI *N. naja* venom which may presumably be due to the non-existence of sequences of these enzymes in snake venom protein databases.

EI *N. naja* venom demonstrated considerable AChE activity (Table 2) and this finding corroborated well with our earlier report [3] as well as proteomic analysis of the venom under study (Table 1, Fig. 3). By biochemical assay, EI *N. naja* venom demonstrated negligible PDE activity

Table 2
Summary of enzymatic activities of EI *Naja naja* venom at the tested dose of 20 μg/ml.

Biochemical assays	Activity (units/mg)
Phospholipase A_2[a]	2017.5 ± 0.011
Fibrinogenolytic[b]	10.0 ± 0.001
Fibrinolytic[b]	20.1 ± 0.002
LAAO[c]	17.7 ± 0.003
ATPase[d]	5224.0 ± 0.002
ADPase[d]	3770.8 ± 0.010
AMPase[d]	4211.8 ± 0.010
Hyaluronidase[e]	62.0 ± 0.010
AChE[f]	4105.8 ± 0.263
PDE[g]	1.3 ± 0.001
TAME[h]	12.3 ± 0.001
BAEE[i]	51.3 ± 0.01

Values are mean ± S.D. of triplicate determinations.
[a] Unit activity is defined as the amount of protein which produces a decrease in 0.01 absorbance in 10 min at 740 nm.
[b] Unit activity is defined as 1.0 μg of tyrosine equivalent liberated per min per ml of enzyme.
[c] Unit activity is defined as nmol kynurenic acid produced/min under the assay conditions.
[d] Unit activity is defined as μM Pi released per min.
[e] Unit activity is defined as the relative decrease in turbidity reduction unit (TRU) per min per mg of protein in 30 min of reaction at 37 °C.
[f] Unit activity is defined as the amount of protein which hydrolysed 0.01 mg of acetylcholine bromide in 1 min in 3 ml of 0.0092 M acetylcholine bromide;
[g] Unit activity is defined as μmol of *p*-nitrophenol released per min (using 17,600 as molar extinction coefficient).
[h] Unit activity is defined as increase of 0.01 absorbance unit at 244 nm during the first 10 min of the reaction at 37 °C.
[i] Unit activity is defined as increase of 0.01 absorbance unit at 254 nm during the first 10 min of the reaction at 37 °C.

(Table 2) which is correlated to proteomic analysis showing occurrence of a low proportion of this enzyme (2.1%) in crude venom (Table 1, Fig. 3, Supplementary Fig. S1). EI *N. naja* venom demonstrated TAME as well as BAEE-esterase activities (Table 2) nonetheless, LC-MS/MS analysis of the venom fractions did not identify any esterase enzyme (Table 1, Supplementary Fig. S1). In general, esterase activity is shown by SVSPs [30,91]; however, esterase activity of the unique SVSP (gi|387935404) identified in EI *N. naja* venom is unknown.

The distress of crude *N. naja* venom on a hemostasis system was rarely explored. An adult Indian cobra contains 200–225 mg of venom (personal communication from Mr. D. Mitra, in-charge, Calcutta Snake Park, Kolkata). If we consider a full bite from a cobra, the concentration of injected venom will be equivalent to ~40 μg/ml in an adult human blood. EI *N. naja* venom delayed the clotting time of whole blood from 68.5 ± 2.3 to 86.0 ± 2.9 s (mean ± SD, $n = 3$) at the tested dose of 40 μg/ml. It dose-dependently prolonged the Ca^{2+} clotting time (Fig. 4A), prothrombin time (PT) and activated partial thromboplastin time (APTT) (Fig. 4B) of PPP suggesting that EI *N. naja* venom under *in vitro* conditions exerts anticoagulant action by interfering with both extrinsic and intrinsic pathways. The above findings contradicted the previous reports demonstrating in *in vitro* conditions *N. naja* venom from EI exerted pro-coagulant activity owing to containing prothrombin activating enzyme(s) [15,91]. EI *N. naja* venom at a maximum dose of 40 μg/ml did not demonstrate prothrombin activation or thrombin-like (fibrinogen clotting) activity (data not shown). Further, tandem mass spectrometry analysis did not show occurrence of prothrombin activator or thrombin-like protease in the venom under study (Table 1) which supports our observation.

Absence of appreciable fibrin(ogen)olytic activity in EI *N. naja* venom unambiguously suggests that it exerts anticoagulant activity by targeting other factor(s) of the blood coagulation cascade. The EI *N. naja* venom at the tested doses (10 and 40 μg/ml) did not show FXa inhibition activity (Supplementary Fig. S2). Noteworthy, to date no FXa inhibitor is reported from *N. naja* venom. This result is suggestive of the fact that an anticoagulant mechanism of *N. naja* venom by inhibition of FXa is unlikely.

Thrombin, a key regulator of blood coagulation cascade converts fibrinogen to fibrin thus facilitatingblood coagulation. EI *N. naja* venom dose-dependently inhibited the fibrinogen clotting activity of thrombin (Fig. 4C) suggesting that thrombin inhibition is a predominant non-enzymatic mechanism of its anticoagulant action [21]. Because the venom under study exhibited feeble fibrinogenolytic activity (Table 2, Fig. 3), therefore fibrinogen degradation may not contribute to the observed *in vitro* anticoagulant effect of *N. naja* venom. An acidic PLA_2 (accession no. gi|129514) identified in this *N. naja* venom (Table 1) showed sequence similarity with a major anticoagulant PLA_2 enzyme ($NnPLA_2$-I) purified from Burdwan (EI) *N. naja* venom [21]. Similarly, another acidic PLA_2 enzyme (accession no. gi|24638468) identified in EI *N. naja* venom

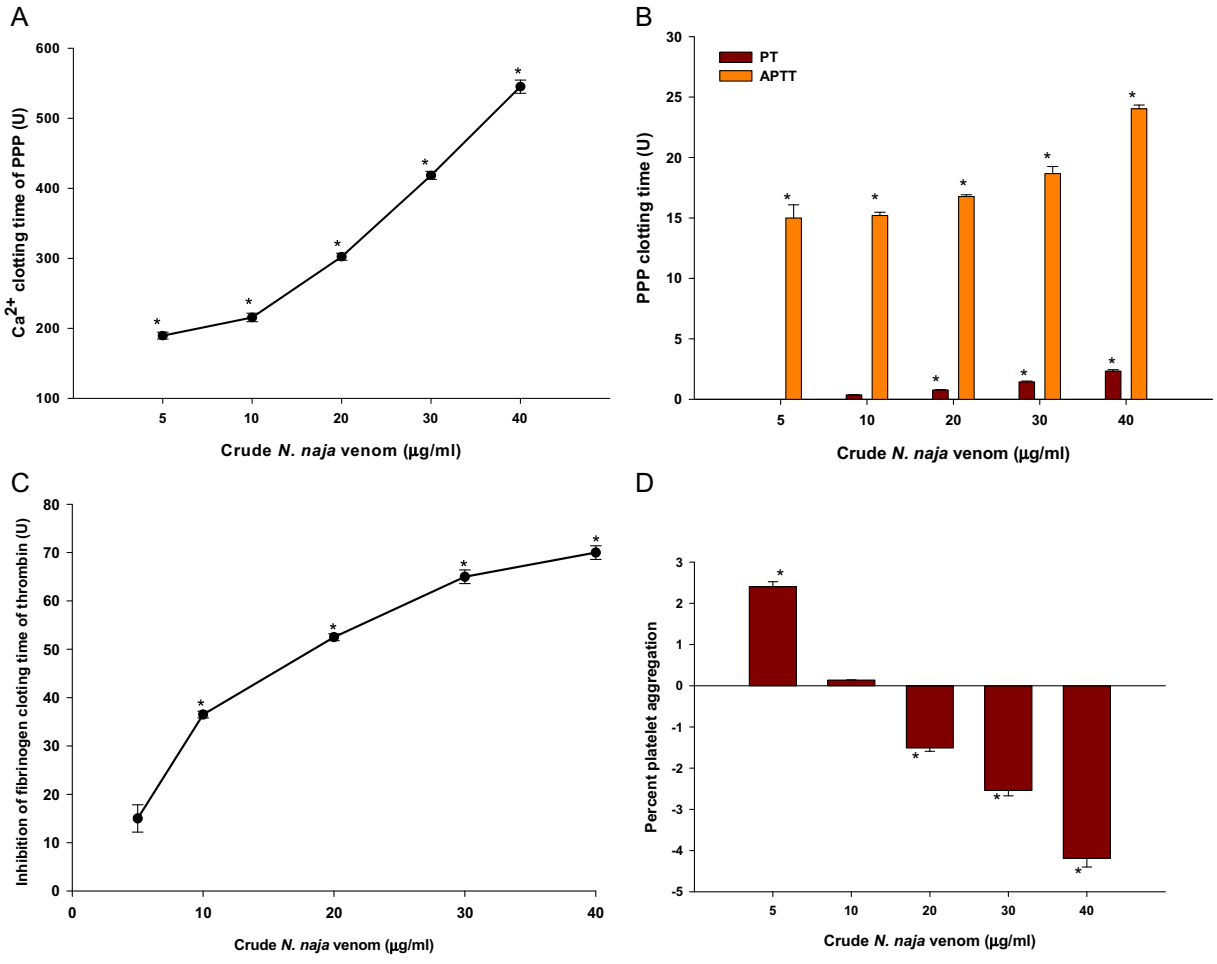

Fig. 4. Dose-dependent (5 to 40 μg/ml) *in vitro* pharmacological properties of EI *N. naja* venom. (A) Calcium-clotting time of PPP, (B) PT and APTT of PPP. The Ca^{2+} clotting time of control PPP was recorded as 180.1 ± 6.2 s, whereas the PT and APTT value of the control plasma was 14.0 ± 0.3 s and 38.3 ± 0.3 s, respectively. (C) Inhibition of fibrinogen clotting time of thrombin by EI *N. naja* venom. Fibrinogen clotting time of control thrombin was determined at 117.5 ± 3.5 s. One unit of inhibitory activity is defined as 1 s increase in the fibrinogen clotting time of thrombin treated with venom as compared to fibrinogen clotting time of untreated thrombin (control). (D) Dose-dependent platelet modulating effect of EI *N. naja* venom against platelet rich plasma (PRP). The platelet modulation in the presence or absence of crude *N. naja* venom is expressed in terms of percent aggregation of platelets in PRP. Values are mean ± SD of triplicate determinations. Significance of difference $^*p < 0.05$.

(Table 1) shared sequence similarity with an anticoagulant PLA_2 enzyme isolated from Egyptian cobra *N. haje* venom [92]. Both the above PLA_2 enzymes exerted anticoagulant activity *via* thrombin inhibition [21,92] reinforcing that this is the principle mechanism of anticoagulation by EI *N. naja* venom. In addition, anticoagulant activity may also be attributed to plasma phospholipid hydrolytic activity of the PLA_2 isoenzymes identified in EI *N. naja* venom (Tables 1 and 2, Fig. 3) [2,21]. Furthermore, 5′-NTs and KSPIs identified in an EI *N. naja* venom sample (Table 1, Fig. 3, Supplementary Fig. S1) may also significantly contribute to its anticoagulant property [23,62,85].

Crude *N. naja* venom demonstrated dose-dependent aggregation or de-aggregation (anti-platelet activity) of PRP; at a lower dose (5 μg/ml), it caused aggregation of PRP whereas at higher concentrations (20 to 40 μg/ml), it induced de-aggregation of PRP (Fig. 4D). This result advocates that platelet de-aggregation is also a precise mechanism to prolong the blood coagulation by EI *N. naja* venom [12]. Various proteins of cobra venom such as PLA_2 [21], SVMP [55], LAAO [56], NT [62], and 3FTxs [63,64] were shown as platelet aggregation inhibitors; by proteomic analysis several of these classes of protein were identified in EI *N. naja* venom (Table 1, Figs. 3A, B). For example, $NnPLA_2$-I, a major PLA_2 enzyme from Burdwan (EI) *N. naja* venom was shown to modulate the platelet function in a dose-dependent manner [21]; proteomic analysis ascertained the presence of this enzyme in the venom under study. Similarly, Kaouthiagin (gi|32469675) like hemorrhagic SVMP present in the EI *N. naja* venom (Table 1, Supplementary Fig. S1) may also be responsible for specific cleavage of human von Willebrand factor (VWF) thereby inhibiting platelet aggregation [93]. The high lethal potency (LD_{50}) of *N. naja* venom samples from three neighboring districts of West Bengal, EI was estimated in the range of 0.4 to 0.63 mg/kg body weight of mice suggesting predominance of highly toxic enzymes and non-enzymatic 3FTxs (such as CTx and NTxs) in these cobra venom samples [2], which is in close agreement with proteomic analysis of EI *N. naja* venom proteome (Table 1, Figs. 3A, B).

There is no published clinical data on cobra envenomation from eastern India; however, a few hospital based studies showed that neurological symptoms, rapid respiratory paralysis, and loss of consciousness are the major pathophysiological symptoms in cobra bite patients from Maharashtra, western India [7,41]. Identical symptoms including neurotoxicity, weakening and decreased movements of hind limbs, and difficulty in breathing (respiratory paralysis) were also observed in mice treated with cobra venom samples from EI [3]. The above clinical manifestations/biological activity (neurotoxicity) can be attributed to occurrence of abundant 3FTxs (63.8%) in an EI *N. naja* venom sample (Table 1, Fig. 3) [65,94]. NTxs, a type of 3FTxs, have been reported to bind almost irreversibly and rapidly to the nAchRs which may not be reversed by antivenom treatment [65]; therefore, the occurrence of a relatively high proportion of 3FTxs in EI *N. naja* venom (Table 1) as compared to *N. naja* venom from other locales of the Indian subcontinent [20] might be a great concern for efficient treatment of cobra bite patients in EI.

In addition, CdTx also inflicts circulatory and respiratory failure, cardiac arrhythmias, heart block, and ultimately cardiac arrest in cobra envenomed victims [65,95]. Further, a considerable proportion of AChE (6.3%) and ChE (6.0%) enzymes identified in *N. naja* venom from the Nadia district of EI (Tables 1, 2; Fig.3A) may also be responsible for inflicting neurotoxicity in victims or in experimental animals [96]. Noteworthy, anti-ChE therapy reversed the neuromuscular dysfunction of cobra envenomed patients [7] advocating the role of AchE and ChE in venom induced neurotoxicity. Although Ohanin-like protein (OLP) represents a minor component of *N. naja* venom from Nadia, EI (Table 1, Fig. 3); nevertheless, it may also contribute significantly to retard the locomotion and induction of hyperalgesia [87] in EI *N. naja* venom-treated experimental mice [2,3]. The biological function of OLP and predominated 3FTxs of *N. naja* venom may be attributed to subduing the agile mammalian prey before being swallowed by the predator.

Previous studies demonstrated that rodents injected with EI *N. naja* venom resulted in damage to cardiac and skeletal muscles, liver, and kidney tissues [2,97]. In addition to myotoxicity, oedema-induction by EI *N. naja* venom was also reported [2,3,97]. All of the above pharmacological effects can be well correlated with the occurrence of significant amounts (11.4%) of PLA_2 enzymes (Tables 1, 2) in EI *N. naja* venom under study [12,31,98,99].

Proteomic and biochemical analyses provide an overall view of EI *N. naja* venom inflicted pharmacological activity and toxicity. Following a bite, hyaluronidase helps the spreading of cobra venom by damaging the extracellular matrix of the tissues thereby allowing the systemic influx of toxic venom components [100]. Existence of a high percentage of 3FTxs (post-synaptic NTx, CTx and CdTx) in *N. naja* venom from Nadia, EI (Table 1, Supplementary Fig. 1) might be accountable for paralysis and eventually cardiac arrest to cause the death of the victims or experimental animals after systemic envenomation [2,20,63,95]. In addition, myotoxic and cytotoxic PLA_2s as well as CTxs inflict local edema, blistering, and tissue necrosis [6,97] and in combination they are also accountable for damage to liver and cardiac tissues [2,97]. The primary function of snake venom is to subdue large, agile prey such as rodents (rats/mice) or rabbit before being swallowed [85]. Therefore, abundant low molecular mass basic 3FTxs act synergistically with other proteins of cobra venom such as PLA_2 [63,101] to rapidly paralyze small mammal prey followed by its death by cardiac arrest and respiratory paralysis within minutes of envenomation.

Although the effect of *N. naja* venom on blood coagulopathy has not been well documented in an envenomed human [102]; nonetheless, clinical manifestations like thrombocytopenia, spontaneous bleeding and positive 20 minute-whole blood clotting time (20WBCT) observed in a cobra envenomed human [6, personal communication by Dr. D. Punde, Punde Hospital, Maharashtra] may be inflicted by the presence of a high proportion of anticoagulant and antiplatelet proteins such as PLA_2, SVMP, and NT in *N. naja* venom (Table 1, Figs. 4A–D) [21,55,103].

The hypotension observed in *N. naja* bite victims [104] may be attributed to the occurrence of NPs identified in EI *N. naja* venom (Table 1) as these proteins are reported to affect the pressure-volume homeostasis by causing vasodilation and increasing water-electrolyte excretion in experimental animals [74]. Due to these complex and expeditious interplay of various cobra venom components, management of victims has always been a challenging task for the attending physicians.

4. Conclusion

The analysis of proteome composition of the eastern India *N. naja* venom revealed the occurrence of 43 enzymatic and non-enzymatic proteins which are distributed over 15 families of snake venom proteins. By LC-MS/MS analysis, the occurrence of AChEs, PDEs, ChEs and a SVSP in *N. naja* venom is reported for the first time; however, by proteomic analysis ATPase, ADPase, and hyaluronidase enzymes detected by enzymatic analysis could not be identified in this venom. The present study suggested that ~75% of the venom proteome was composed of low molecular weight (<18 kDa) non-enzymatic components (3FTxs, KSPIs, NPs and OLP) as well as PLA_2 isoenzymes and together they are accountable for exerting the systemic effect of envenomation. In a nutshell, the complex array of identified cobra venom toxins through their diverse biochemical properties and pharmacological activities are responsible for inducing a multitude of clinical manifestations in cobra envenomed victims.

Supplementary data to this article can be found online at http://dx.doi.org/10.1016/j.jprot.2016.12.018.

Conflict of interest

None.

Acknowledgements

The authors thank Dr. Vikash Kumar, mass spectrometry facility, C-CAMP, NCBS, Bangalore for LC-MS/MS analysis. SD and TI are recipients of the DST-INSPIRE Fellowship. AC is a recipient of a Junior Research fellowship award from a DBT Indo-Russia project grant. BK and AP are recipients of a Junior Research fellowship award from a DBT U-Excel project grant. This project received financial support from the DBT, New Delhi sponsored Unit of Excellence in Biotechnology in NER of India grant (BT/412/NE/U-Excel/2013) to AKM.

References

[1] B. Mohapatra, D.A. Warrell, W. Suraweera, P. Bhatia, N. Dhingra, R.M. Jotkar, P.S. Rodriguez, K. Mishra, R. Whitaker, P. Jha, Snakebite mortality in India: a nationally representative mortality survey, PLoS Negl. Trop. Dis. 5 (4) (2011), e1018. .
[2] A.K. Mukherjee, C.R. Maity, The composition of *Naja naja* venom samples from three districts of West Bengal, India, Comp. Biochem. Physiol. A Mol. Integr. Physiol. 119 (2) (1998) 621–627.
[3] A.K. Mukherjee, C.R. Maity, Biochemical composition, lethality and pathophysiology of venom from two cobras—*Naja naja* and *N. kaouthia*, Comp. Biochem. Physiol. B: Biochem. Mol. Biol. 131 (2) (2002) 125–132.
[4] World Health Organization, WHO, WHO Guidelines for the Production, Control and Regulation of Snake Antivenom Immunoglobulins, WHO, Geneva, 2010 134.
[5] H.S. Bawaskar, P.H. Bawaskar, Envenoming by the common krait (*Bungarus caeruleus*) and Asian cobra (*Naja naja*): clinical manifestations and their management in a rural setting, Wilderness Environ. Med. 15 (2004) 257–266.
[6] S.A.M. Kularatne, B.D.S.S. Budagoda, I.B. Gawarammana, W.K.S. Kularatne, Epidemiology, clinical profile and management issues of cobra (*Naja naja*) bites in Sri Lanka: first authenticated case series, Trans. R. Soc. Trop. Med. Hyg. 103 (9) (2009) 924–930.
[7] S. Raut, P. Raut, Snake bite management experience in western Maharastra (India), Toxicon 103S (2015) 89–90.
[8] S. Nirthanan, M.C.E. Gwee, Three-finger and alpha-neurotoxins and the nicotinic acetylcholine receptor, forty years on, J. Pharm. Sci. 94 (1) (2004) 1–17.
[9] C. Montecucco, J.M. Gutiérrez, B. Lomonte, Cellular pathology induced by snake venom phospholipase A_2 myotoxins and neurotoxins: common aspects of their mechanisms of action, Cell. Mol. Life Sci. 65 (18) (2008) 2897–2912.
[10] C.W. Vogel, R. Bredehorst, D.C. Fritzinger, T. Grunwald, P. Ziegelmüller, M.A. Kock, Structure and Function of Cobra Venom Factor, the Complement-activating Protein in Cobra Venom, Natural Toxins, 2, Springer, US, 1996 97–114.
[11] J.M. Gutiérrez, A.V. Rucavado, Snake venom metalloproteinases: their role in the pathogenesis of local tissue damage, Biochimie 82 (9) (2000) 841–850.
[12] R.M. Kini, Anticoagulant proteins from snake venoms: structure, function and mechanism, Biochem. J. 397 (3) (2006) 377–387.
[13] R. Thangam, P. Gunasekaran, K. Kaveri, G. Sridevi, S. Sundarraj, M. Paulpandi, S. Kannan, A novel disintegrin protein from *Naja naja* venom induces cytotoxicity and apoptosis in human cancer cell lines in vitro, Process Biochem. 47 (8) (2012) 1243–1249.
[14] M. Li Lee, I. Chung, S. Yee Fung, M.S. Kanthimathi, N. Hong Tan, Antiproliferative activity of king cobra (*Ophiophagus hannah*) venom l-amino acid oxidase, Basic Clin. Pharmacol. Toxicol. 114 (4) (2014) 336–343.
[15] R. Shashidharamurthy, D.K. Jagadeesha, K.S. Girish, K. Kemparaju, Variation in biochemical and pharmacological properties of Indian cobra (*Naja naja naja*) venom due to geographical distribution, Mol. Cell. Biochem. 229 (1–2) (2002) 93–101.
[16] J.J. Calvete, P. Juárez, L. Sanz, Snake venomics. Strategy and applications, J. Mass Spectrom. 42 (11) (2007) 1405–1414.
[17] J.J. Calvete, L. Sanz, Y. Angulo, B. Lomonte, J.M. Gutiérrez, Venoms, venomics, antivenomics, FEBS Lett. 583 (11) (2009) 1736–1743.
[18] S. Li, J. Wang, X. Zhang, Y. Ren, N. Wang, K. Zhao, X. Chen, C. Zhao, X. Li, J. Shao, J. Yin, M.B. West, N. Xu, S. Liu, Proteomic characterization of two snake venoms: *Naja naja atra* and *Agkistrodon halys*, Biochem. J. 384 (1) (2004) 19–127.
[19] S.A. Ali, D.C. Yang, T.N. Jackson, E.A. Undheim, I. Koludarov, K. Wood, B.G. Fry, Venom proteomic characterization and relative antivenom neutralization of two medically important Pakistani elapid snakes (*Bungarus sindanus* and *Naja naja*), J. Proteome 89 (2013) 15–23.
[20] K. Sintiprungrat, K. Watcharatanyatip, W.D.S.T. Senevirathne, P. Chaisuriya, D. Chokchaichamnankit, C. Srisomsap, K. Ratanabanangkoon, A comparative study of venomics of *Naja naja* from India and Sri Lanka, clinical manifestations and antivenomics of an Indian polyspecific antivenom, J. Prot. 132 (2016) 131–143.
[21] S. Dutta, D. Gogoi, A.K. Mukherjee, Anticoagulant mechanism and platelet deaggregation property of a non-cytotoxic, acidic phospholipase A_2 purified from Indian cobra (*Naja naja*) venom: inhibition of anticoagulant activity by low molecular weight heparin, Biochimie 110 (2015) 93–106.
[22] O.H. Lowry, N.J. Rosebrough, A.L. Farr, R.J. Randall, Protein measurement with the Folin phenol reagent, J. Biol. Chem. 193 (1) (1951) 265–275.
[23] A.K. Mukherjee, B. Kalita, R. Thakur, Two acidic, anticoagulant PLA_2 isoenzymes purified from the venom of monocled cobra *Naja kaouthia* exhibit different potency to inhibit thrombin and factor Xa via phospholipids independent, non-enzymatic mechanism, PLoS One 9 (8) (2014), e101334.
[24] A.K. Mukherjee, S.P. Mackessy, S. Dutta, Characterization of a Kunitz-type protease inhibitor peptide (Rusvikunin) purified from *Daboia russelii russelii* venom, Int. J. Biol. Macromol. 67 (2014) 154–162.
[25] A.K. Mukherjee, B. Kalita, S.P. Mackessy, A proteomics analysis of Pakistan *Daboia russelii russelii* venom and assessment of potency of Indian polyvalent and monovalent antivenom, J. Prot. 144 (2016) 73–86.
[26] A. Chapeaurouge, M.A. Reza, S.P. Mackessy, P.C. Carvalho, R.H. Valente, A. Teixeira-Ferreira, J. Perales, Q. Lin, R.M. Kini, Interrogating the venom of the viperid snake *Sistrurus catenatus edwardsii* by a combined approach of electrospray and MALDI mass spectrometry, PLoS One 10 (5) (2015), e0092091. .
[27] H. Choi, D. Fermin, A.I. Nesvizhskii, Significance analysis of spectral count data in label-free shotgun proteomics, Mol. Cell. Proteomics 7 (2008) 2373–2385.
[28] R.H. Ziganshin, S.I. Kovalchuk, G.P. Arapidi, V.G. Starkov, A.N. Hoang, T.T.T. Nguyen, K.C. Nguyen, B.B. Shoibonov, V.I. Tsetlin, Y.N. Utkin, Quantitative proteomic analysis of Vietnamese krait venoms: neurotoxins are the major components in *Bungarus multicinctus* and phospholipases A_2 in *Bungarus fasciatus*, Toxicon 107 (2015) 197–209.
[29] K.Y. Tan, C.H. Tan, S.Y. Fung, N.H. Tan, Venomics, lethality and neutralization of *Naja kaouthia* (monocled cobra) venoms from three different geographical regions of Southeast Asia, J. Prot. 120 (2015) 105–125.
[30] A.K. Mukherjee, The pro-coagulant fibrinogenolytic serine protease isoenzymes purified from *Daboia russelii russelii* venom coagulate the blood through factor V activation: role of glycosylation on enzymatic activity, PLoS One 9 (2) (2014), e86823. .
[31] R. Doley, A.K. Mukherjee, Purification and characterization of an anticoagulant phospholipase A_2 from Indian monocled cobra (*Naja kaouthia*) venom, Toxicon 41 (1) (2003) 81–91.
[32] H. Weissbach, A.V. Robertson, B. Witkop, S. Udenfriend, Rapid spectrophotometric assays for snake venom L-amino acid oxidase based on the oxidation of L-kynurenine or 3,4-dehydro-L-proline, Anal. Biochem. 1 (1960) 286–290.
[33] A.K. Mukherjee, S.K. Ghosal, C.R. Maity, Some biochemical properties of Russell's viper (*Daboia russelli*) venom from Eastern India: correlation with clinico-pathological manifestation in Russell's viper bite, Toxicon 38 (2) (2000) 163–175.
[34] L. Cariani, L. Thomas, J. Brito, J.R. del Castillo, Bismuth citrate in the quantification of inorganic phosphate and its utility in the determination of membrane-bound phosphatases, Anal. Biochem. 324 (1) (2004) 79–83.
[35] S. Pukrittayakamee, D.A. Warrell, V. Desakorn, A.J. McMichael, N.J. White, D. Bunnag, The hyaluronidase activities of some Southeast Asian snake venoms, Toxicon 26 (7) (1988) 629–637.
[36] A.K. Mukherjee, S.P. Mackessy, Biochemical and pharmacological properties of a new thrombin-like serine protease (Russelobin) from the venom of Russell's Viper (*Daboia russelii russelii*) and assessment of its therapeutic potential, Biochim. Biophys. Acta 1830 (6) (2013) 3476–3488.
[37] G.L. Ellman, K.D. Courtney, V. Andres Jr., R.M. Feather-Stone, A new and rapid colorimetric determination of acetylcholinesterase activity, Biochem. Pharmacol. 7 (1961) 88–95.
[38] E. Sulkowski, M. Laskowski, Inactivation of 5′-nucleotidase in commercial preparations of venom exonuclease (phosphodiesterase), Biochim. Biophys. Acta Nucl. Acids Prot. Syn. 240 (3) (1971) 443–447.
[39] R. Thakur, P. Chattopadhyay, S.S. Ghosh, A.K. Mukherjee, Elucidation of procoagulant mechanism and pathophysiological significance of a new prothrombin activating metalloprotease purified from *Daboia russelii russelii* venom, Toxicon 100 (2015) 1–12.
[40] B. Bednar, C. Condra, R.J. Gould, T.M. Connolly, Platelet aggregation monitored in a 96-well microplate reader is useful for evaluation of platelet agonists and antagonists, Thromb. Res. 51 (1995) 453–463.
[41] D.P. Punde, Management of snake-bite in rural Maharashtra: a 10-year experience, Natl Med. J. India 18 (2005) 71–75.
[42] R.J. Pedro, D.E. Arnold, Y. Clemmer, J.P. Li, Q. Reilly, H. Sheng, Z. Tang, R. Xun, P. Zeng, Radivojac, Fast and accurate identification of semi-tryptic peptides in shotgun proteomics, Bioinformatics 24 (2008) 102–109.
[43] C.M. Modahl, R. Doley, R.M. Kini, Venom analysis of long-term captive Pakistan cobra (*Naja naja*) populations, Toxicon 55 (2) (2010) 612–618.
[44] B. Lomonte, A. Tarkowski, U. Bagge, L.A. Hanson, Neutralization of the cytolytic and myotoxic activities of phospholipases A_2 from *Bothrops asper* snake venom by glycosaminoglycans of the heparin/heparan sulfate family, Biochem. Pharmacol. 47 (1994) 1509–1518.
[45] R. Doley, G.F. King, A.K. Mukherjee, Differential hydrolysis of erythrocyte and mitochondrial membrane phospholipids by two phospholipase A_2 isoenzymes (NK-PLA_2-I and NK-PLA_2-II) from the venom of the Indian monocled cobra *Naja kaouthia*, Arch. Biochem. Biophys. 425 (1) (2004) 1–13.
[46] R. Shashidharamurthy, K. Kemparaju, A neurotoxic phospholipase A_2 variant: isolation and characterization from eastern regional Indian cobra (*Naja naja*) venom, Toxicon 47 (7) (2006) 727–733.
[47] D. Saikia, N.K. Bordoloi, P. Chattopadhyay, S. Choklingam, S.S. Ghosh, A.K. Mukherjee, Differential mode of attack on membrane phospholipids by an acidic phospholipase A_2 (RVVA-PLA_2-I) from *Daboia russelli* venom, Biochim. Biophys. Acta Biomembr. 1818 (12) (2012) 3149–3157.
[48] Y. Frobert, C. Créminon, X. Cousin, M.H. Rémy, J.M. Chatel, S. Bon, J. Grassi, Acetylcholinesterases from Elapidae snake venoms: biochemical, immunological and enzymatic characterization, Biochim. Biophys. Acta Protein Struct. Mol. Enzymol. 1339 (2) (1997) 253–267.
[49] R. Raba, A. Aaviksaar, M. Raba, J. Siigur, Cobra venom acetylcholinesterase, Eur. J. Biochem. 96 (1) (1979) 151–1580.
[50] R. Thakur, A.K. Mukherjee, A brief appraisal on Russell's Viper venom (*Daboia russelii russelii*) proteinases, Snake Venom, Springer, Netherlands 2015, pp. 1–18.

[51] H.J. Evans, Purification and properties of a fibrinogenase from the venom of *Naja nigricollis*, Biochim. Biophys. Acta Gen. Subj. 802 (1) (1984) 49–54.
[52] Y. Yamakawa, T. Omori-Satoh, A protease from the venom of king cobra (*Ophiophagus hannah*): purification, characterization and substrate specificity on oxidized insulin B-chain, Toxicon 26 (1988) 1145–1155.
[53] C.M. Ward, D.V. Vinogradov, R.K. Andrews, M.C. Berndt, Characterization of mocarhagin, a cobra venom metalloproteinase from *Naja mocambique mocambique*, and related proteins from other Elapidae venoms, Toxicon 34 (10) (1996) 1203–1206.
[54] J. Hamako, T. Matsui, S. Nishida, S. Nomura, Y. Fujimura, M. Ito, K. Titani, Purification and characterization of kaouthiagin, a von Willebrand factor-binding and -cleaving metalloproteinase from *Naja kaouthia* cobra venom, Thromb. Haemost. 80 (1998) 499–505.
[55] D.K. Jagadeesha, K.S. Girish, K. Kemparaju, A non-toxic anticoagulant metalloprotease: purification and characterization from Indian cobra (*Naja naja naja*) venom, Toxicon 40 (6) (2002) 667–675.
[56] X.Y. Du, K.J. Clemetson, Snake venom L-amino acid oxidases, Toxicon 40 (6) (2002) 659–665.
[57] M. Samel, K. Tõnismägi, G. Rönnholm, H. Vija, J. Siigur, N. Kalkkinen, E. Siigur, L-Amino acid oxidase from *Naja naja oxiana* venom, Comp. Biochem. Physiol. B: Biochem. Mol. Biol. 149 (4) (2008) 572–580.
[58] M.K.K. Yap, S.Y. Fung, K.Y. Tan, N.H. Tan, Proteomic characterization of venom of the medically important Southeast Asian *Naja sumatrana* (Equatorial spitting cobra), Actatropica 133 (2014) 15–25.
[59] I. Malih, T.Y. Tee, R. Saile, N. Ghalim, I. Othman, Proteomic analysis of Moroccan cobra *Naja haje legionis* venom using tandem mass spectrometry, J. Prot. 96 (2014) 240–252.
[60] H.W. Huang, B.S. Liu, K.Y. Chien, L.C. Chiang, S.Y. Huang, W.C. Sung, W.G. Wu, Cobra venom proteome and glycome determined from individual snakes of *Naja atra* reveal medically important dynamic range and systematic geographic variation, J. Prot. 128 (2015) 92–104.
[61] S.D. Aird, Ophidian envenomation strategies and the role of purines, Toxicon 40 (4) (2002) 335–393.
[62] B.L. Dhananjaya, A. Nataraju, R. Rajesh, C.R. Gowda, B.K. Sharath, B.S. Vishwanath, C.J. D'Souza, Anticoagulant effect of *Naja naja* venom 5′ nucleotidase: demonstration through the use of novel specific inhibitor, vanillic acid, Toxicon 48 (4) (2006) 411–421.
[63] Y.N. Utkin, Three-finger toxins, a deadly weapon of elapid venom—milestones of discovery, Toxicon 62 (2013) 50–55.
[64] R.M. Kini, R. Doley, Structure, function and evolution of three-finger toxins: mini proteins with multiple targets, Toxicon 56 (6) (2010) 855–867.
[65] U.K. Ranawaka, D.G. Lalloo, H.J. de Silva, Neurotoxicity in snakebite—the limits of our knowledge, PLoS Negl. Trop. Dis. 7 (10) (2013), e2302. .
[66] J.P. Changeux, The TiPS lecture. The nicotinic acetylcholine receptor: an allosteric protein prototype of ligand-gated ion channels, Trends Pharmacol. Sci. 11 (12) (1990) 485–492.
[67] G.A. Grant, V.A. Chiappinelli, kappa-Bungarotoxin: complete amino acid sequence of a neuronal nicotinic receptor probe, Biochemist 24 (6) (1985) 1532–1537.
[68] V.V. Kukhtina, C. Weise, T.A. Muranova, V.G. Starkov, P. Franke, F. Hucho, Y.N. Utkin, Muscarinic toxin-like proteins from cobra venom, Electron. J. Biochem. 267 (23) (2000) 6784–6789.
[69] C. Chung, B.N. Wu, C.C. Yang, L.S. Chang, Muscarinic toxin-like proteins from Taiwan banded krait (*Bungarus multicinctus*) venom: purification, characterization and gene organization, Biol. Chem. 383 (9) (2002) 1397–1406.
[70] M.J. Dufton, R.C. Hider, Structure and pharmacology of elapid cytotoxins, Pharmacol. Ther. 36 (1) (1988) 1–40.
[71] A. Bilwes, B. Rees, D. Moras, R. Menez, A. Menez, X-ray structure at 1.55 Å of toxin γ, a cardiotoxin from *Naja nigricollis* venom: crystal packing reveals a model for insertion into membranes, J. Mol. Biol. 239 (1) (1994) 122–136.
[72] L.S. Pierre, S. Flight, P.P. Masci, K.J. Hanchard, R.J. Lewis, P.F. Alewood, M.F. Lavin, Cloning and characterisation of natriuretic peptides from the venom glands of Australian elapids, Biochimie 88 (12) (2006) 1923–1931.
[73] A.S. Siang, R. Doley, F.J. Vonk, R.M. Kini, Transcriptomic analysis of the venom gland of the red-headed krait (*Bungarus flaviceps*) using expressed sequence tags, BMC Mol. Biol. 11 (1) (2010) 1.
[74] Y. Zhang, J. Wu, G. Yu, Z. Chen, X. Zhou, S. Zhu, Q. Lu, A novel natriuretic peptide from the cobra venom, Toxicon 57 (1) (2011) 134–140.
[75] Y. Yamazaki, T. Morita, Structure and function of snake venom cysteine-rich secretory proteins, Toxicon 44 (3) (2004) 227–231.
[76] R.L. Brown, T.L. Haley, K.A. West, J.W. Crabb, Pseudechetoxin: a peptide blocker of cyclic nucleotide-gated ion channels, Proc. Natl. Acad. Sci. 96 (2) (1999) 754–759.
[77] Y. Yamazaki, R.L. Brown, T. Morita, Purification and cloning of toxins from elapid venoms that target cyclic nucleotide-gated ion channels, Biochemist 41 (38) (2002) 11331–11337.
[78] K. Sunagar, T.N.W. Jackson, T. Reeks, B.G. Fry, Cysteine-rich secretory proteins, Venomous Reptiles and their Toxins: Evolution, Pathophysiology and Biodiscovery, Oxford University Press 2015, pp. 239–246.
[79] H. Takahashi, K. Hayashi, Purification and characterization of anticomplement factor (cobra venom factor) from the *Naja naja atra* venom, Biochim. Biophys. Acta 701 (1982) 102–110.
[80] C.W. Vogel, D.C. Fritzinger, Cobra venom factor: structure, function, and humanization for therapeutic complement depletion, Toxicon 56 (7) (2010) 1198–1222.
[81] T. Kostiza, J. Meier, Nerve growth factors from snake venoms: chemical properties, mode of action and biological significance, Toxicon 34 (7) (1996) 787–806.
[82] H. Takahashi, S. Iwanaga, Y. Hokama, T. Suzuki, T. Kitagawa, Primary structure of proteinase inhibitor II isolated from the venom of Russell's viper (*Vipera russelli*), FEBS Lett. 38 (2) (1974) 217–221.
[83] S.T. Earl, R. Richards, L.A. Johnson, S. Flight, S. Anderson, A. Liao, M.F. Lavin, Identification and characterisation of Kunitz-type plasma kallikrein inhibitors unique to *Oxyuranus* sp. snake venoms, Biochimie 94 (2) (2012) 365–373.
[84] C.B. Mourão, E.F. Schwartz, Protease inhibitors from marine venomous animals and their counterparts in terrestrial venomous animals, Mar. Drugs 11 (6) (2013) 2069–2112.
[85] A.K. Mukherjee, S.P. Mackessy, Pharmacological properties and pathophysiological significance of a Kunitz-type protease inhibitor (Rusvikunin-II) and its protein complex (Rusvikunin complex) purified from *Daboia russelii russelii* venom, Toxicon 89 (2014) 55–66.
[86] C.T. Guo, S. McClean, C. Shaw, P.F. Rao, M.Y. Ye, A.J. Bjourson, Trypsin and chymotrypsin inhibitor peptides from the venom of Chinese *Daboia russellii siamensis*, Toxicon 63 (2013) 154–164.
[87] Y.F. Pung, P.T. Wong, P.P. Kumar, W.C. Hodgson, R.M. Kini, Ohanin, a novel protein from king cobra venom, induces hypolocomotion and hyperalgesia in mice, J. Biol. Chem. 280 (13) (2005) 13137–13147.
[88] A.K. Mukherjee, Correlation between the phospholipids domains of the target cell membrane and the extent of *Naja kaouthia* PLA_2-induced membrane damage: evidence of distinct catalytic and cytotoxic sites in PLA_2 molecules, Biochim. Biophys. Acta Gen. Subj. 1770 (2) (2007) 187–195.
[89] A.K. Mukherjee, S.K. Ghosal, C.R. Maity, Lysosomal membrane stabilization by α-tocopherol against the damaging action of *Vipera russelli* venom phospholipase A_2, Cell. Mol. Life Sci. 53 (2) (1997) 152–155.
[90] D. Mebs, A comparative study of enzyme activities in snake venoms, Int. J. Biochem. 1 (3) (1970) 335–342.
[91] C.R. Gowda, A. Nataraju, R. Rajesh, B.L. Dhananjaya, B.K. Sharath, B.S. Vishwanath, Differential action of proteases from *Trimeresurus malabaricus*, *Naja naja* and *Daboia russellii* venoms on hemostasis, Comp. Biochem. Physiol. C: Toxicol. Pharmacol. 143 (3) (2006) 295–302.
[92] A.V. Osipov, D.Y. Mordvintsev, V.G. Starkov, L.V. Galebskaya, E.V. Ryumina, P.P. Bel'tyukov, L.V. Kozlov, S.V. Romanov, Y. Doljansky, V.I. Tsetlin, Y.N. Utkin, *Naja melanoleuca* cobra venom contains two forms of complement-depleting factor (CVF), Toxicon 46 (2005) 394–403.
[93] M. Ito, J. Hamako, Y. Sakurai, M. Matsumoto, Y. Fujimura, M. Suzuki, K. Hashimoto, K. Titani, T. Matsui, Complete amino acid sequence of kaouthiagin, a novel cobra venom metalloproteinase with two disintegrin-like sequences, Biochemist 40 (14) (2001) 4503–4511.
[94] C.C. Chang, S.T. Chuang, C.Y. Lee, J.W. Wei, Role of cardiotoxin and phospholipase A in the blockade of nerve conduction and depolarization of skeletal muscle induced by cobra venom, Br. J. Pharmacol. 44 (1972) 752–764.
[95] H.S. Bawaskar, P.H. Bawaskar, Snake bite poisoning, J. M. Gandhi Inst. Med. Sci. 20 (1) (2015) 5.
[96] R. Guieu, J.P. Rosso, H. Rochat, Anticholinesterases and experimental envenomation by *Naja*, Comp. Biochem. Physiol. C: Pharmacol. Toxicol. Endocrinol. 109 (3) (1994) 265–268.
[97] R. Shashidharamurthy, Y.H. Mahadeswaraswamy, L. Ragupathi, B.S. Vishwanath, K. Kemparaju, Systemic pathological effects induced by cobra (*Naja naja*) venom from geographically distinct origins of Indian peninsula, Exp. Toxicol. Pathol. 62 (6) (2010) 587–592.
[98] J.M. Gutiérrez, B. Lomonte, Phospholipases A_2: unveiling the secrets of a functionally versatile group of snake venom toxins, Toxicon 62 (2013) 27–39.
[99] B. Lomonte, Y. Angulo, L. Caldern, An overview of Lysine-49 phospholipase A_2 myotoxins from crotalid snake venoms and their structural determinants of myotoxic action, Toxicon 42 (2003) 885–901.
[100] K.S. Girish, R. Shashidharamurthy, S. Nagaraju, T.V. Gowda, K. Kemparaju, Isolation and characterization of hyaluronidase a "spreading factor" from Indian cobra (*Naja naja*) venom, Biochimie 86 (3) (2004) 193–202.
[101] A.K. Mukherjee, Non-covalent interaction of phospholipase A_2 (PLA_2) and kaouthiotoxin (KTX) from venom of *Naja kaouthia* exhibits marked synergism to potentiate their cytotoxicity on target cells, J. Venom Res. 1 (2010).
[102] I.B. Sundell, M. Ranby, M. Zuzela, K.A. Robinson, R.D.G. Theakston, In vitro procoagulant and anticoagulant properties of *Naja naja naja* venom, Toxicon 42 (2003) 239–247.
[103] B.L. Dhananjaya, C.J. D'Souza, The pharmacological role of nucleotidases in snake venoms, Cell Biochem. Funct. 28 (3) (2010) 171–177.
[104] D.A. Warrell, Snake bite, Lancet 375 (9708) (2010) 77–88.

BBA - Biomembranes 1861 (2019) 958–977

Contents lists available at ScienceDirect

BBA - Biomembranes

journal homepage: www.elsevier.com/locate/bbamem

Binding of a *Naja naja* venom acidic phospholipase A_2 cognate complex to membrane-bound vimentin of rat L6 cells: Implications in cobra venom-induced cytotoxicity

Sumita Dutta[a], Archana Sinha[b], Suman Dasgupta[b], Ashis K. Mukherjee[a,*]

[a] Microbial Biotechnology and Protein Research Laboratory, Department of Molecular Biology and Biotechnology, Tezpur University, Tezpur 784028, Assam, India
[b] Molecular Endocrinology and Metabolism Laboratory, Department of Molecular Biology and Biotechnology, Tezpur University, Tezpur 784028, Assam, India

ARTICLE INFO

Keywords:
Phospholipase A_2
Cobra venom cognate complex
Rat L6 myoblasts
LC-MS/MS
2D SDS-PAGE
Cytotoxicity

ABSTRACT

An acidic phospholipase A_2 enzyme ($NnPLA_2$-I) interacts with three finger toxins (cytotoxin and neurotoxin) from *Naja naja* venom to form cognate complexes to enhance its cytotoxicity towards rat L6 myogenic cells. The cytotoxicity was further enhanced in presence of trace quantity of venom nerve growth factor. The purified rat myoblast cell membrane protein showing interaction with $NnPLA_2$-I was identified as vimentin by LC-MS/MS analysis. The ELISA, immunoblot and spectrofluorometric analyses showed greater binding of $NnPLA_2$-I cognate complex to vimentin as compared to the binding of individual $NnPLA_2$-I. The immunofluorescence and confocal microscopy studies evidenced the internalization of $NnPLA_2$-I to partially differentiated myoblasts post binding with vimentin in a time-dependent manner. Pre-incubation of polyvalent antivenom with $NnPLA_2$-I cognate complex demonstrated better neutralization of cytotoxicity towards L6 cells as compared to exogenous addition of polyvalent antivenom 60–240 min post treatment of L6 cells with cognate complex suggesting clinical advantage of early antivenom treatment to prevent cobra venom-induced cytotoxicity. The *in silico* analysis showed that 19–22 residues, inclusive of Asp48 residue, of $NnPLA_2$-I preferentially binds with the rod domain (99–189 and 261–335 regions) of vimentin with a predicted free binding energy (ΔG) and dissociation constant (K_D) values of -12.86 kcal/mol and 3.67×10^{-10} M, respectively; however, $NnPLA_2$-I cognate complex showed greater binding with the same regions of vimentin indicating the pathophysiological significance of cognate complex in cobra venom-induced cytotoxicity.

1. Introduction

Phospholipase A_2 enzymes occur unambiguously in all snake venoms and exhibit a wide array of pharmacological effects [1–5] by binding to target through a "pharmacological site" on the surface of the enzyme which is independent of the catalytic site [6–8]. However, the pharmacological properties of a snake venom PLA_2 enzyme may or may not be dependent on its catalytic activity [4,9–11].

Studies have shown that group IB mammalian $sPLA_2$s bind to PLA_2 receptor (PLA_2R), which is a transmembrane glycoprotein resembling C-type animal lectin family of receptors [12,13], to induce cell proliferation, cell migration, and production of lipid mediator(s) in mammalian cells [12,13]. Nevertheless, snake venom PLA_2s have been reported to differentially bind and attack phospholipid micro-domains or

Abbreviations: 1D, one dimensional; 2D, two dimensional; 3FTx, three finger toxin; ANOVA, analysis of variance; AO, acridine orange; ATCC, American type cell culture; BSA, bovine serum albumin; CK, creatine kinase; CTx, cytotoxin; DAPI, 4′,6-diamidino-2-phenylindole; DMEM, Dulbecco's Modified Eagle's medium; EB, ethidium bromide; ELISA, enzyme-linked immune sorbent assay; FBS, fetal bovine serum; FITC, fluorescein isothiocyanate; HRP, horse-radish peroxidase; L6CP, L6 cytosolic protein; L6MP, L6 membrane protein; LC, liquid chromatography; LC-MS/MS, liquid chromatography-tandem mass spectrometry; LDH, lactate dehydrogenase; LNTx, long chain neurotoxins; MOPS, 3-(*N*-morpholino)propanesulfonic acid; MS, mass spectrometry; MTT, 3-(4,5-dimethylthiazol-2-Yl)-2,5-diphenyltetrazolium bromide; NCBI, National Center for Biotechnology Information; NGF, nerve growth factor; NHS, *N*-hydroxysuccinimide; NnV, *Naja naja* venom; PAV, polyvalent antivenom; PBS-T, phosphate buffered saline containing 0.1% tween-20; PC, phosphatidylcholine; PE, phosphatidylethanolamine; PLA_2, phospholipase A_2; PRP, platelet rich plasma; PS, phosphatidylserine; PVDF, polyvinylidene difluoride; QTOF, quadrupole time-of-flight; RP-HPLC, reverse phase high performance liquid chromatography; SDS-PAGE, sodium dodecyl sulfate polyacrylamide gel electrophoresis; TMB, 3,3′,5,5′-tetramethylbenzidine; U-HPLC, ultra-high performance liquid chromatography

* Corresponding author.
E-mail address: akm@tezu.ernet.in (A.K. Mukherjee).

https://doi.org/10.1016/j.bbamem.2019.02.002
Received 25 August 2018; Received in revised form 25 January 2019; Accepted 5 February 2019
Available online 15 February 2019
0005-2736/

rafts present on the mammalian cells; therefore, phospholipid types in different plasma membrane of cells determines the extent of PLA_2 hydrolysis [14–16]. Studies have also revealed the presence of certain elusive PLA_2 receptors on the plasma membranes which may or may not be directly involved in the toxic effects of snake venom PLA_2s [17]. In 1990, Lambeau and colleagues [18] demonstrated the high affinity binding of a high molecular weight (180 kDa) monomeric membrane protein in rabbit myotubes to a PLA_2 from *Oxyuranus scutellatus* venom; however, the exact pathophysiological significance of PLA_2-membrane protein interaction was unknown. Another Lys49 myotoxic PLA_2 from venom of *Agkistrodon piscivorus piscivorus* was shown to bind to a kinase insert domain containing receptor (KDR) [17,19]. However, such interactions may not always demonstrate a functional relevance in the pathophysiology exhibited by the snake venom PLA_2 enzymes [20].

Neurotoxicity is the major symptom of cobra envenomation [21,22], albeit coagulopathy, edema, necrosis, renal failure, and cardiotoxicity leading to hypotension and cardiac arrest are also reported [21,22]. Myotoxicity is one of the major signs of cobra envenomation that results in permanent morbidities in snakebite victims [23,24]. Non-enzymatic three finger toxins (3FTxs) and enzymatically active/inactive homologs of venom PLA_2s in elapid venoms induce myotoxicity by disruption of cellular integrity of myotubes [25,26]. Catalytically inactive snake venom PLA_2s possessing Lys49, Ser49, Asn49, Glu49 or Arg49 instead of Asp49 [27] are also reported to induce myotoxicity [9,28,29]. Recently it has been demonstrated that a myotoxic Lys49 PLA_2 (Mt-II) from *Bothrops asper* binds to membrane-bound nucleolin at low temperatures [30]. However, at physiological temperature, this binding was followed by internalization and co-localization of Mt-II and nucleolin in paranuclear and nuclear areas of myotubes showing the role of this association in myotoxicity exhibited by the PLA_2 [30].

The myotoxic PLA_2s are primarily basic in nature and their basic charge might play an important role in membrane binding and subsequent damage to the cells [31]. The present study shows that an acidic PLA_2 purified from Indian cobra *Naja naja* venom (NnV) is devoid of cytotoxicity towards myogenic cells; however, it forms a cognate complex with other components of cobra venom to show considerable cytotoxicity against rat myogenic L6 cells in *in vitro* conditions indicating PLA_2 cognate complex may play a pivotal role in cobra venom-induced cytotoxicity. The present study is also the first report showing binding of cobra venom acidic PLA_2 and its cognate complex with membrane bound vimentin of rat myogenic L6 cells to induce cytotoxicity and internalization of PLA_2 to cytosol post binding with vimentin.

2. Material and methods

2.1. Materials

Human breast adenocarcinoma (MCF-7), rat myoblast or myogenic cells (L6), human embryonic kidney (HEK-293) and rat pheochromocytoma (PC-12) cell lines were obtained from American Type Culture Collection (ATCC), USA. Dulbecco's Modified Eagle's Medium (DMEM) and fetal bovine serum (FBS) were obtained from HiMedia Laboratories, USA; Penicillin-Streptomycin Solution was obtained from Gibco™, Thermo Fisher Scientific, USA; Fluorescein isothiocyanate (FITC) was procured from Sigma-Aldrich, USA; while all other cell culture accessories were procured from Corning®, Sigma-Aldrich, USA. All other analytical grade reagents were procured from Sigma-Aldrich, USA. The NHS-activated Sepharose 4 Fast Flow matrix was purchased from GE Healthcare, Sweden. The polyvalent antivenom (PAV) raised against Big Four snake (*Naja naja*, *Daboia russelii*, *Echis carinatus* and *Bungarus caeruleus*) venoms was obtained from Premium Serum and Vaccines Pvt. Ltd., Maharashtra, India (Batch no. 012015, expiry date: December 2018). The anticoagulant phospholipase A_2 enzyme ($NnPLA_2$-I) was purified from NnV of eastern India as described previously [4]. Polyclonal antibodies against $NnPLA_2$-I were raised in rabbit and serum IgG was purified by affinity (protein A/G resins) chromatography. Anti-vimentin antibody (Cat. No. ab92547, Abcam, USA) was a generous gift from Dr. Biplab Bose, Indian Institute of Technology (IIT), Guwahati. Bright field and fluorescence microscopy were performed using Leica DMi8 microscope, Leica Microsystems, Germany; confocal microscopy was done using a Zeiss LSM 880 confocal microscope, Zeiss, Germany at IIT, Guwahati.

2.2. Two-dimensional SDS-PAGE followed by immuno-blot and LC-MS/MS analyses to identify $NnPLA_2$-I interacting components of the cognate complex

The 2D electrophoresis of NnV was done under both reduced and non-reduced conditions. Lyophilized NnV (1.0 mg) was dissolved in 20 mM Tris-HCl buffer, pH 7.4 and centrifuged at 11,760*g* for 10 min. The supernatant was cleaned using 2-D Clean-Up kit (GE Healthcare, Sweden) and thereafter quantified using 2-D Quant kit (GE Healthcare, Sweden). 300 μg of cleaned-up NnV in rehydration buffer was gently added to pH 3–10, 7 cm Immobiline DryStrip gel (GE Healthcare, Sweden) and rehydrated for 16 h. The Immobilin DryStrip gels were then subjected to isoelectric focusing (1D electrophoresis) on an Ettan IPGphor 3 Isoelectric Focusing System (GE Healthcare, Sweden) for 11,350 kVh (300 V for 4 h, 300–1000 V in 1 h, 1000–5000 V in 90 min, 5000 V for 1 h). After completion of 1D electrophoresis, equilibration of the IPG strip was done with equilibration buffer containing 65 mM dithiothreitol (for reduction) and 135 mM iodoactetamide (for alkylation) for 10 min each at room temperature. For the non-reduced 2D SDS-PAGE, the DTT and IAA treatment steps were avoided and both the strips (containing reduced and non-reduced venom) were subjected to 12% SDS-PAGE at 120 V, 40 mA. The proteins spots were visualized by staining the gel with PhastGel Blue R (GE Healthcare, Sweden) for overnight and distaining with methanol/acetic acid/water (40:10:50). The gels were scanned on an EPSON scanner using Silver Fast software and the protein spots were counted and analyzed by ImageMaster™ 2D Platinum v7.0 Software (GE Healthcare, Sweden).

The NnV proteins separated by 2D SDS-PAGE were transferred from gels to Immobilon-P PVDF membranes by semi-dry gel transfer system at 78 mA (1.2 mA/cm^2) for 2 h. Thereafter, the membrane was blocked with 5% skimmed milk in Tris-buffered saline (0.05 M Tris buffer, 0.138 M NaCl and 2.7 mM KCl) containing 0.1% Tween-20 (TBS-T) for overnight at 4 °C. The membrane was washed three times with TBS-T (10 min each) with constant shaking and thereafter incubated with rabbit anti-$NnPLA_2$-I antibodies (1:2000 dilutions) for 30 min. The membrane was again washed with TBS-T followed by incubation with HRP-conjugated goat anti-rabbit IgG (1: 5000 dilutions) for 30 min. After washing, the blot was developed by adding 3,3′,5,5′-Tetramethylbenzidine (TMB) Liquid Substrate System for Membranes (T0565, Sigma-Aldrich, USA) [32].

The 2D gel spots, corresponding to that recognized by anti-$NnPLA_2$-I antibodies in PVDF membrane, were excised and subjected to LC-MS/MS analysis for proteins identification after in-gel trypsin digestion [33]. Briefly, the tryptic peptides were desalted and concentrated by ZipTip C_{18} (Merck, USA) and separated on a Zorbax C_{18} column (Rapid Resolution HT 2.1 × 50 mm, 1.8 μm) coupled to an Agilent 1260 UHPLC system [34]. The column compartment temperature was set at 40 °C source and analyzed on an Agilent 6530 QTOF mass spectrometer. The MS and MS/MS spectra were acquired in the range of 100 to 2000 *m/z*, with a scan rate of 6 and 3 spectra/s for MS and MS/MS, respectively. The raw MS/MS data was searched against the *Naja naja* (taxid 35,670) protein entries of the non-redundant NCBI database using Morpheus software [35]. Carbamidomethylation of cysteine and the oxidation of methionine residues were set as fixed and variable modifications, respectively. Precursor and fragment mass error tolerances were set to 2.1 Da and 0.025 Da, respectively; up to two missed cleavages were allowed, and the false discovery rate was set to < 1%. Identification of at least one unique peptide per protein entry was

considered to be the minimum pre-requisite for protein identification [33]. The relative abundance of venom proteins in 2D SDS-PAGE spots (cognate complexes) were determined by MS2 (normalized spectral count)–based label free quantification technique [32,36] using the following Eqs. 1 and 2:

$$\text{Mean spectral count for protein } X = \frac{\Sigma \text{ spectral count against MS2 peptides of } X}{\text{number of identified peptides}} \quad (1)$$

$$\text{Relative abundance of protein } X = \frac{\text{mean spectral count of } X}{\text{total mean spectral count of all proteins}} \times 100\% \quad (2)$$

2.3. Isolation and determination of molecular mass of NnPLA$_2$-I cognate complex

The cation-exchange Nn(N)CM2 fraction of NnV was isolated as previously described by us [33]. 100 μg of Nn(N)CM2 was subjected to in-solution trypsin digestion followed by LC-MS/MS analysis [33]. Thereafter, the relative abundance of venom proteins in Nn(N)CM2 was determined by MS2 (normalized spectral count)–based label free quantification technique [32,36] using the Eqs. 1 and 2 above. Based on the percent relative abundance, the quantity of each protein (in moles) in 100 μg of Nn(N)CM2 was calculated using eq. 3, and thereafter the stoichiometry of each protein in the complex was determined.

$$\text{Protein } X \text{ (in moles)} = \frac{\text{microgram of } X \text{ in } 100\ \mu g \text{ of cognate complex}}{\text{molecular mass of } X \text{ (in Da)}} \quad (3)$$

The LC-MS/MS analysis demonstrated that the composition of Nn (N)CM2 fraction [33] was similar to the cognate complex of NnPLA$_2$-I (present study); therefore, this fraction was chosen as a representative NnPLA$_2$-I cognate complex. To confirm the non-covalent interaction of NnPLA$_2$-I with other venom toxins, 40 μg each of NnPLA$_2$-I, Nn(N)CM2 and NnV were separated by 12.5% SDS-PAGE under both reducing and non-reducing conditions at 120 V, 400 mA. The protein bands were visualized by staining the gel with PhastGel Blue Rand distaining with methanol: glacial acetic acid: water (40:10:50). From densitometry analysis of the gel (ImageJ software, NIH, USA), ELISA of Nn(N)CM2 fraction with anti-NnPLA$_2$-I antibody, and label-free quantification (see above) the concentration and relative abundance of NnPLA$_2$-I in its cognate complex [Nn(N)CM2 fraction] was also determined.

To determine the molecular mass, 0.5 mg of the cognate complex [(Nn(N)CM2)] was subjected to size exclusion chromatography on a HiLoad 16/600 Superdex 75 pg column pre-equilibrated with 20 mM Tris-HCl buffer containing 150 mM NaCl, pH 7.4 and coupled to an AKTA Purifier FPLC system. A mixture of standard proteins (Immunoglobulin, 150 kDa; serum albumin, 67 kDa; α-lactoglobulin, 35 kDa; cytochrome C, 12.4 kDa and Vitamin B_{12}, 1.3 kDa) were also separated under identical conditions to determine the molecular mass of the complex. From the log molecular weight of standard proteins *vs* Ve/Vo plot the molecular mass range of the NnPLA$_2$-I-cognate complex was calculated.

2.4. Isolation of individual components of the NnPLA$_2$-I cognate complex

The NnPLA$_2$-I cognate complex [Nn(N)CM2, 150 μg] was subjected to RP-HPLC fractionation on a Dionex Acclaim C_{18} column (2.1 × 150 mm, 3.0 μm) pre-equilibrated with 95% solvent A (Type I water containing 0.1% TFA) and 5% solvent B (90% acetonitrile containing 0.1% TFA), coupled to a Dionex Ultimate 3000 U-HPLC system (Thermo Fisher Scientific, Germany). The proteins were eluted using a multi-step gradient of solvent B with a flow rate of 0.5 ml/min. The eluted protein peaks were pooled and lyophilized, and the protein content of individual peak was determined [37]. Further, each major fraction (30 μg) was subjected to in-solution trypsin digestion followed by LC-MS/MS analysis as described above.

2.5. Cytotoxicity of purified NnPLA$_2$-I and its cognate complex on different mammalian cells

Erythrocytes, platelet-rich plasma (PRP), and washed platelets were isolated from citrated goat blood as described previously [4,38]. The hemolytic activity of NnPLA$_2$-I (10.0 μg/ml or 0.70 μM) and its cognate complex (12.5 μg/ml and 25.0 μg/ml) was assayed against 2.0 ml of 5% (*v*/v) erythrocytes suspension [15]. Hemolytic activity, if any, was expressed as % hemolysis compared to hemolysis induced by 0.1% triton X-100 (100%). Similarly, NnPLA$_2$-I (0.7 μM) or its cognate complex (12.5 and 25.0 μg/ml containing 0.35 μM and 0.70 μM NnPLA$_2$-I, respectively) or PBS (control) was incubated with 100 μl of washed platelets (1×10^6 platelets/ml) for 4 h at 37 °C, 5% CO_2. Platelets viability or decrease in number of platelets, if any, was determined by counting the trypan blue stained platelets in a hemocytometer using Motic Images plus 3.0 ML software [39]. Antibacterial activity of NnPLA$_2$-I (0.70 μM) and its cognate complex (25.0 μg/ml) against Gram positive *Bacillus subtilis* and Gram negative *Escherichia coli* was assayed as described previously [16].

The mammalian cell lines L6, MCF-7, PC-12, and HEK-293 cells (1×10^3 cells/ml) were grown in DMEM containing 10% heat-inactivated FBS and 1% pen-strep antibiotic solution (Gibco™, Thermo Fisher Scientific, USA) in a 96-well plate at 37 °C in a 5% CO_2 humidified incubator for 24 h. For L6 cells, the myoblasts were allowed to partially differentiate by replacing the medium with fresh DMEM containing 2% FBS. The process was repeated after every 24 h for 5–7 days. After allowing the cells to grow and adhere to the culture plates, the medium was replaced with a fresh medium containing NnPLA$_2$-I (0.70 μM) or NnPLA$_2$-I-cognate complex (12.5 and 25.0 μg/ml containing 0.35 μM and 0.70 μM NnPLA$_2$-I NnPLA$_2$-I, respectively) or PBS (control).

In another set of experiments, the partially differentiated myoblasts were treated with - (i) RP-HPLC purified 2.2 μg/ml or 0.35 μM of the cytotoxin (CTx), (ii) 4.8 μg/ml or 0.62 μM of neurotoxin (LNTx), (iii) reconstituted complexes of CTx (0.35 μM)-LNTx (0.62 μM), and (iv) CTx (0.35 μM)-LNTx (0.62 μM)-NnPLA$_2$-I (0.35 μM). The concentration of the above 3FTxs/NnPLA$_2$-I was calculated based on their percent relative abundance in the cognate complex as determined by LC-MS/MS analysis of Nn(N)CM2. After 24 h of incubation, cytotoxicity was determined by observation of the cells under the bright field of a fluorescence microscope followed by counting using Motic Images plus 3.0 ML software, after acridine orange/ethidium bromide (AO/EB) staining (see below), and MTT-based cell viability assay [40]. Cytotoxicity was expressed as % cell death by comparing the values to that of control (100%) [41].

The cytotoxicity towards L6 myogenic cells was also confirmed by assaying the release of creatine kinase (CK) and lactate dehydrogenase (LDH) in growth medium 24 h post treatment with NnPLA$_2$-I and its cognate complex [Nn(N)CM2 fraction] using commercial diagnostic kits (Tulip Diagnostics Ltd., India).

To study the morphological changes induced in L6 myogenic cells by NnPLA$_2$-I and its cognate complex, the treated cells were stained with ethidium bromide and acridine orange (100 μg/ml in PBS, 1:1). After 5 min of incubation at 37 °C in a humidified CO_2 incubator, the cells were washed in PBS for three times and then observed under a fluorescence microscope (Leica DMi8, Leica Microsystems, Germany) at 20× magnification using rhodamine (for red) and FITC (for green) filters [42]. The treated L6 cells were also observed under a bright field microscope (Leica DMi8, Leica Microsystems, Germany) at 10× magnification.

2.6. Assessment of neutralization of $NnPLA_2$-I cognate complex-induced cytotoxicity and phospholipase A_2 activity by polyvalent antivenom and anti-$NnPLA_2$-I antibody

Prior to addition to partially differentiated myoblasts, the $NnPLA_2$-I cognate complex (12.5 μg/ml) was pre-incubated with graded concentrations of PAV (protein: protein (*w*/w) ratio of 1:6.25, 1:12.5, and 1:25.0) or with anti-$NnPLA_2$-I antibody (at 1:25 w/w ratio for abolishing the PLA_2 activity) for 30 min at 37 °C. In another set of experiments, the PAV was added to culture media at 1:25 ratio after 60, 120, and 240 min post treatment of partially differentiated myoblasts with $NnPLA_2$-I cognate complex (12.5 μg/ml). After 24 h of incubation the cytotoxicity was assayed by MTT-based method as mentioned above. The cytotoxicity induced by $NnPLA_2$-I cognate complex was considered as 100% activity and other values were compared to that.

To determine the extent of neutralization of PLA_2 activity of the $NnPLA_2$-I cognate complex, the cognate complex was incubated with commercial PAV / anti-$NnPLA_2$-I antibody or PBS, pH 7.4 (control) for 30 min at 37 °C and PLA_2 activity was assayed using a $sPLA_2$ assay kit according to the manufacturer's protocol (Cayman's Chemical Company, USA) [43].

2.7. Assessment of inhibition of $NnPLA_2$-I cognate complex-induced cytotoxicity and PLA_2 activity by chemical modification of His48 residue

The Nn(N)CM2 (25.0 μg/ml) was pre-incubated with 5.0 mM *p*-bromophenacyl bromide (*p*-BPB) at 37 °C for 30 min. The un-reacted/excess *p*-BPB was separated by filtering the reaction mixture through a 3 kDa cut-off membrane (Pall Corporation, USA). The inhibition of PLA_2 activity of cognate complex was ascertained by PLA_2 enzyme assay as described in Section 2.6. The supernatant containing $NnPLA_2$-I-alkylated cognate complex was used to assay the residual toxicity against rat myogenic cells as described above (Section 2.5).

2.8. Determination of binding of $NnPLA_2$-I and its cognate complex to L6 cells by ELISA

The L6 cells were grown in DMEM as stated above. The adherent cells were isolated by trypsinization and were seeded in the wells of a 96-well tissue culture plate at a density of 1×10^3 cells per well. The cells were allowed to adhere to the well surface by incubating them in medium under regular growth conditions for 18 h and further allowed to partially differentiate (as mentioned above).

The wells coated with L6 cells (partially differentiated myoblasts)/PBS (control) were blocked using 5% FBS in PBS for 30 min at room temperature and then the wells were washed for three times with PBS-T (10 mM phosphate buffer containing 150 mM NaCl and 0.05% tween-20) for 10 min each with constant shaking. A set of blank wells (without cells) were also blocked in a similar way. Thereafter, increasing concentrations of $NnPLA_2$-I (0.17, 0.35, 0.70 μM) or $NnPLA_2$-I cognate complex (6.25, 12.5, 25.0 μg/ml) or PBS (blank and control) were added to the cells and incubated for 30 min at room temperature. The wells were washed with PBS-T for three times followed by addition of 100 μl of 1:2000 diluted rabbit anti-$NnPLA_2$-I antibodies (100 ng per well, except blank) and incubated for 2 h at room temperature. The wells were again washed with PBS-T and 100 μl of 1:5000 diluted anti-rabbit IgG-HRP conjugated secondary antibodies was added and incubated for 2 h at room temperature. After washing the wells with PBS-T, 100 μl of 3,3′,5,5′-Tetramethylbenzidine (TMB)/H_2O_2 was added and the plates were incubated in dark at room temperature for 30 min. The reaction was terminated by adding 50 μl of 2.0 M H_2SO_4 and the absorbance was measured at 492 nm in a microplate reader (Multiskan GO, Thermo Scientific, USA). To avoid false signals, the absorbance of the blank was subtracted from the absorbance of the control and test wells during data analysis.

2.9. Immunofluorescence and confocal microscopy studies to determine the binding followed by internalization of $NnPLA_2$-I to L6 cells

L6 myoblasts grown on coverslips were allowed to undergo partial differentiation (as mentioned above) and incubated with 0.70 μM of $NnPLA_2$-I in culture medium for 30, 60, 120, and 240 min at 37 °C, 5% CO_2. The cells were washed with PBS, pH 7.4 for three times and thereafter fixed with 4% paraformaldehyde for 10 min followed by washing three times for 5 min each with ice-cold PBS, pH 7.4. The fixed cells were then permeabilized using 0.1% triton X-100 in PBS, pH 7.4 for 5 min and then washed in ice-cold PBS, pH 7.4 for three times. Thereafter, the cells were blocked with 1% BSA solution in PBS, pH 7.4 containing 0.3 M glycine and 0.1% tween-20. The cells were then washed with ice-cold PBS, pH 7.4 for three times, and incubated with anti-$NnPLA_2$-I polyclonal antibody (1:250 in PBS-T) at 4 °C for overnight. The following day, myoblasts adhered to cover slips were washed with ice cold PBS, pH 7.4 and incubated with 1:200 diluted (in PBS-T) Alexa Fluor 488 conjugated anti-rabbit IgG (Invitrogen, Thermo Scientific, USA) for 60 min at room temperature (~23 °C). The cells were then washed, stained with DAPI for 5 min and mounted on glass slides using ProLong® Gold Antifade Mountant (Thermo Fisher Scientific, Germany) and visualized under Leica DMi8 fluorescence microscope at 40× magnification using FITC (for green) and DAPI (for blue) filters.

In another set of experiments, $NnPLA_2$-I was conjugated with FITC [44] and thereafter incubated with partially differentiated myoblasts for 30–240 min at 37 °C in a humidified incubator as described above. Briefly, $NnPLA_2$-I (10 mg/ml) was dissolved in MOPS [3-(*N*-morpholino)propanesulfonic acid] buffer and incubated with FITC (protein:FITC ratio of 1:2) for 2 h at room temperature. Then β-mercaptoethanol (1.0 mM) was added to the reaction mixture to block the free FITC groups. The conjugated $NnPLA_2$-I (0.70 μM) after filtering through a 3 kDa cut-off membrane (Pall Corporation, USA) was added to the growth medium of myoblasts. After incubation, the culture media was aspirated out, the cells were washed with ice-cold PBS, pH 7.4, stained with DAPI for 5 min, washed with PBS, pH 7.4, and mounted on glass slides using ProLong® Gold Antifade Mountant. The cells were then visualized under a Zeiss LSM 880 confocal microscope at 63× magnification using bright field, FITC (488 nm excitation wavelength), and DAPI (358 nm excitation wavelength) filters. To confirm the time-dependent internalization of $NnPLA_2$-I, the confocal microscopic images of treated rat myoblasts were subjected to z-stack projection analysis [45] by ZEN System software, ZEISS, Germany. A set of 9–15 z-stack images in different planes (separated by 1 μm) was analyzed for time-dependent internalization of FITC-conjugated $NnPLA_2$-I.

2.10. Determination of binding of $NnPLA_2$-I and its cognate complex to membrane and cytosolic proteins of L6 cells by ELISA

Membrane proteins of partially differentiated L6 myoblasts were isolated using the Mem-PER™ Plus Membrane Protein Extraction Kit (Thermo Fisher Scientific, USA). The isolated membrane and cytosolic proteins were quantitated [46], desalted in PD 10 column (GE Healthcare, Sweden) and lyophilized (CentriVap Benchtop Vacuum Concentrator, Labconco Corporation, USA) until further use.

To determine the binding, 1.0 μg of L6 cytosolic protein (L6CP) or membrane protein (L6MP)/BSA (negative control)/PBS (control to avoid the false signal, if any) was coated in triplicate to a 96-well ELISA plate (Nunc MaxiSorp™, Thermo Fisher Scientific, USA) and incubated for 18 h at 4 °C. The wells were washed with PBS-T for three times and then blocked with 5% fat-free milk (in PBS, pH 7.4) for 30 min. After washing the wells with PBS-T (three times), 100 μl of 0.70 μM of $NnPLA_2$-I (~1.0 μg per well) or 25.0 μg/ml cognate complex [Nn(N)CM2 containing ~1.0 μg per well or 0.70 μM PLA_2] was added to the wells. An equivalent volume of PBS-T was added to the wells serving as negative controls (BSA). After incubation for 30 min at room temperature, the wells were washed with PBS-T and binding of $NnPLA_2$-I

and $NnPLA_2$-I in its cognate complex to L6MP and L6CP was determined by ELISA as stated above (Section 2.8).

2.11. Determination of binding of purified PLA_2 and its cognate complex to L6MP by immunoblot analysis

Eighty microgram of L6MP was separated by 12.5% non-reduced SDS-PAGE (two sets of gel run under identical conditions). The proteins from one set of gel were transferred to an Immobilon-P PVDF membrane (Merck, Germany) by semi-dry gel transfer system (Amersham Bioscience, UK) at 38 mA (1.2 mA/cm^2) for 2 h whereas another set of gel was kept aside. The protein transfer efficiency was verified by 0.5% Ponceau-S red staining of the PVDF membrane as well as PhastGel Blue R staining of the post transfer gel. Thereafter, the membrane was blocked in 5% skimmed milk (*w/v*) dissolved in TBS-T for overnight at 4 °C. Following day, the membrane was washed three times with TBS-T (10 min for each wash), cut into two pieces and immersed in a small tray containing 0.35 μM of 0.70 μM of $NnPLA_2$-I or 25.0 μg/ml of Nn (N)CM2 (PLA_2-cognate complex containing 0.70 μM of $NnPLA_2$-I). After incubation for 30 min at room temperature, the membrane was washed with TBS-T and then 100 μl of 1:2000 diluted rabbit anti-$NnPLA_2$-I antibodies were added and incubated at room temperature for 1 h. After washing the membrane with TBS-T (three times) it was incubated with HRP-conjugated goat anti-rabbit IgG secondary antibodies (1:5000 dilutions) at room temperature for 1 h. Thereafter, the membrane was washed with TBS-T and the blot was developed using TMB Liquid Substrate System for Membranes. The gels were scanned on an EPSON scanner using SilverFast software. The experiment was repeated three times to assure the reproducibility. As a positive control, 80 μg NnV was separated by 12.5% SDS-PAGE under reduced conditions, transferred to PVDF membrane, and the membrane was developed by using anti-$NnPLA_2$-I antibody as mentioned above.

From the second set of gel the membrane protein bands showing binding with $NnPLA_2$-I (individual as well as with cognate complex) were excised and identified by mass spectrometry analysis as described above.

2.12. Isolation and purification of $NnPLA_2$-I binding L6MP

The $NnPLA_2$-I binding L6MP was isolated by affinity chromatography using immobilized $NnPLA_2$-I as the ligand. Briefly, 200 μl of NHS-activated Sepharose 4 Fast Flow matrix was packed in a 1.0 ml column and incubated with 200 μg of $NnPLA_2$-I for overnight (~18 h) at 4 °C. The column was washed with 1.0 ml of PBS, pH 7.4 to wash out the unbound $NnPLA_2$-I, if any, which was determined by estimating the protein content [46] and assay of PLA_2 activity of post wash buffer. Thereafter, 400 μg of membrane proteins were loaded onto the column and incubated at room temperature (25 °C) for 2 h with constant shaking. The unbound L6MPs were eluted by washing the column with 5 column volumes (CV) of PBS, pH 7.4; while the bound proteins were eluted with a step gradient of 2 CV of 0.02 mM glycine, pH 2.0, followed by 5 CV of 0.1 M glycine, pH 2.0 [47]. The pH of the eluted bound L6MP was immediately neutralized by adding equal volume of 1.0 M Tris-HCl, pH 9.0.

The $NnPLA_2$-I binding L6MP was quantitated, desalted, lyophilized, and then subjected to RP-HPLC fractionation (Dionex Ultimate 3000 U-HPLC system, Thermo Fisher Scientific, Bremen, Germany) in a Acclaim C_{18} column (2.1 × 150 mm, 3 μm) pre-equilibrated with 95% of solvent A (0.1% trifluoroacetic acid) and 5% solvent B (90% acetonitrile containing 0.1% TFA). After eluting the hydrophilic proteins with solvent A, the bound L6MPs were eluted with a multi-step gradient of solvent B. The proteins fractions were collected and lyophilized. L6MP (100 ng) from each RP-HPLC peak was coated in a 96 well plate and it's binding with $NnPLA_2$-I was determined by ELISA using anti-$NnPLA_2$-I antibodies. The RP-HPLC fraction of L6MP that bind to $NnPLA_2$-I was subjected to in-solution trypsin digestion followed by LC-MS/MS analysis for protein identification and quantification.

2.13. Spectrofluorometric analysis to determine dose- and time-dependent binding of $NnPLA_2$-I and its cognate complex to vimentin

The interaction between $NnPLA_2$-I/cognate complex with vimentin (purified from L6MP) was determined by our previously described method [48] with slight modifications. Briefly, to determine the dose-dependent binding, graded concentrations of $NnPLA_2$-I (0.17–0.70 μM) or its cognate complex (6.25–25.0 μg/ml containing 0.17–0.70 μM $NnPLA_2$-I) were added to the wells of a Nunc™ F96 MicroWell™ Black Polystyrene Plate (Thermo Fisher Scientific, Denmark) containing vimentin (10.0 μg/ml) in a reaction mixture of 100 μl. For time-dependent binding study, 0.17 μM of $NnPLA_2$-I or 6.25 μg/ml of its cognate complex was incubated with 10.0 μg/ml of vimentin for different time intervals (7.5–60 min) in a 100 μl reaction mixture. The reaction mixtures were excited at 280 nm with a monochromator light source. The slit width was maintained at 12 nm and emission was monitored from 300 to 500 nm using a Varioskan LUX Multimode Microplate Reader (Thermo Fisher Scientific, Denmark). As a control, the fluorescence spectrum of individual protein was also determined and compared with the relative intensity of the fluorescence spectra (λ_{max}) of $NnPLA_2$-I and its cognate complex with vimentin. The change in λmax (Δλmax) was plotted against the concentrations (μM) or pre-incubation time (min) of $NnPLA_2$-I/cognate complex with vimentin using GraphPad Prism 5.0 software.

2.14. In silico study to determine the interaction between $NnPLA_2$-I and vimentin

The complete FASTA sequence of P15445 ($NnPLA_2$-I), P25671 (LNTx), P86538 (CTx), and P01140 (NGF) were obtained from NCBI database and submitted to I-TASSER software for structure prediction [49]. The PDB structures for four regions of the rod region of vimentin were available at the Protein Data Bank data with accession numbers 3s4r (chain B: 99–189), 3uf1 (chain A: 146–249), 3trt (chain A: 261–335), and 1gk4 (chain D: 330–407). Molecular dynamics for each of these structures were run using MDWeb server [50] and for docking analysis chains B, A, A, and D of 3s4r, 3uf1, 3trt, and 1gk4, respectively, were used [51]. The binding of $NnPLA_2$-I with each of the structures of vimentin was studied using ClusPro 2.0 [52] and FireDock servers [53]. The docking servers calculate the global energy of interaction and the model with the lowest energy was considered as the best model [53]. The vimentin structures (mentioned above) showing the best interaction with $NnPLA_2$-I was further considered for studying their binding with the $NnPLA_2$-I cognate complex and its individual components. Further, PDBsum server tool was used to determine the residue-to-residue interactions between $NnPLA_2$-I and its cognate complex to vimentin [54,55].

In order to calculate the predicted values of ΔG (free binding energy) and K_D (dissociation constant) of $NnPLA_2$-I-vimentin interaction, the full sequences of $NnPLA_2$-I and vimentin were submitted to PPA-Pred2 (Protein-Protein Affinity Predictor) online server [56].

To confirm the results of *in silico* studies by wet lab experiment, 1.0 μg of RP-HPLC purified vimentin was coated on a 96 well plate for overnight. Prior to addition of 10.0 μg/ml or 0.70 μM of $NnPLA_2$-I or 25.0 μg/ml of $NnPLA_2$-I cognate complex (containing 0.70 μM of $NnPLA_2$-I), the vimentin was pre-incubated with anti-vimentin antibody (ab92547, Abcam, USA) raised against the tail region of vimentin or PBS, pH 7.4 (control) for 30 min at room temperature. Thereafter, binding of $NnPLA_2$-I or its cognate complex to treated vimentin was assessed by ELISA as mentioned above. The binding of $NnPLA_2$-I or its cognate complex to control was considered as 100% binding and other values were compared to that.

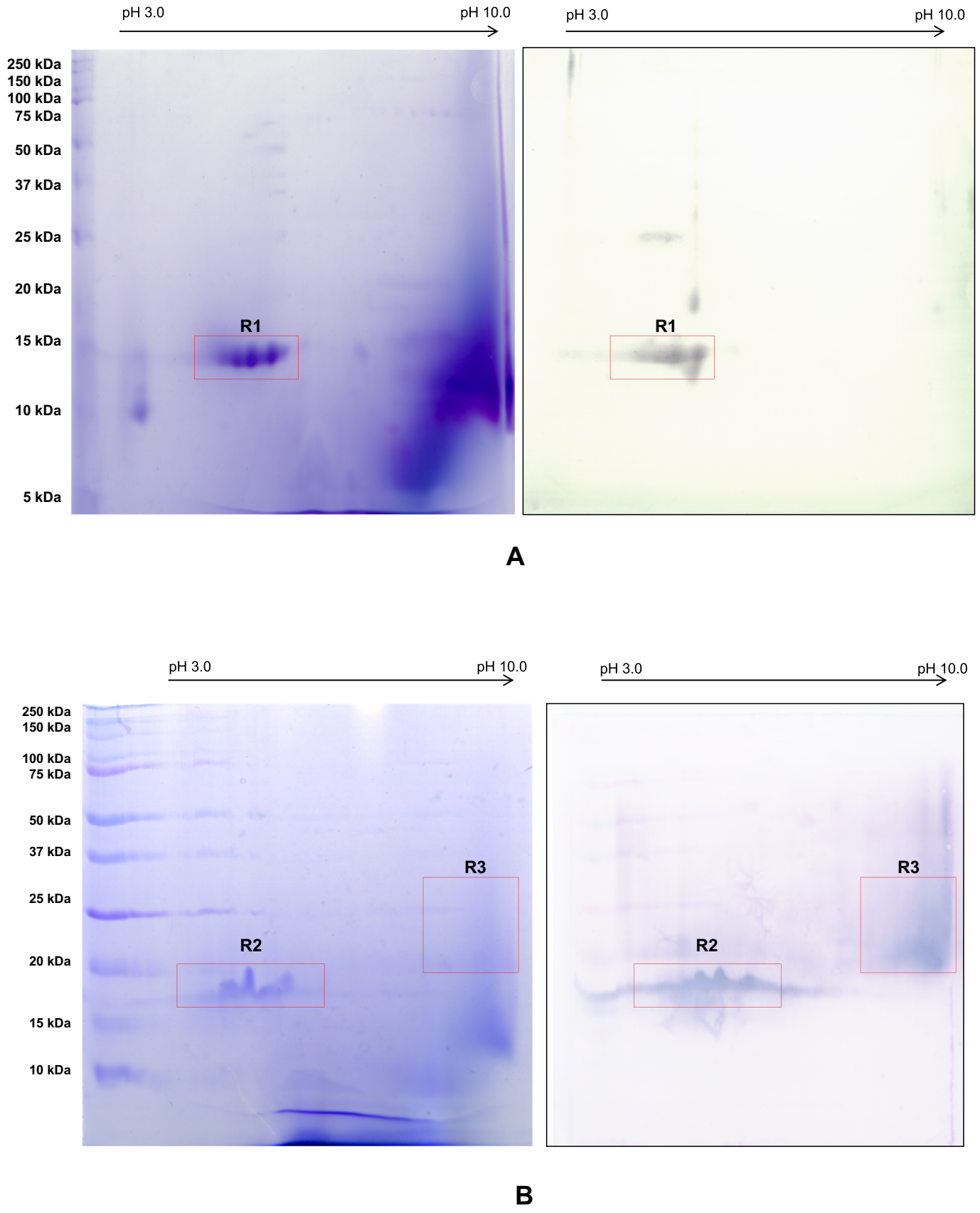

Fig. 1. 2D SDS-PAGE (left panels) of *N. naja* venom (300 μg) under (A) reduced and (B) non-reduced conditions, and their corresponding immunoblots (right panels) developed with rabbit anti-NnPLA$_2$-I antibody and HRP-conjugated goat anti-rabbit IgG secondary antibody.

Table 1
List of proteins identified by LC-MS/MS analysis of protein spots in 2D SDS-PAGE of *N. naja* venom under reduced (R1) and non-reduced (R2, R3) conditions. The protein spots were detected by immunoblot analysis against anti-NnPLA$_2$-I polyclonal antibody.

Protein Description	Accession no.	Organism	Coverage (%)	Molecular mass (Da)	Summed Morpheus Score	Unique peptides	Region
Acidic phospholipase A_2 2	P15445	*Naja naja*	67.23	13,346	117.35	6	R1, R2, R3
Long neurotoxin 3	P25671	*Naja naja*	60.56	7833	60.47	4	R2, R3
Venom nerve growth factor	P01140	*Naja naja*	55.17	13,023	63.33	5	R2, R3
Cytotoxin 3	P24780	*Naja naja*	33.33	6745	23.46	2	R3
Cytotoxin 2a	P86538	*Naja naja*	33.33	6711	28.45	2	R2, R3
Cysteine-rich venom protein (Fragment)	P86543	*Naja naja*	30.30	3910	12.09	1	R3

2.15. Statistical analysis

Student's *t*-test and one way ANOVA were done using Sigma Plot 10.0 for Windows (version 10.0) and MS Excel, respectively to test the significance of difference in cell cytotoxicity and binding of NnPLA$_2$-I and its cognate complex (Nn(N)CM2 fraction) with respect to control as well as between them. A value of $p \leq 0.05$ was considered significant.

3. Results

3.1. 2D SDS-PAGE analysis shows non-covalent interaction of NnPLA$_2$-I with three finger toxins and nerve growth factor from NnV to form cognate complexes

The 2D SDS-PAGE of *N. naja* venom resolved the proteins according to their mass and charge. When NnV was separated under reduced conditions the anti-NnPLA$_2$-I antibodies recognized only 3 spots (R1 region) of ~15 kDa mass acidic protein(s) (Fig. 1A). The LC-MS/MS analysis of the spots of R1 (Table 1, Supplementary Table S1A) identified the presence of isoforms of acidic PLA$_2$ enzymes (Uniprot ID P15445); the major one was previously identified as NnPLA$_2$-I [4]. However, when NnV was separated under non-reduced conditions, the anti-NnPLA$_2$-I antibodies recognized proteins from two broad regions R2 (20–24 kDa, pI 3.5–5.5) and R3 (22–37 kDa; pI 8.5–10) (Fig. 1B). The LC-MS/MS analysis of R2 demonstrated co-migration of isoforms of an acidic PLA$_2$ (P15445), a long chain neurotoxin (LNTx; UniProt ID P25671), a cytotoxin (CTx; UniProt ID P86538), and a venom nerve growth factor (NGF; UniProt ID P01140) from NnV with a relative abundance (RA) of 41.0%, 34.9%, 19.3%, and 4.7%, respectively (Supplementary Fig. S1A, Table 1, Supplementary Table S1B). The LC-MS/MS analysis of R3 demonstrated co-migration of LNTx (P25671; RA – 43.6%), CTxs (P86538 and P24780; RA – 20.3%), NGF (P01140; RA – 4.2%), and a cysteine-rich secretory protein (UniProt ID P86543; RA – 1.6% RA) along with the isoforms of an acidic PLA$_2$ enzyme (P15445; RA – 30.3%) from NnV (Supplementary Fig. S1B, Table 1, Supplementary Table S1B). Tandem mass spectrometry analysis of NnPLA$_2$-I and *de novo* sequencing of its tryptic peptides showed 100% sequence similarity to P15445 (Supplementary Table S2).

The proteomic composition of Nn(N)CM2 fraction (Supplementary Fig. S2A) was found to consists of 38.2% PLA$_2$, 39.0% LNTx, 17.8% CTx, and 5.0% NGF [33] (Supplementary Fig. S2B). Fascinatingly, the composition as well as percent relative abundance of each toxin present in Nn(N)CM2 fraction was comparable to the composition and relative abundance of toxins of R2 region of NnV (Supplementary Figs. S1A, S2B). Furthermore, the acidic charge of Nn(N)CM2 fraction (Supplementary Fig. S2A) correlates well with the acidic pI of R2 proteins (Fig. 1B). Therefore, the Nn(N)CM2 fraction was considered as a cognate complex of PLA$_2$ and was used for subsequent studies. From the relative abundance of the components of the cognate complex, it was determined that 100 µg of Nn(N)CM2 fraction contains 2.9 nmol, 5.0 nmol, 2.7 nmol, and 0.4 nmol of PLA$_2$ (P15445), LNTx (P25671), CTx (P86538), and NGF (P01140), respectively showing that the approximate molar stoichiometric ratio of PLA$_2$:LNTx:CTx:NGF is 1.0:1.7:0.9:0.1. Considering the nearest integer, this ratio become 1:2:1 of PLA$_2$:LNTx:CTx and NGF may not be a real component of the complex but an associated protein formed by non-covalent interaction with the PLA$_2$ cognate complex.

RP-HPLC of Nn(N)CM2 resolved it into three major protein peaks Nn(N)CMRP1 to Nn(N)CMRP3 (Supplementary Fig. S3A). The LC-MS/MS analysis of each of these peaks identified Nn(N)CM2RP1, Nn(N)CM2RP2, and Nn(N)CM2RP3 as LNTx (P25671), PLA$_2$ (NnPLA$_2$-I; P15445), and CTx (P86538), respectively (data not shown). However, trace amounts of NGF present in the complex could not be purified by RP-HPLC.

The SDS-PAGE analysis of Nn(N)CM2 fraction under reduced conditions showed two prominent protein bands at 5–7 kDa and ~15 kDa regions (Supplementary Fig. S3B). Nevertheless, under non-reduced conditions this fraction showed a broad aggregated protein band in the molecular mass range of 14–37 kDa (Supplementary Fig. S3B) which is much higher as compared to the molecular weight of R2 region of non-reduced 2D SDS-PAGE of NnV (Fig. 1B). Snake venom proteins are known to form higher mass aggregates when stored in solution [48] and this may be the reason for which the molecular mass range of NnPLA$_2$-I-cognate complex was found to be higher by 1D SDS-PAGE analysis (Supplementary Fig. S3B). The NnPLA$_2$-I under reduced and non-reduced conditions showed a sharp and diffused band of ~15 kDa, respectively (Supplementary Fig. S3B). Size exclusion chromatography of Nn(N)CM2 demonstrated the elution of cognate complex as a single prominent broad peak from 49.8 to 62.0 ml with the highest intensity at 59.8 ml (Supplementary Fig. S3C) which corresponds to molecular mass of the cognate complex in the range of 22–39.8 kDa (Supplementary Fig. S3D). This data corroborates with the molecular mass of the cognate complex determined by 1D SDS-PAGE analysis of Nn(N)CM2 under non-reduced conditions (Supplementary Fig. S3B). Taken together, LC-MS/MS, 1D SDS-PAGE, and SEC of Nn(N)CM2 fraction demonstrated that the components of the cognate complex (PLA$_2$:LNTx:CTx) exist in a stoichiometric ratio of 1:2:1 which corresponds to molecular mass of the cognate complex at ~36 kDa. The RP-HPLC analysis did not show NGF peak (Supplementary Fig. S3A), albeit LC-MS/MS analysis suggested presence of trace amount of NGF in this complex which may not be a real component of this complex.

3.2. Cytotoxicity of PLA$_2$ and its cognate complex to mammalian and bacterial cells

The cytotoxicity exhibited by NnPLA$_2$-I (10.0 µg/ml or 0.70 µM) and two different doses of cognate complex [containing 0.35 µM and 0.70 µM of NnPLA$_2$-I, respectively as determined by ELISA (Supplementary Fig. S4) and MS2 based spectral count analysis] is shown in Fig. 2A. The NnPLA$_2$-I-cognate complex exhibited cytotoxicity against the mammalian cells in the following order - partially differentiated L6 myoblasts > platelets > PC-12 (Fig. 2A). The NnPLA$_2$-I and its cognate complex did not demonstrate cytotoxicity against erythrocytes, MCF-7, and HEK-29 cells or antibacterial activity against *B. subtilis* and *E.coli* cells (data not shown), nevertheless they exhibited marginal toxicity against platelets (Fig. 2A). However, non-covalent interaction of NnPLA$_2$-I with basic proteins of NnV to form a cognate complex did not result in increase in its catalytic activity (data not

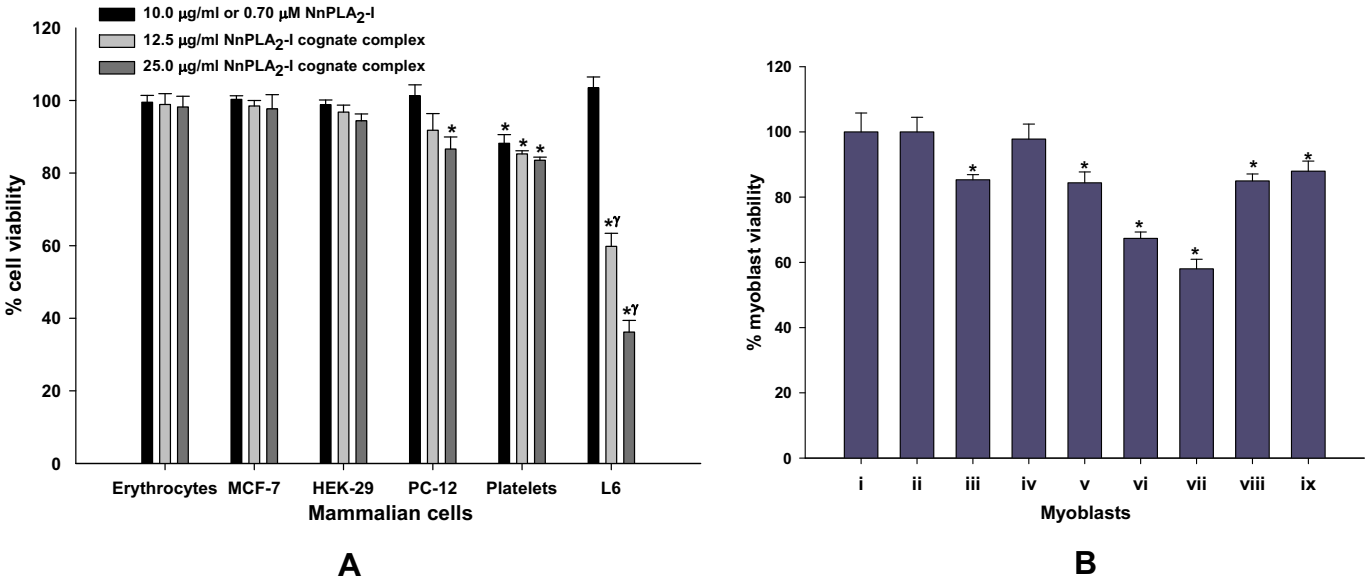

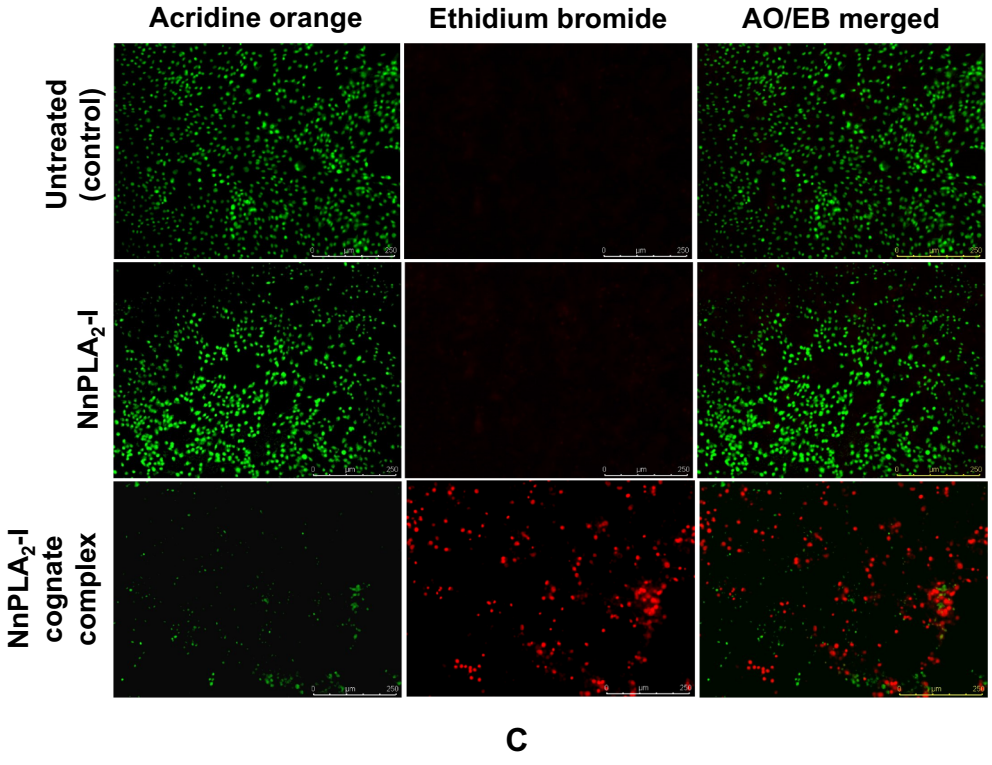

Fig. 2. Evaluation of cytotoxicity of $NnPLA_2$-I and its cognate complex. (A) Cytotoxicity (post 24 h) of $NnPLA_2$-I and its cognate complex [Nn(N)CM2] against different mammalian cells. The L6 cells used for the assay were partially differentiated myoblasts. Values are mean ± SD of three experiments. Significance of difference $^*p < 0.05$ and $^{\gamma}p < 0.05$ as compared to control and 0.70 μM $NnPLA_2$-I induced toxicity, respectively. (B) Percent cell viability determined by analysis of the bright field images (Supplementary Fig. S4B) of untreated myoblasts (i) and myoblast treated with (ii) $NnPLA_2$-I (0.70 μM), (iii) CTx (0.35 μM), (iv) LNTx (0.62 μM), (v) reconstituted CTx (0.35 μM)-LNTx (0.62 μM) complex, (vi) reconstituted CTx (0.35 μM)-LNTx (0.62 μM)-$NnPLA_2$-I (0.35 μM) complex, (vii) native $NnPLA_2$-I cognate complex (12.5 μg/ml), (viii) $NnPLA_2$-I cognate complex (12.5 μg/ml) pre-incubated with anti-$NnPLA_2$-I antibodies at 1: 25 ratio, (ix) $NnPLA_2$-I cognate complex (12.5 μg/ml) pre-incubated with 5.0 mM *p*-BPB. The myoblasts were initially seeded with cell count of 1×10^3 cells per well, and allowed to partially differentiate for 5 days in DMEM containing 2% FBS. Values are mean ± SD of three sets of experiments. Significance of difference $^*p < 0.05$ and $^{\gamma}p < 0.05$ as compared to control and 12.5 μg/ml $NnPLA_2$-I cognate complex- induced cytoxicity, respectively. (C) Fluorescent microscopic images (10 X) of AO/EB stained partially differentiated L6 myoblasts treated with PBS (control), $NnPLA_2$-I (0.70 μM), and $NnPLA_2$-I cognate complex (12.5 μg/ml containing 0.35 μM of $NnPLA_2$-I). The green colour shows live cell nuclei whereas red colour shows dead nuclei of treated cells.

shown).

The NnPLA$_2$-I cognate complex showed highest toxicity against partially differentiated rat myoblasts which was also confirmed by measuring the enhanced release of CK and LDH from the treated cells compared to control cells. The NnPLA$_2$-I had no effect on release of these enzymes albeit NnPLA$_2$-I-cognate complex significantly enhanced the release of CK and LDH from L6 cells to the culture media (Supplementary Table S3). The cytotoxicity exhibited by the native cognate complex was significantly higher as compared to the individual components of this complex (NnPLA$_2$-I, LNTx, and CTx), re-constituted CTx-LNTx complex and re-constituted CTx-LNTx-PLA$_2$ complex (Supplementary Table S4). Furthermore, pre-incubation of NnPLA$_2$-I-cognate complex with PAV, anti-NnPLA$_2$-I antibody, and *p*-BPB resulted in a significant reduction of its cytotoxicity against partially differentiated rat myoblasts; PAV was more effective in reducing the cytotoxicity of NnPLA$_2$-I-cognate complex whereas anti-NnPLA$_2$-I antibody showed higher inhibition of PLA$_2$ activity of the cognate complex (Supplementary Table S4). Treatment with *p*-BPB resulted in a significant reduction of the catalytic activity and cytotoxic property of the NnPLA$_2$-I cognate complex (Supplementary Table S4). However, addition of PAV to rat myoblast culture medium post 60–240 min of treatment with NnPLA$_2$-I cognate complex resulted in a gradual loss of its cytotoxicity inhibition property (Supplementary Table S4).

The NnPLA$_2$-I-cognate complex-induced cytotoxicity towards partially differentiated L6 myoblasts was also evident from the bright field microscopic observation of the treated cells (Supplementary Fig. S5, Fig. 2B). The L6 myoblasts (Supplementary Fig. S5A) were allowed to partially differentiate to elongated spindle shaped myoblasts before treatment [Supplementary Fig. S5B, panel (i)]. The cells treated with reconstituted CTx-LNTx-NnPLA$_2$-I complex [Supplementary Fig. S5B, panel (vi)] or NnPLA$_2$-I native cognate complex [Supplementary Fig. S5B, panel (vii)] demonstrated significant decrease in cell number and changes in the cellular morphology (marked with red arrows) as compared to the cells treated with the individual toxins (NnPLA$_2$-I, CTx, and LNTx) of the complex [Supplementary Fig. S5B, panels (ii), (iii) and (iv)] or re-constituted CTx-LNTx complex [Supplementary Fig. S5B, panel (v)]. In addition to decrease in cell number, the partially differentiated myoblasts treated with reconstituted 3FTx-NnPLA$_2$-I complex [Supplementary Fig. S5B, panel (vi)] and native cognate complex [Supplementary Fig. S5B, panel (vii)] showed loss of well distended elongated structure of the cells (shown with arrows); albeit the latter showed significantly higher toxicity than that of the former. The higher toxicity of cognate complex compared to reconstituted complex (devoid of NGF) (Fig. 2B) suggests that NGF present in the native cognate complex plays a role in the cytotoxic property of this complex. Pre-incubation of NnPLA$_2$-I-cognate complex with anti-NnPLA$_2$-I antibodies [Supplementary Fig. S5B, panel (viii)] or 5 mM *p*-BPB [Supplementary Fig. S5B, panel (ix)] significantly inhibited its cytotoxic property against rat myogenic cells (Fig. 2B). The fluorescent microscopic observation of NnPLA$_2$-I-cognate complex treated myogenic cells after acridine orange and ethidium bromide (AO/EB) staining showed dead nuclei stained red with dispersed nuclear matter (Fig. 2C) due to disintegration of nuclei.

3.3. Time-dependent binding and internalization of NnPLA$_2$-I in rat myogenic cells

It was found that NnPLA$_2$-I alone and in association with other basic proteins of NnV (cognate complex) binds to partially differentiated L6 myoblasts; however, in cognate complex form it showed significantly higher binding ($p < 0.05$) compared to binding of individual NnPLA$_2$-I (Fig. 3A). Time-dependent (30, 60, 120, and 240 min) incubation of these cells with 0.70 μM of NnPLA$_2$-I followed by fluorescent staining demonstrated binding followed by time-dependent internalization of NnPLA$_2$-I in myogenic cells (Fig. 3B). Observation under a confocal microscope confirmed the time-dependent internalization of FITC conjugated NnPLA$_2$-I (Fig. 3C). The *Z*-stack analysis of each image, which has been used for deconvolution of confocal microscopy data [45], demonstrated localization of NnPLA$_2$-I (green colour) in the cytoplasm of the myogenic cells (Supplementary Fig. S6).

3.4. The NnPLA$_2$-I in its cognate complex compared to individual NnPLA$_2$-I showed significantly higher binding to vimentin of L6MP

The ELISA revealed the binding of NnPLA$_2$-I and its cognate complex to L6MP albeit they showed insignificant binding to L6CP (Fig. 4A). Further, by immunoblot analysis we could not detect the binding of NnPLA$_2$-I and its cognate complex to L6CP (data not shown). The NnPLA$_2$-I in its cognate complex showed significantly higher binding ($p < 0.05$) to L6MPs compared to individual NnPLA$_2$-I (Fig. 4A). Immuno-blot analysis indicated binding of NnPLA$_2$-I to ~55 kDa and to a lesser extent ~48 kDa L6MP (Fig. 4B, C, Supplementary Fig. S7A) and this binding was significantly enhanced when the NnPLA$_2$-I was in its cognate complex with other proteins of NnV (Fig. 4B, C). Immunoblot analysis also demonstrated binding of NnPLA$_2$-I cognate complex with a L6MP protein band of ~40 kDa (lane 2 of Fig. 4B). Because no corresponding band was detected in lane 1 (L6MP incubated with NnPLA$_2$-I), therefore, this band was not considered for further analysis.

The RP-HPLC fractionation of NnPLA$_2$-I-bound L6MP isolated by affinity chromatography was resolved into one major peak (L6RP1) and four minor peaks (L6RP2-L6RP5) (Supplementary Fig. S7B). ELISA demonstrated binding of NnPLA$_2$-I with the major protein peak L6RP1 (data not shown). Tandem mass spectrometry analysis of L6RP1 identified it as vimentin (UniProt ID P31000) (Supplementary Table S5).

The LC-MS/MS analysis of ~48 kDa and ~55 kDa membrane protein bands showing binding with Nn-PLA$_2$-I and its cognate complex demonstrated highest resemblance with vimentin (M_r = 53.5 kDa) from *Rattus norvegicus* (UniProt ID P31000), an intermediate filament of the cytoskeletal (Supplementary Table S5). The proteomic analysis of ~48 kDa protein demonstrated a truncated vimentin where its 20 amino acid residues (~5.4 kDa) from N-terminal region (head-region) were found to be missing. Strikingly, the ~48 kDa L6MP band primarily comprised of tubulin α3 (40%), tubulin β5 (12%) chains of myoblast cytoskeleton, and vimentin (5.3%) whereas the ~55 kDa L6MP band primarily consists of vimentin (58.1%) followed by protein disulfide-isomerase (P04785; 26.9%) and caveolae-associated protein 1 (UniProt ID P85125; 15.0%) (data not shown). However, NnPLA$_2$-I bound L6MP and RP-HPLC purified L6RP1 was composed of 89.3% and 100% vimentin (P31000), respectively.

3.5. Spectrofluorometric analysis evidenced the dose and time-dependent increase in binding of NnPLA$_2$-I and its cognate complex to vimentin

Increasing concentration of NnPLA$_2$-I and its cognate complex led to decrease in fluorescence of vimentin suggesting protein–protein interactions leading to quenching of aromatic residues of vimentin (Fig. 5A, B). A saturation in binding with vimentin was observed at a 0.35 μM concentration of NnPLA$_2$-I (Fig. 5A inset) and the optimum time for NnPLA$_2$-I-vimentin binding was observed at 15 min post incubation of interacting proteins (Fig. 5C). In a sharp contrast, NnPLA$_2$-I cognate complex at a concentration of 25.0 μg/ml (containing 0.70 μM of NnPLA$_2$-I) did not show saturation of binding with vimentin (Fig. 5B inset). The optimum time of binding of NnPLA$_2$-I cognate complex with vimentin was observed 45 min post incubation (Fig. 5D).

3.6. In silico analysis demonstrated superior binding of NnPLA$_2$-I in its cognate complex compared to individual NnPLA$_2$-I with the rod region of vimentin

The interaction between the different regions of vimentin (as receptor) and NnPLA$_2$-I (as ligand) was predicted to be strong and stable

with predicted binding free energy (ΔG) and dissociation constant (K_D) values of −12.86 kcal/mol and 3.67×10^{-10} M, respectively. The best predicted structure of $NnPLA_2$-I (Supplementary Fig. S8) showed interaction with all the four chains (PDB IDs 3s4rB, 3uf1A, 3trtA, and 1gk4D) of vimentin with negative global energy; the highest binding was noted with 3s4rB followed by 3trtA chains (Table 2A). PDBSum analysis of the $NnPLA_2$-I – 3s4rB model (Fig. 6A, panels I, II) showed that 19 residues of $NnPLA_2$-I interacted with 15 residues of 3s4rB *via* 120 non-bonded contacts, 12H-bonds, and 4 salt bridges suggesting strong affinity between the these two proteins (Fig. 6A, panel III; Table 2A). Nevertheless, 22 residues of $NnPLA_2$-I interacted with 3trtA region of vimentin (15 residues) by 147 non-bonded contacts, 12H-bonds and 2 salt bridges (Fig. 6B, Table 2A). Interestingly, the Asp48 residue of $NnPLA_2$-I has been predicted to be involved in salt bridge and/or H-bonds formation with the two regions of vimentin (panel III of Fig. 6A, B). The $NnPLA_2$-I also showed binding to 3uf1A (Supplementary Fig. S9A) and 1gk4D (Supplementary Fig. S9B) regions of vimentin *via* non-bonded contacts and H-bonds; however, this binding strength was determined to be less as compared to that of 3s4rB and 3trtA regions (Table 2A).

The *in silico* analysis showed that $NnPLA_2$-I forms a stable complex with 3FTxs and NGF of NnV (Supplementary Fig. S10A, B) with negative global energies (Table 2B). Although individual components of $NnPLA_2$-I-cognate complex showed binding to 3s4rB and 3trtA chains of vimentin (Supplementary Fig. S11A–F) albeit the 3FTx-$NnPLA_2$-I complex showed slightly lower binding efficiency to 3s4rB (Fig. 6C) and 3trtA (Fig. 6D) chains as compared to binding to these regions by individual $NnPLA_2$-I (Table 2B). In this complex, only $NnPLA_2$-I showed binding to 3s4rB region of vimentin *via* 94 non-bonded contacts, 6H-bonds and 3 salt bridges (Fig. 6C). The PDBsum server did not predict direct interactions between 3FTxs of the cognate complex and 3s4rB region of vimentin (Fig. 6C). However, both $NnPLA_2$-I and LNTx interacted with 3trtA region of vimentin *via* non-bonded contacts (88 and 49, respectively) and H-bonds (4 and 2, respectively) (Fig. 6D). However, the $NnPLA_2$-I-3FTx-NGF complex showed higher binding to both 3s4rB and 3trtA regions of vimentin (Table 2B). In the complex, both $NnPLA_2$-I and NGF showed binding to 3s4rB region of vimentin *via* non-bonded contacts (94 and 48, respectively), H-bonds (6 and 3, respectively), and salt bridges (3 each) (Fig. 6E, Supplementary Table S6A). Similar interactions were predicted for the interaction between $NnPLA_2$-I cognate complex and 3trtA region of vimentin (Supplementary Table S6B). It was observed that $NnPLA_2$-I interacted with vimentin *via* 118 non-bonded contacts, 7H-bonds and 2 salt bridges, whereas NGF interacted with 3trtA region of vimentin through 35 non-bonded contacts, 4H-bonds and 1 salt bridge (Fig. 6F, Supplementary Table S6B). The presence of NGF in the complex, therefore, may enhance the binding with vimentin which corroborates with the *in vitro* results.

ELISA result demonstrated that pre-incubation of vimentin with anti-vimentin monoclonal antibodies against the tail region of vimentin did not affect the binding of $NnPLA_2$-I or its cognate complex to vimentin (data not shown), suggesting that $NnPLA_2$-I binds to vimentin other than its tail region. However, due to unavailability of commercial monoclonal antibodies against the rod and head regions of vimentin, the interaction of $NnPLA_2$-I with the rod region of vimentin could not be further confirmed by *in vitro* analysis.

4. Discussion

Toxin synergism, a fascinating phenomenon to enhance toxicity of interacting components has been well documented in many different snake venoms albeit this phenomenon is poorly investigated and understood to date [57–60]. The LC-MS/MS analysis of NnV separated by 2D SDS-PAGE under reduced and non-reduced conditions unambiguously demonstrated the formation of $NnPLA_2$-I-3FTxs-NGF cognate complex, may be by weak non-covalent interactions among the components of cognate complex [61,62]. The significant enhancement of cytotoxicity of $NnPLA_2$-I as a component of the cognate complex compared to individual $NnPLA_2$-I is evident from the facts that – (a) $NnPLA_2$-I alone cannot induce cytotoxicity in partially differentiated rat myoblasts, and (b) neutralization with anti-$NnPLA_2$-I antibodies or alkylation of His48 active site of $NnPLA_2$-I significantly reduced the cytotoxic effect of $NnPLA_2$-I cognate complex. This result is in accordance with previous reports demonstrating several snake venom toxins tend to form a stable or cognate complex of higher molecular mass that significantly potentiate their cytotoxicity and pharmacological property against target cells and/or organisms [48,61,63–65]. It has also been well documented that cytotoxins and neurotoxins from cobra venom can form a stable cognate complex with the catalytically active PLA_2s from the same venom [58,59,62,66,67]; however, this binding may not enhance the catalytic activity of PLA_2 enzyme which is according to our previous observation [62]. Therefore, it is not surprising that $NnPLA_2$-I cognate complex would show a significantly higher cytotoxicity as compared to individual components of the complex. Further, partially differentiated rat myoblast are of mesenchymal origin and a significantly higher cytotoxicity of $NnPLA_2$-I cognate complex on this cell suggests the probable pathophysiological role of this complex in cobra venom-induced myopathy and muscular damage [21,22,68]. However, the other pathophysiological function(s) of this complex in cobra bite patients, if any, remains to be explored.

The cognate complex of $NnPLA_2$-I showed significantly higher cytotoxicity in myogenic cells as compared to other mammalian cells. Several factors including phospholipids composition of the target cell membrane, cholesterol/phospholipids ratio, physicochemical properties of a membrane, and/or presence of a specific toxin receptor in the cell surface may play an important role in snake venom-induced membrane damage and/or cytotoxicity [25,26,58,59]. Our previous study has demonstrated preferential binding of $NnPLA_2$-I to phosphatidylcholine (PC) as compared to phosphatidylethanolamine (PE) or phosphatidylserine (PS) [4]. The differential composition of PC as well as occurrence of a large number of PLA_2-sensitive PC domain in the outer plasma membrane of the treated mammalian cells may explain the higher cytotoxicity of $NnPLA_2$-I and/or its cognate complex towards rat myogenic cells compared to other mammalian cells [16,58]. Further, the PLA_2-interacting cobra venom neurotoxins are also reported to display cell-specific cytotoxicity on mammalian cells [58] which further supports the differential cytotoxicity of $NnPLA_2$-I-cognate complex on mammalian cells. Furthermore, $NnPLA_2$-I and its cognate complex cannot show antibacterial activity due to absence of PC and low number of PLA_2 sensitive phospholipid (PE) domains on the outer membrane of bacterial cells [15].

It has been well documented that snake venom PLA_2s bind to certain phospholipid micro-domains of cell membranes that acts as a platform for PLA_2 adhesion and catalysis leading to cellular disintegration [14,16]; nevertheless, only few studies have shown the binding of snake venom PLA_2s to protein receptor(s) present on outer surface of cell membrane [18,19,30,69,70]. Further, except for plasma membrane bound nucleolin [30], there is dearth of knowledge regarding the consequence or pathophysiological significance of interaction/binding of snake venom PLA_2 to other cell surface receptors/acceptors. The present study suggests a high affinity binding of $NnPLA_2$-I to a ~55 kDa protein acceptor, vimentin, present in outer membrane of rat myoblasts and this binding as well as cytotoxicity against the myoblasts was significantly enhanced when $NnPLA_2$-I exists in a cognate complex. Cobra venom cytotoxins and PLA_2-interacting neurotoxins have been shown to kill the cells by non-selectively disrupting the cell membranes [58,59,66,67]. These reports corroborate well with the present study showing $NnPLA_2$-I cognate complex also retains a part of its cytotoxicity after treatment with anti-PLA_2 antibodies or alkylation of His-48 of $NnPLA_2$-I with *p*-BPB. Therefore, it may be anticipated that after binding with rat myoblasts, the cytotoxin and neurotoxin components of the cognate complex first destabilize the phospholipids bilayer of the

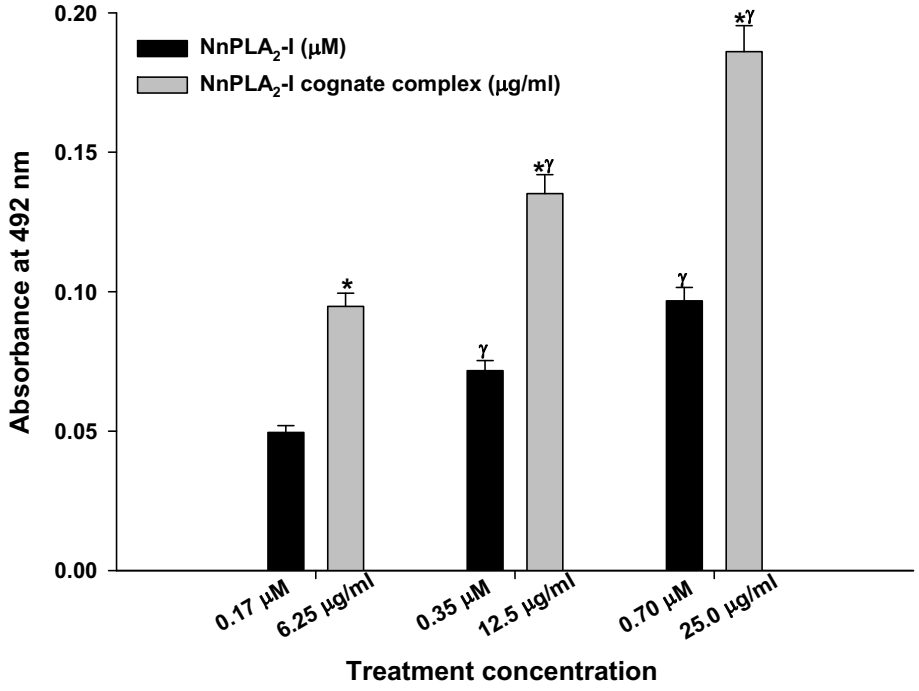

A

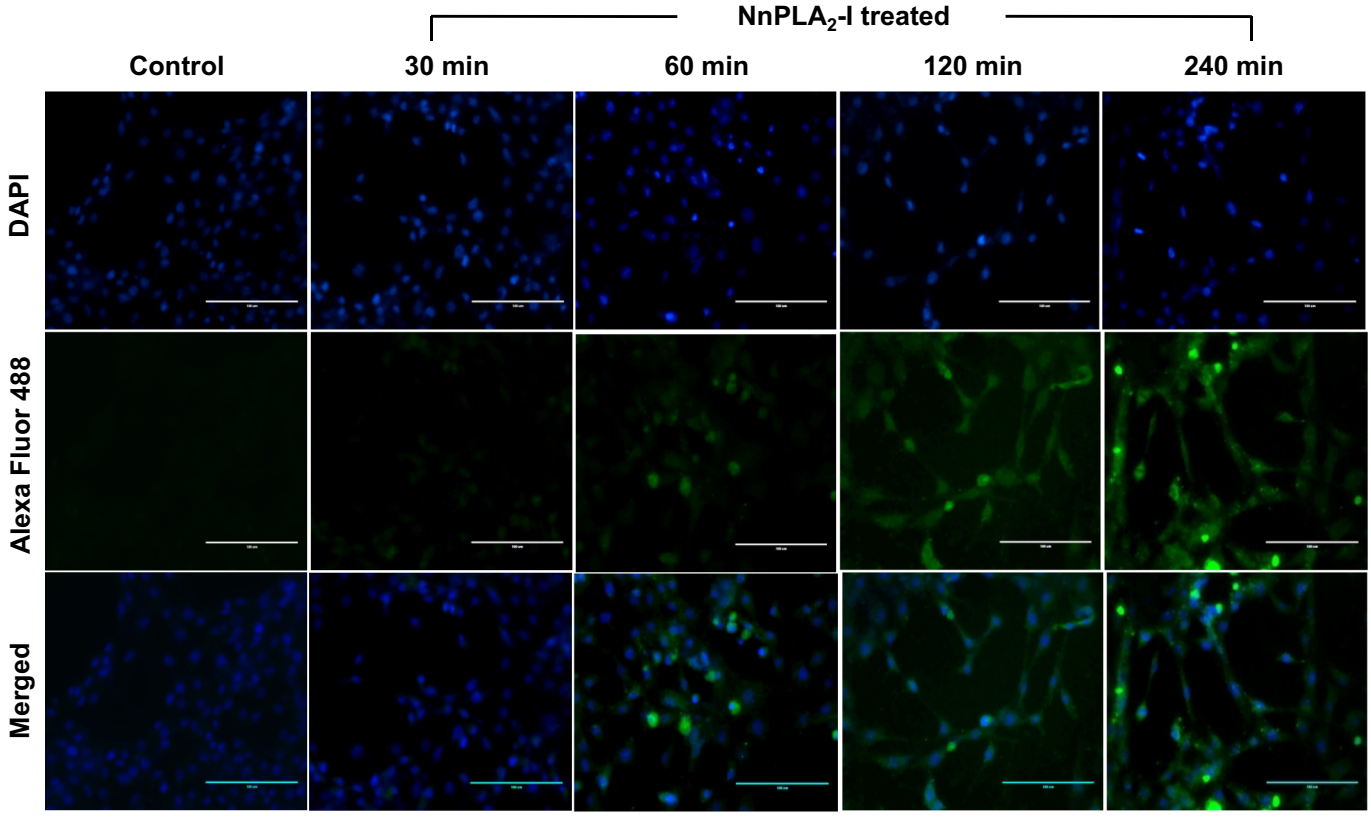

B

(caption on next page)

Fig. 3. Binding followed by internalization of $NnPLA_2$-I in L6 rat myoblasts. (A) Dose-dependent binding of $NnPLA_2$-I (0.17–0.70 μM) and its cognate complex (6.25–25.0 μg/ml) to L6 myoblasts. The binding was determined by ELISA using anti-$NnPLA_2$-I antibodies and HRP conjugated goat anti-rabbit IgG. Values are mean ± SD of triplicate determinations. Significance of difference *$p < 0.05$ with respect to $NnPLA_2$-I, and $^{\gamma}p < 0.05$ as compared to the cognate complex (6.25 μg/ml). (B) Fluorescence microscopic images (40 X) showing time-dependent (30–240 min) internalization of $NnPLA_2$-I (0.70 μM) in L6 rat myoblasts. The $NnPLA_2$-I was detected using anti-$NnPLA_2$-I antibody raised in rabbit. The green images are due to Alexa fluor 488 conjugated anti-rabbit IgG (secondary antibody) visualized under FITC filter whereas blue images for nuclear staining by DAPI were visualized under DAPI filter. (C) Confocal microscopic images (63× magnification) showing time-dependent internalization of FITC-conjugated $NnPLA_2$-I (0.70 μM) after 30–240 min incubation with L6 myoblasts. Green (for $NnPLA_2$-I) and blue (for nucleus) images were visualized under FITC and DAPI filters, respectively. Bar scale = 10 μM.

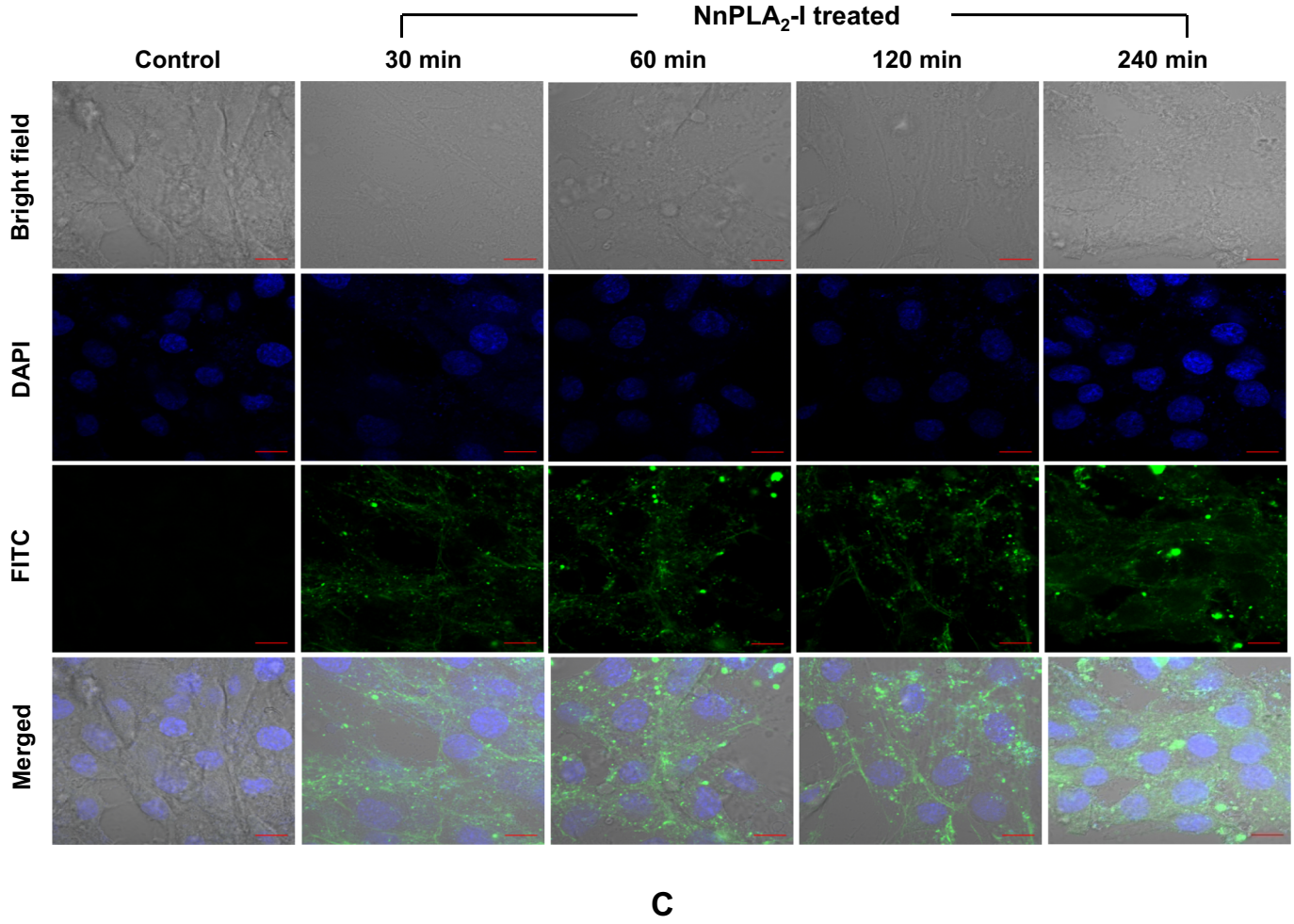

Fig. 3. (*continued*)

target cell membranes that leads to higher binding of PLA_2 on dislocated and disorganized phospholipids bilayer of myoblasts resulting in a significantly higher ($p < 0.01$) membrane damage and cell death by $NnPLA_2$-I-cognate complex compared to individual $NnPLA_2$-I or 3FTxs [59,62,66].

Studies have shown a synergism between PLA_2s and 3FTxs [58,59,62,64,66,67]; however, their exact mechanism of pathophysiological function in complex form remains to be explored. Another minor component associated with the $NnPLA_2$-I complex was determined to be an NGF which is one of the most fascinating proteins found in cobra venom [71,72]. The presence of NGF significantly enhanced the cytoxicity of the cognate complex. Although non-toxic in isolation [72], this class of proteins in association with other venom toxins is known to elicit severe toxicity against different cell lines [71]. Owing to its specificity towards vimentin, it may be anticipated that cobra venom PLA_2 and/or 3FTxs employ NGF as a carrier to specific target sites [71,73] to enhance the toxicity of the cognate complex. This phenomenon reinstates the effect of toxin synergism wherein the presence of even a trace quantity of one or more venom toxin potentiates the pharmacological effect of other venom proteins [48,65]. Nevertheless, further characterization of each individual component of cognate complex is necessary to study their exact stoichiometry of interactions to form a stable complex [48] as well as to explore their definite role in binding with membrane lipids and/or proteins.

Vimentin is a type III intermediate filament (IF) protein of the cytoskeleton known to be constitutively expressed in mesenchymal cells [74] and is mainly involved in tissue integrity. Vimentin serves as a target for human group IIA (hGIIa) PLA_2 enzyme to enhance the binding of the latter to activated T-cells in inflamed synovium of rheumatoid arthritis patients [75]. Further, hGIIa internalizes and co-localizes with vimentin in rheumatoid fibroblast-like synoviocytes [76] which indicates the association of PLA_2 with vimentin in a pathophysiological process. Vimentin is also one of the fifteen proteins that interacted and co-localized with *Bothrops asper* Lys49 myotoxin II (Mt-II) in C2C12 myotubes [30] thereby re-instating the involvement of such an interaction with pathophysiology of snakebite.

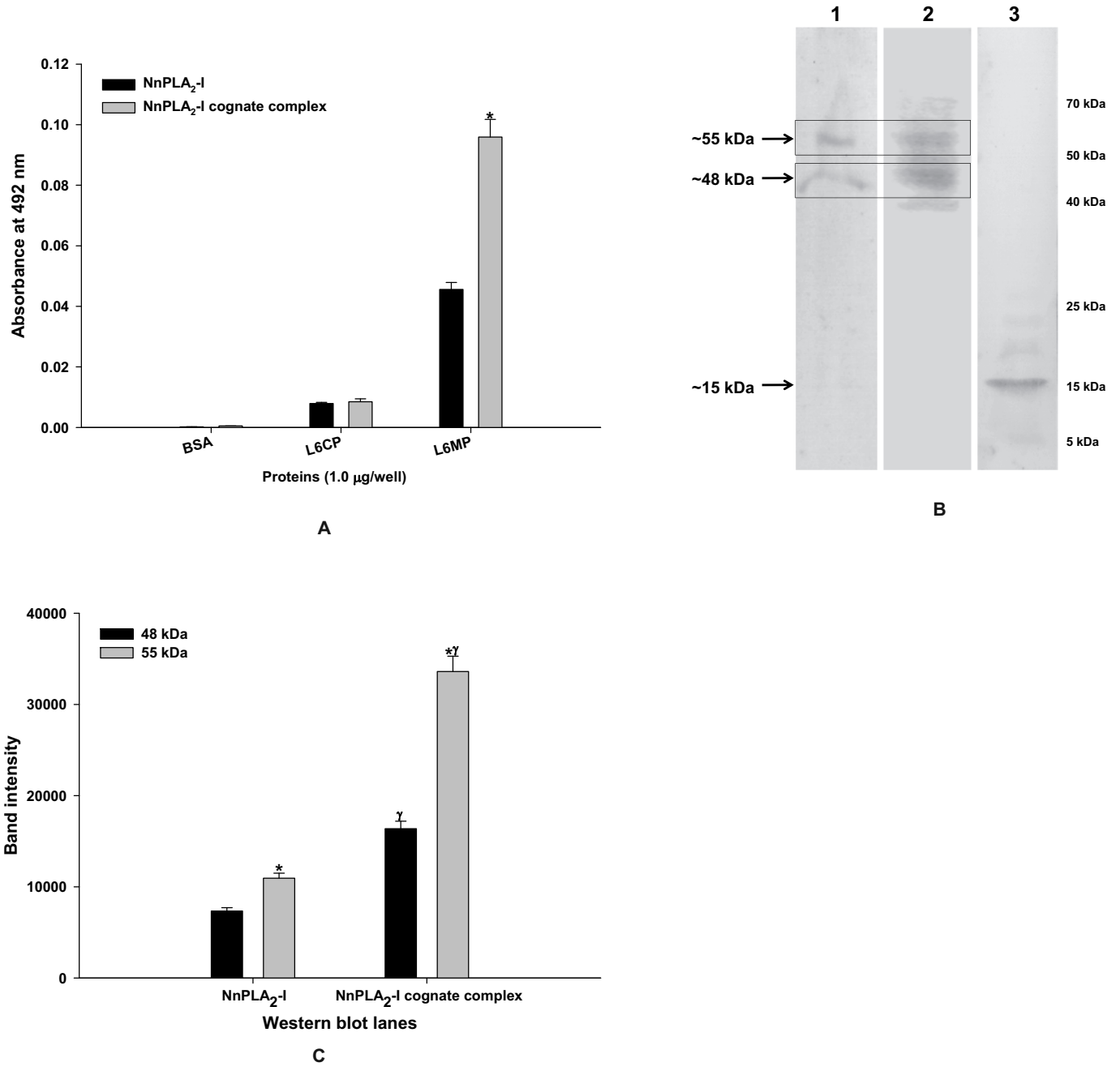

Fig. 4. Binding of $NnPLA_2$-I and its cognate complex to membrane protein(s) of rat myoblasts. **(A)** ELISA to determine the binding of $NnPLA_2$-I (0.70 µM) and $NnPLA_2$-I in its cognate complex (25.0 µg/ml containing 0.70 µM $NnPLA_2$-I) to L6CP, L6MP, and BSA (negative control). The binding was detected using rabbit anti-$NnPLA_2$-I antibodies (primary antibody) and HRP-conjugated anti-rabbit IgG (secondary antibodies). Values are mean ± SD of triplicate determinations. Significance of difference with respect to binding of $NnPLA_2$-I, *$p < 0.05$. (B) Immunoblot analysis to determine the binding of $NnPLA_2$-I and $NnPLA_2$-I-cognate complex to L6MP. The L6MP (80 µg, non-reduced) and NnV (80 µg, reduced) were separated by 12.5% SDS-PAGE and transferred to PVDF membrane: lane 1, L6MP incubated with $NnPLA_2$-I (0.70 µM); lane 2, L6MP incubated with cognate complex (25.0 µg/ml containing 0.70 µM $NnPLA_2$-I); lane 3, NnV (positive control). The detected protein bands detected by anti-Nn-PLA_2-I antibodies are shown with arrows. (C) Densitometry analysis of ~48 kDa and ~55 kDa L6MPs showing interaction with $NnPLA_2$-I/cognate complex. Values are mean ± SD of triplicate determinations. Significance of difference *$p < 0.05$ with respect to 48 kDa band intensity; $^{\gamma}p < 0.05$ as compared to binding by $NnPLA_2$-I.

Vimentin is reported to be expressed on the surface of different cells such as apoptotic neutrophils, T cells [77], activated macrophages [78], vascular endothelial cells [79], skeletal muscle cells [80], and platelets [81] by some unknown mechanism or by post-translational modification of vimentin [82]. The involvement of cell surface vimentin in binding with several extracellular proteins, toxins, and microorganisms has been well documented [51,79,83]; nevertheless, this is the first report suggesting the role of membrane bound vimentin as a myogenic cell surface acceptor for NnV acidic PLA_2 enzyme. It has been suggested that there may be several receptor(s) in a cell responsible for binding to different types of PLA_2 enzymes [18]. The binding with vimentin was found to be critical for initiation of infection and pathogenesis by the virulent strain of Japanese encephalitis virus [84] and the present study shows a crucial vimentin – *N. naja* venom PLA_2 interaction which may

have a role in inducing cytotoxicity. Further, pre-incubation of cognate complex with polyvalent antivenom has shown to reduce its cytotoxicity towards rat myoblasts which advocates early antivenom therapy for successful management of cobra bite patients. Although it was expected that $NnPLA_2$-I and its cognate complex should also show binding to intracellular vimentin present in cytosolic proteins of partially differentiated rat myoblasts, however, our observation was quite contrary. Interference from other cytosolic proteins or specific conformational changes of cytosolic vimentin may influence this binding; however, extensive studies would be required to pin-point the differences in binding between membrane bound and cytosolic vimentin.

Vimentin is composed of three regions - a head, which initiates and direct the filament assembly; a rod region and a tail region [85]. The *in silico* analysis indicated that the rod region of vimentin may be involved in high affinity binding to $NnPLA_2$-I by a mechanism similar to the binding of dengue virus and *Clostridium botulinum* C3 exoenzyme to the rod region of vimentin present in outer surface of vascular endothelial cells and hippocampal HT22 cells, respectively [79,86]. $NnPLA_2$-I internalization in myoblasts may be associated to its binding with vimentin in a manner similar to vimentin mediated uptake of C3 exoenzyme to hippocampal HT22 cells [83,86]. Further, the *in silico* study has provided a strong evidence of higher binding of $NnPLA_2$-I-cognate complex to vimentin compared to individual $NnPLA_2$-I.

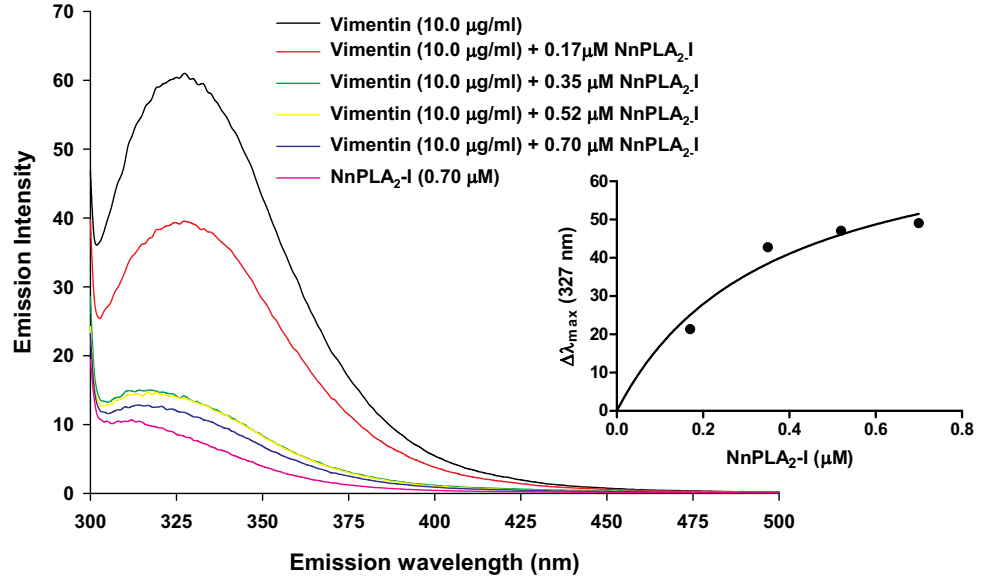

A

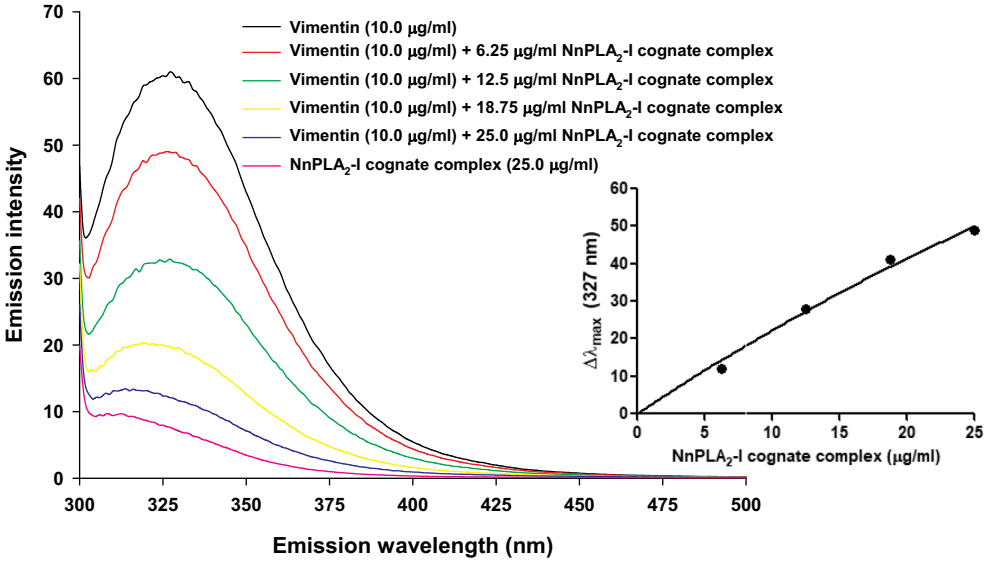

B

Fig. 5. Spectrofluorometric analysis to determine the dose-dependent binding of (A) $NnPLA_2$-I (0.17–0.70 µM), and (B) $NnPLA_2$-I cognate complex (6.25–25.0 µg/ml) to vimentin (10.0 µg/ml). The time-dependent (7.5–60 min) binding of (C) $NnPLA_2$-I (0.17 µM), and (D) $NnPLA_2$-I cognate complex (6.25 µg/ml) to vimentin (10.0 µg/ml).

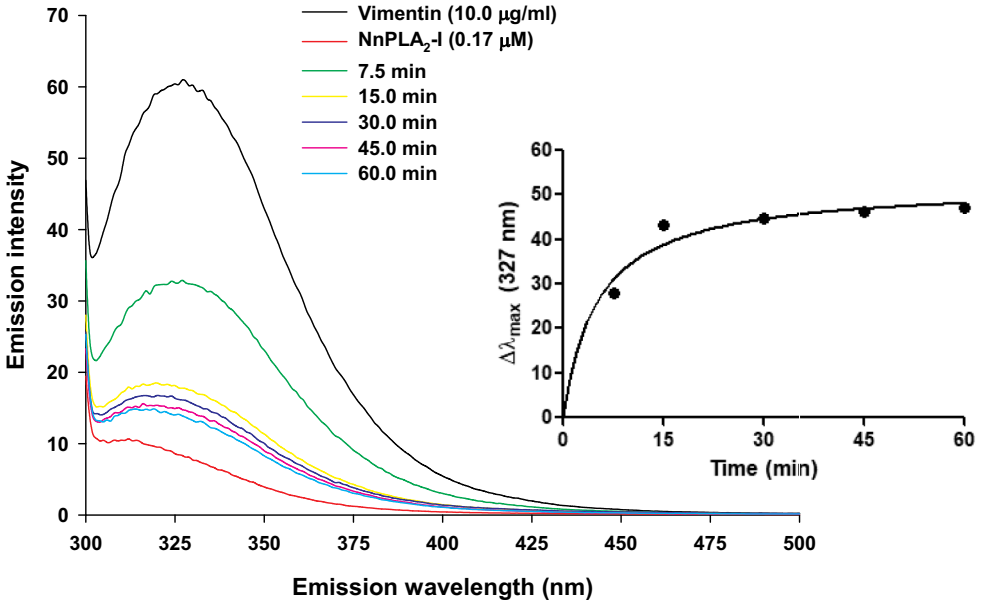

C

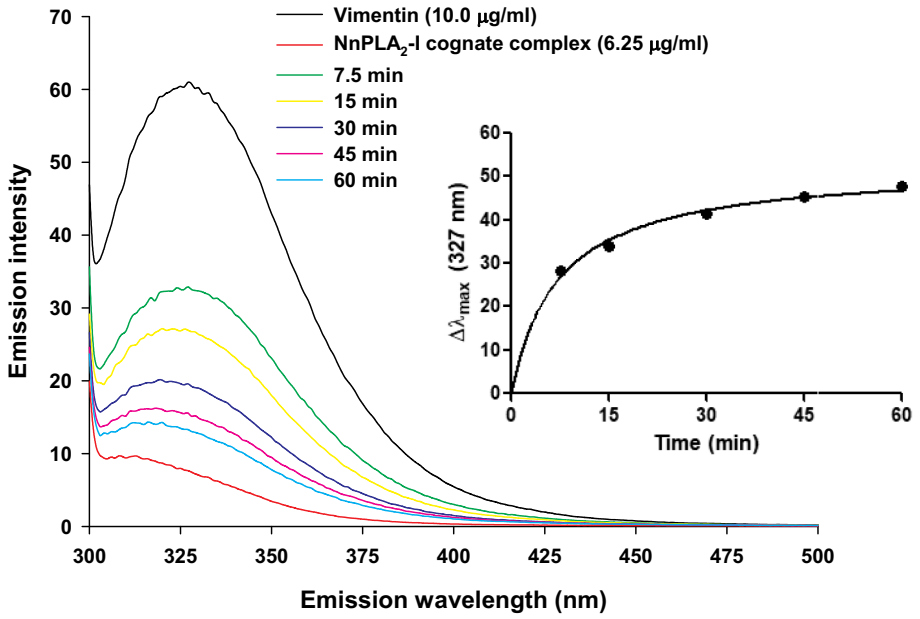

D

Fig. 5. (*continued*)

Table 2A
A comparison of the global energy of binding of $NnPLA_2$-I to different regions of rod structure of vimentin. The global energy values were predicted using Firedock server and the types of interactions were determined using PDBSum server.

Chain of vimentin (PDB ID)	Amino acid region	Global energy	Non-bonded contacts	Hydrogen bonds	Salt bridges
3s4rB	99–189	−111.04	120	12	4
3uf1A	146–249	−82.55	86	8	0
3trtA	261–335	−107.58	147	12	2
1gk4D	330–407	−100.68	156	7	0

5. Conclusion

The study reports for the first time a strong interaction between an acidic PLA_2 from NnV and membrane bound vimentin of partially differentiated rat myoblasts. In addition to phospholipid microdomains of the plasma membranes, the membrane bound vimentin may serve as an additional acceptor for snake venom PLA_2 enzymes for exerting cytolytic and/or cytotoxic effects. The enhanced binding and toxicity of PLA_2-CTx-LNTx-NGF cognate complex as compared to individual $NnPLA_2$-I sheds light on the possible role of vimentin as a cellular acceptor in cobra venom PLA_2 complexes induced cytotoxicity. Further studies are required to understand the stoichiometry of each component in the cognate complex and their associated roles in pathophysiology of cobra bite.

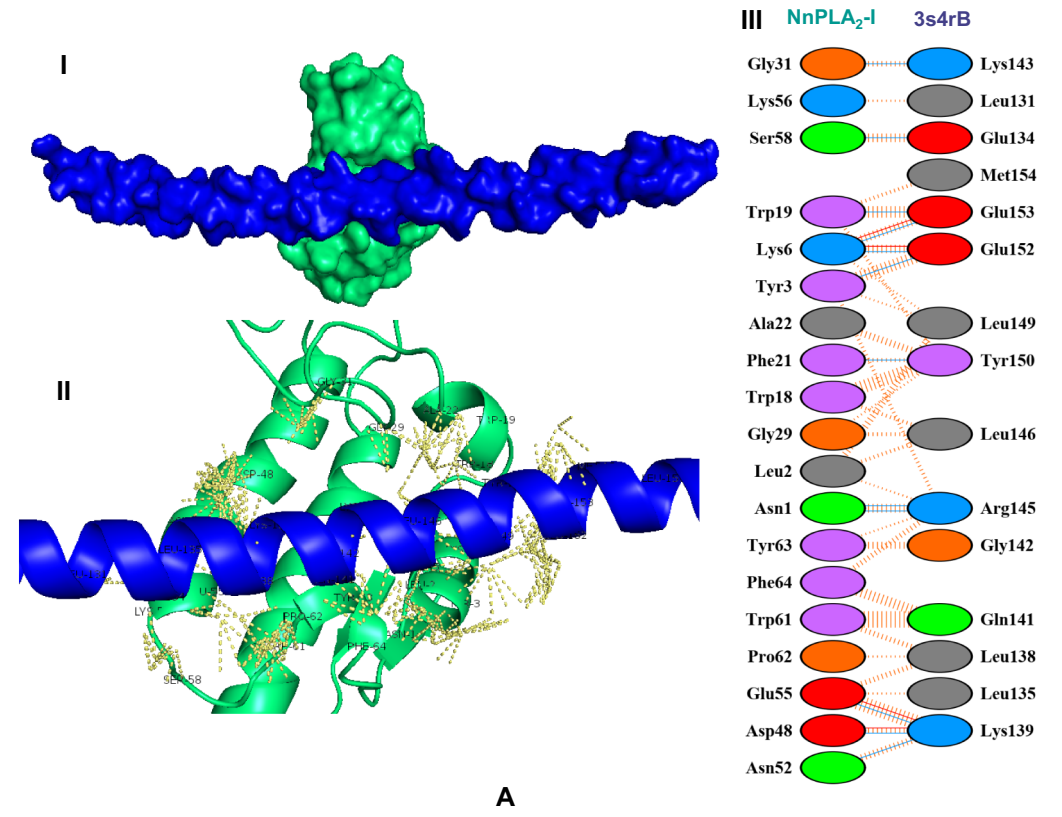

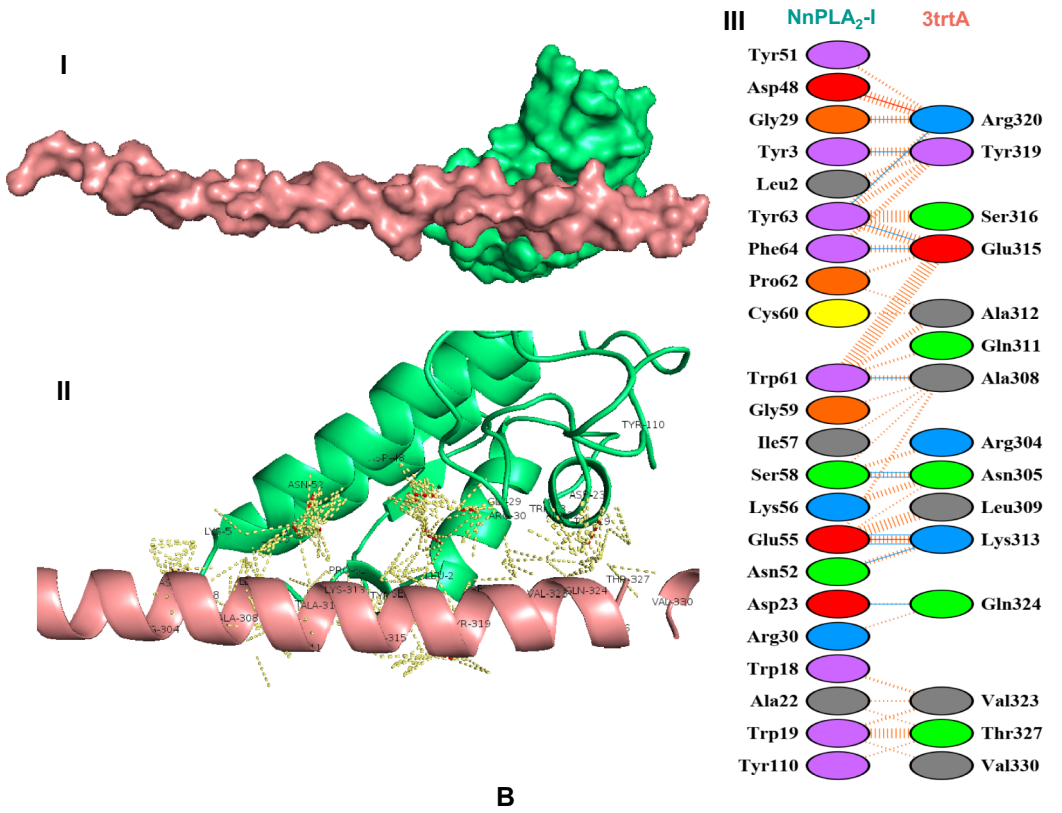

Fig. 6. Most favorable docking models predicted by ClusPro 2.0 server and refined by Firedock server for determining the interaction of $NnPLA_2$-I (green chain) with (A) 3s4rB chain (blue colour) and (B) 3trtA chain (light pink colour) of vimentin. Best docking model of $NnPLA_2$-I-3FTx complex with (C) 3s4rB and (D) 3trtA chains of vimentin. Best docking model of $NnPLA_2$-I-3FTx-NGF complex with (E) 3s4rB and (F) 3trtA chains of vimentin. All models have been visualized using PyMol software.

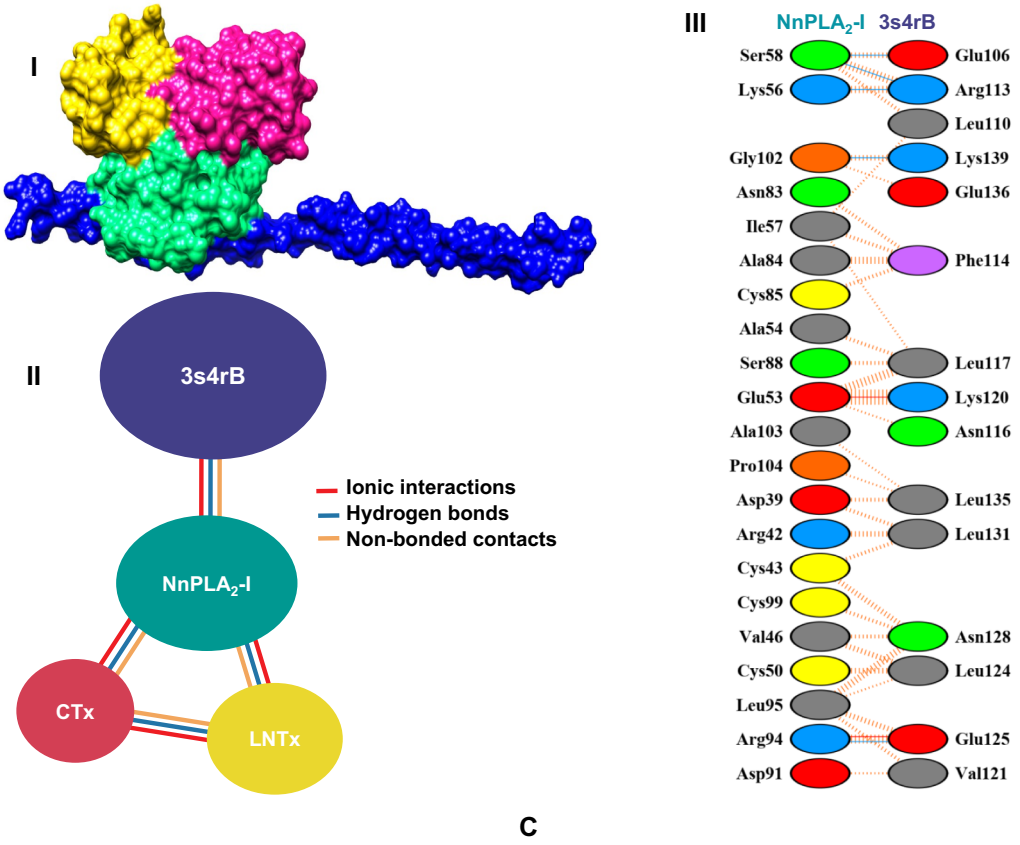

C

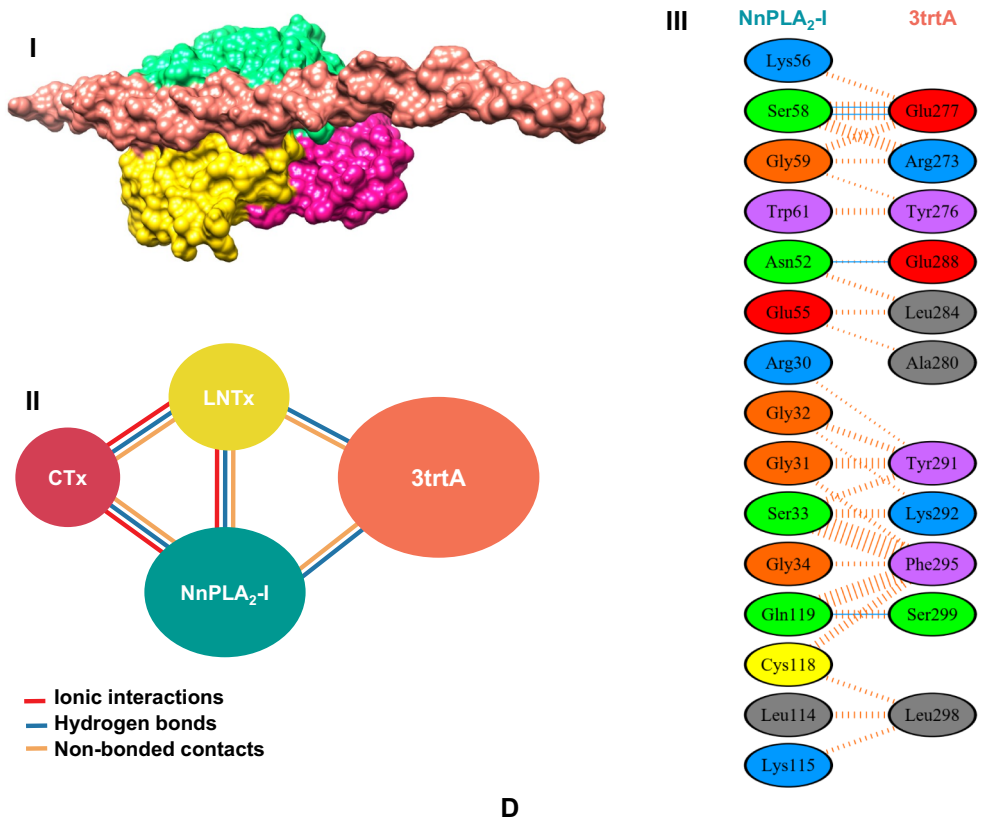

D

Fig. 6. (*continued*)

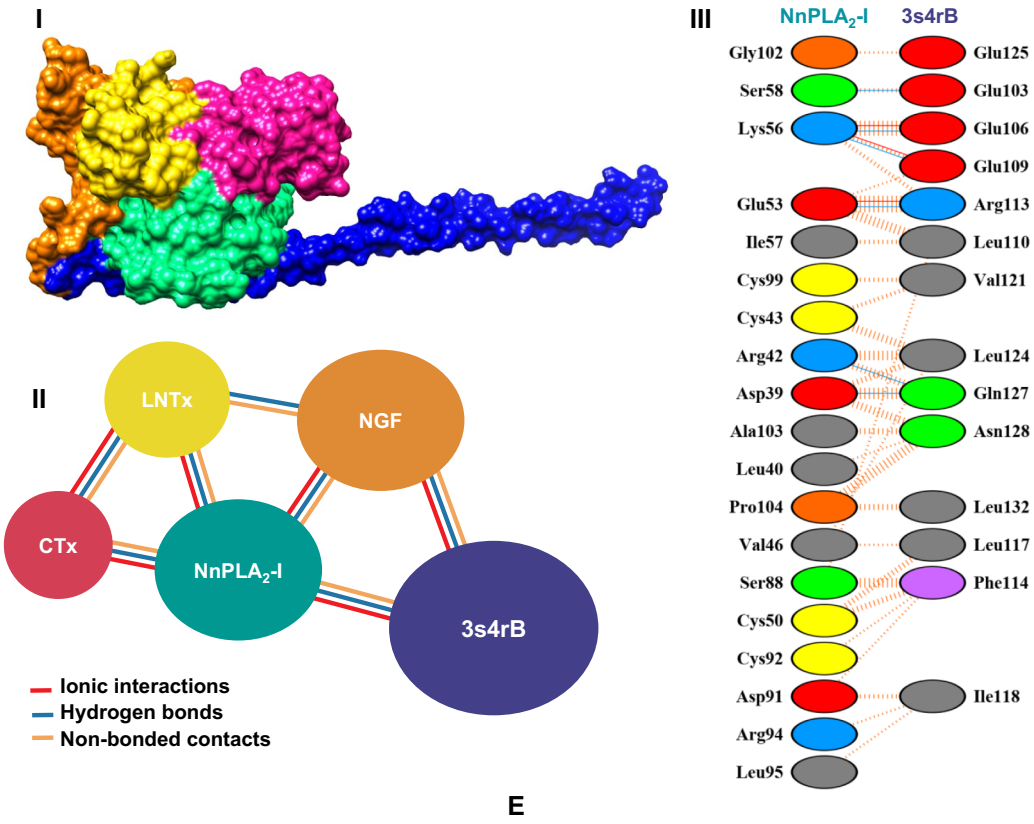

E

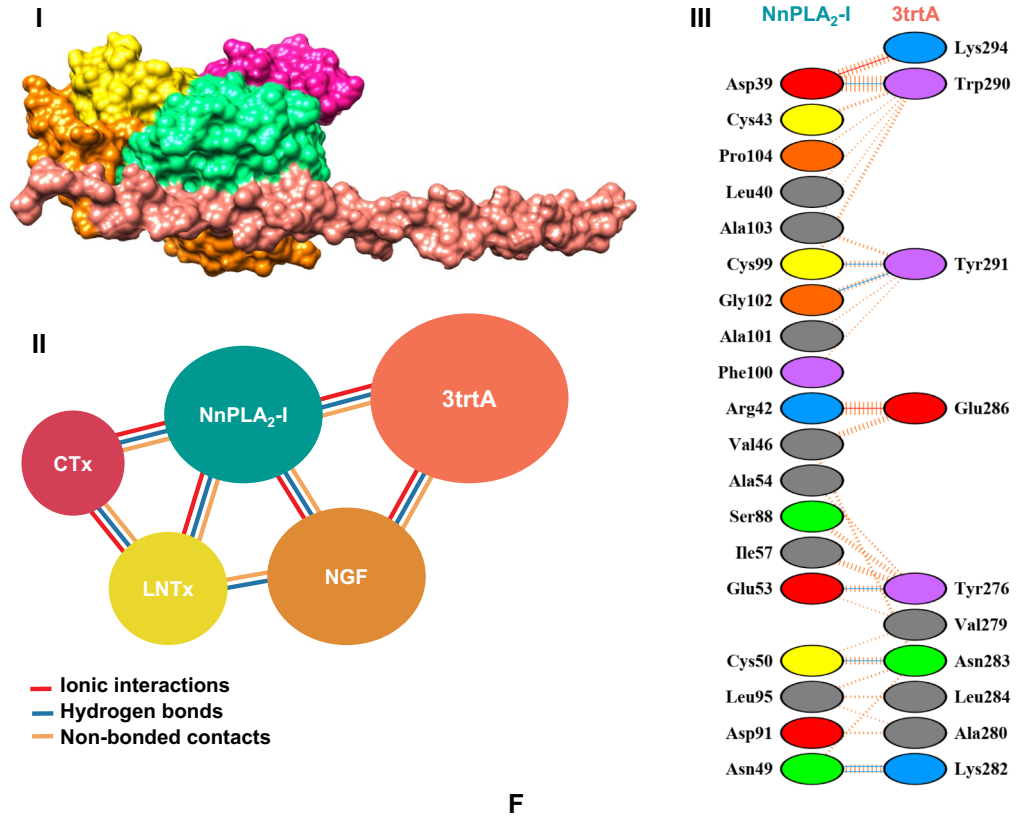

F

Fig. 6. (*continued*)

Table 2B
A comparison of the global energy of binding of the components of $NnPLA_2$-I cognate complex to two regions of the rod structure of vimentin: 3s4rB (rod region; 99–189) and 3trtA (rod region; 261–335). The global energy values were predicted using Firedock server.

Protein	Global energy of complex	Global energy of interaction with 3s4rB region of vimentin	Global energy of interaction with 3trtA region of vimentin
$NnPLA_2$-I	–	−111.04	−107.58
CTx	–	−114.77	−101.74
LNTx	–	−90.12	−84.55
NGF	–	−125.62	−132.73
$NnPLA_2$-I-CTx	−111.55	−104.28	−97.63
$NnPLA_2$-I-LNTx	−123.37	−104.43	−94.14
$NnPLA_2$-I-NGF	−136.94	−131.94	−107.42
$NnPLA_2$-I-CTx-LNTx	−91.30	−109.69	−95.61
$NnPLA_2$-I-CTx-LNTx-NGF	−174.54	−138.20	−113.19

Transparency document

The Transparency document associated with this article can be found, in online version.

Acknowledgements

Authors acknowledge BioBharati Life Sciences Private Limited, Kolkata for raising the antibodies against $NnPLA_2$-I, and Technology Business Incubator, KIIT University, Bhubaneswar for LC-MS/MS analysis, Dr. B. Bose, Indian Institute of Technology, Guwahati for providing the anti-vimentin antibody, Dr. S.S. Ghosh and Mr. A.P. Bidkar, Indian Institute of Technology, Guwahati for confocal microscopy analysis, and Mr. T. Islam, Tezpur University for technical assistance in the FITC-conjugation. SD is the recipient of Department of Science and Technology – Innovation in Science Pursuit for Inspired Research Programme (DST-INSPIRE) senior research fellowship. This study received partial financial support from the Department of Biotechnology National Bioscience Award grant (BT/HRD/NBA/34/01/2012-13/(ix)) to AKM.

Authors' contributions

A.K.M. conceived the idea and designed the experiments; S.D. performed the experiments including *in silico* studies. S.D.G. and A.S. provided help with cell culture experiments and spectrofluorometric analysis. S.D. wrote the manuscript and A.K.M. edited and approved the final manuscript.

Conflict of interests

The authors declare that they have no conflict of interests.

Appendix A. Supplementary data

Supplementary data to this article can be found online at https://doi.org/10.1016/j.bbamem.2019.02.002.

References

[1] R.M. Kini, Structure–function relationships and mechanism of anticoagulant phospholipase A_2 enzymes from snake venoms, Toxicon 45 (2005) 1147–1161.
[2] A.K. Mukherjee, B. Kalita, R. Thakur, Two acidic, anticoagulant PLA_2 isoenzymes purified from the venom of monocled cobra *Naja kaouthia* exhibit different potency to inhibit thrombin and factor Xa via phospholipids independent, non-enzymatic mechanism, PLoS One 9 (2014) e101334.
[3] A.K. Mukherjee, A major phospholipase A_2 from *Daboia russelii russelii* venom shows potent anticoagulant action via thrombin inhibition and binding with plasma phospholipids, Biochimie 99 (2014) 153–161.
[4] S. Dutta, D. Gogoi, A.K. Mukherjee, Anticoagulant mechanism and platelet deaggregation property of a non-cytotoxic, acidic phospholipase A_2 purified from Indian cobra (*Naja naja*) venom: inhibition of anticoagulant activity by low molecular weight heparin, Biochimie 110 (2015) 93–106.
[5] D. Saikia, A.K. Mukherjee, Anticoagulant and membrane damaging properties of snake venom phospholipase A_2 enzymes, Snake Venoms (2017) 87–104.
[6] E. Condrea, J.E. Fletcher, B.E. Rapuano, C.C. Yang, P. Rosenberg, Dissociation of enzymatic activity from lethality and pharmacological properties by carbamylation of lysines in *Naja nigricollis* and *Naja naja atra* snake venom phospholipases A_2, Toxicon 19 (1981) 705–720.
[7] R.M. Kini, H.J. Evans, Structure-function relationships of phospholipases. The anticoagulant region of phospholipases A_2, J. Biol. Chem. 262 (1987) 14402–14407.
[8] R.M. Kini, H.J. Evans, A model to explain the pharmacological effects of snake venom phospholipases A_2, Toxicon 27 (1989) 613–635.
[9] B. Lomonte, Y. Angulo, L. Calderon, An overview of lysine-49 phospholipase A_2 myotoxins from crotalid snake venoms and their structural determinants of myotoxic action, Toxicon 42 (2003) 885–901.
[10] R.M. Kini, Excitement ahead: structure, function and mechanism of snake venom phospholipase A_2 enzymes, Toxicon 42 (2003) 827–840.
[11] A.V. Osipov, S.Y. Filkin, Y.V. Makarova, V.I. Tsetlin, Y.N. Utkin, A new type of thrombin inhibitor, noncytotoxic phospholipase A_2, from the *Naja haje* cobra venom, Toxicon 55 (2010) 186–194.
[12] K. Hanasaki, H. Arita, Phospholipase A_2 receptor: a regulator of biological functions of secretory phospholipase A_2, Prostaglandins Other Lipid Mediat. 68-69 (2002) 71–82.
[13] K. Hanasaki, Mammalian phospholipase A_2: phospholipase A_2 receptor, Biol. Pharm. Bull. 27 (2004) 1165–1167.
[14] R. Doley, G.F. King, A.K. Mukherjee, Differential hydrolysis of erythrocyte and mitochondrial membrane phospholipids by two phospholipase A_2 isoenzymes (NK-PLA_2-I and NK-PLA_2-II) from the venom of the Indian monocled cobra *Naja kaouthia*, Arch. Biochem. Biophys. 425 (2004) 1–13.
[15] A.K. Mukherjee, Correlation between the phospholipids domains of the target cell membrane and the extent of *Naja kaouthia* PLA_2-induced membrane damage: evidence of distinct catalytic and cytotoxic sites in PLA_2 molecules, Biochim. Biophys. Acta 1770 (2007) 187–195.
[16] D. Saikia, N.K. Bordoloi, P. Chattopadhyay, S. Choklingam, S.S. Ghosh, A.K. Mukherjee, Differential mode of attack on membrane phospholipids by an acidic phospholipase A_2 (RVVA-PLA_2-I) from *Daboia russelli* venom, Biochim. Biophys. Acta Biomembr. 1818 (2012) 3149–3157.
[17] C. Montecucco, J.M. Gutierrez, B. Lomonte, Cellular pathology induced by snake venom phospholipase A_2 myotoxins and neurotoxins: common aspects of their mechanisms of action, Cell. Mol. Life Sci. 65 (2008) 2897–2912.
[18] G. Lambeau, A. Schmid-Alliana, M. Lazdunski, J. Barhanin, Identification and purification of a very high affinity binding protein for toxic phospholipases A_2 in skeletal muscle, J. Biol. Chem. 265 (1990) 9526–9532.
[19] Y. Yamazaki, Y. Matsunaga, Y. Nakano, T. Morita, Identification of vascular endothelial growth factor receptor-binding protein in the venom of eastern cottonmouth. A new role of snake venom myotoxic Lys49-phospholipase A_2, J. Biol. Chem. 280 (2005) 29989–29992.
[20] B. Lomonte, J. Rangel, Snake venom Lys49 myotoxins: from phospholipases A_2 to non-enzymatic membrane disruptors, Toxicon 60 (2012) 520–530.
[21] H.S. Bawaskar, P.H. Bawaskar, D.P. Punde, M.K. Inamdar, R.B. Dongare, R.R. Bhoite, Profile of snakebite envenoming in rural Maharashtra, India, J. Assoc. Physicians India 56 (2008) 88–95.
[22] S.A. Kularatne, B.D. Budagoda, I.B. Gawarammana, W.K. Kularatne, Epidemiology, clinical profile and management issues of cobra (*Naja naja*) bites in Sri Lanka: first authenticated case series, Trans. R. Soc. Trop. Med. Hyg. 103 (2009) 924–930.
[23] C.L. Ownby, T.R. Colberg, Classification of myonecrosis induced by snake venoms: venoms from the prairie rattlesnake (*Crotalus viridis viridis*), western diamondback rattlesnake (*Crotalus atrox*) and the Indian cobra (*Naja naja naja*), Toxicon 26 (1988) 459–474.
[24] A.K. Mukherjee, C.R. Maity, Biochemical composition, lethality and pathophysiology of venom from two cobras—*Naja naja* and *N. kaouthia*, Comp. Biochem. Physiol. B Biochem. Mol. Biol. 131 (2002) 125–132.
[25] J.M. Gutierrez, C.L. Ownby, Skeletal muscle degeneration induced by venom phospholipases A_2: insights into the mechanisms of local and systemic myotoxicity, Toxicon 42 (2003) 915–931.
[26] C.L. Ownby, J.E. Fletcher, T.R. Colberg, Cardiotoxin 1 from cobra (*Naja naja atra*) venom causes necrosis of skeletal muscle in vivo, Toxicon 31 (1993) 697–709.
[27] R.M. Kini, Y.M. Chan, Accelerated evolution and molecular surface of venom phospholipase A_2 enzymes, J. Mol. Evol. 48 (1999) 125–132.
[28] B. Lomonte, E. Moreno, A. Tarkowski, L.A. Hanson, M. Maccarana, Neutralizing interaction between heparins and myotoxin II, a lysine 49 phospholipase A_2 from *Bothrops asper* snake venom. Identification of a heparin-binding and cytolytic toxin region by the use of synthetic peptides and molecular modeling, J. Biol. Chem. 269 (1994) 29867–29873.
[29] F. Tonello, M. Rigoni, Cellular mechanisms of action of snake phospholipase A_2 toxins, Snake Venoms (2017) 49–65.
[30] M.L. Massimino, M. Simonato, B. Spolaore, C. Franchin, G. Arrigoni, O. Marin, L. Monturiol-Gross, J. Fernandez, B. Lomonte, F. Tonello, Cell surface nucleolin interacts with and internalizes *Bothrops asper* Lys49 phospholipase A_2 and mediates its toxic activity, Sci. Rep. 8 (2018) 10619.
[31] J.M. Gutierrez, B. Lomonte, Phospholipases A_2: unveiling the secrets of a functionally versatile group of snake venom toxins, Toxicon 62 (2013) 27–39.

[32] A.K. Mukherjee, B. Kalita, S.P. Mackessy, A proteomic analysis of Pakistan *Daboia russelii russelii* venom and assessment of potency of Indian polyvalent and monovalent antivenom, J. Proteomics 144 (2016) 73–86.

[33] S. Dutta, A. Chanda, B. Kalita, T. Islam, A. Patra, A.K. Mukherjee, Proteomic analysis to unravel the complex venom proteome of eastern India *Naja naja*: correlation of venom composition with its biochemical and pharmacological properties, J. Proteomics 156 (2017) 29–39.

[34] B. Kalita, S. Singh, A. Patra, A.K. Mukherjee, Quantitative proteomic analysis and antivenom study revealing that neurotoxic phospholipase A_2 enzymes, the major toxin class of Russell's viper venom from southern India, shows the least immunorecognition and neutralization by commercial polyvalent antivenom, Int. J. Biol. Macromol. 118 (2018) 375–385.

[35] C.D. Wenger, J.J. Coon, A proteomics search algorithm specifically designed for high-resolution tandem mass spectra, J. Proteome Res. 12 (2013) 1377–1386.

[36] H. Choi, D. Fermin, A.I. Nesvizhskii, Significance analysis of spectral count data in label-free shotgun proteomics, Mol. Cell. Proteomics 7 (2008) 2373–2385.

[37] O.H. Lowry, N.J. Rosebrough, A.L. Farr, R.J. Randall, Protein measurement with the Folin phenol reagent, J. Biol. Chem. 193 (1951) 265–275.

[38] R. Thakur, P. Chattopadhyay, A.K. Mukherjee, Biochemical and pharmacological characterization of a toxic fraction and its cytotoxin-like component isolated from Russell's viper (*Daboia russelii russelii*) venom, Comp. Biochem. Physiol. Toxicol. Pharmacol. 168 (2015) 55–65.

[39] B. Kalita, A. Patra, A.K. Mukherjee, Unraveling the proteome composition and immuno-profiling of Western India Russell's Viper venom for in-depth understanding of its pharmacological properties, clinical manifestations, and effective antivenom treatment, J. Proteome Res. 16 (2017) 583–598.

[40] D. Gerlier, N. Thomasset, Use of MTT colorimetric assay to measure cell activation, J. Immunol. Methods 94 (1986) 57–63.

[41] A.K. Mukherjee, S.P. Mackessy, Biochemical and pharmacological properties of a new thrombin-like serine protease (Russelobin) from the venom of Russell's Viper (*Daboia russelii russelii*) and assessment of its therapeutic potential, Biochim. Biophys. Acta 1830 (2013) 3476–3488.

[42] A.K. Mukherjee, A.J. Saviola, P.D. Burns, S.P. Mackessy, Apoptosis induction in human breast cancer (MCF-7) cells by a novel venom L-amino acid oxidase (Rusvinoxidase) is independent of its enzymatic activity and is accompanied by caspase-7 activation and reactive oxygen species production, Apoptosis 20 (2015) 1358–1372.

[43] C.M. Modahl, A.K. Mukherjee, S.P. Mackessy, An analysis of venom ontogeny and prey-specific toxicity in the Monocled Cobra (*Naja kaouthia*), Toxicon 119 (2016) 8–20.

[44] R.P. Haugland, Coupling of monoclonal antibodies with fluorophores, Methods Mol. Biol. 45 (1995) 205–221.

[45] P.M. Bendix, G.H. Koenderink, D. Cuvelier, Z. Dogic, B.N. Koeleman, W.M. Brieher, C.M. Field, L. Mahadevan, D.A. Weitz, A quantitative analysis of contractility in active cytoskeletal protein networks, Biophys. J. 94 (2008) 3126–3136.

[46] M.M. Bradford, A rapid and sensitive method for the quantitation of microgram quantities of protein utilizing the principle of protein-dye binding, Anal. Biochem. 72 (1976) 248–254.

[47] A.R. Mazzer, X. Perraud, J. Halley, J. O'Hara, D.G. Bracewell, Protein A chromatography increases monoclonal antibody aggregation rate during subsequent low pH virus inactivation hold, J. Chromatogr. A 1415 (2015) 83–90.

[48] A.K. Mukherjee, S. Dutta, B. Kalita, D.K. Jha, P. Deb, S.P. Mackessy, Structural and functional characterization of complex formation between two Kunitz-type serine protease inhibitors from Russell's Viper venom, Biochimie 128-129 (2016) 138–147.

[49] J. Yang, R. Yan, A. Roy, D. Xu, J. Poisson, Y. Zhang, The I-TASSER Suite: protein structure and function prediction, Nat. Methods 12 (2015) 7–8.

[50] A. Hospital, P. Andrio, C. Fenollosa, D. Cicin-Sain, M. Orozco, J.L. Gelpi, MDWeb and MDMoby: an integrated web-based platform for molecular dynamics simulations, Bioinformatics 28 (2012) 1278–1279.

[51] M. Shigyo, T. Kuboyama, Y. Sawai, M. Tada-Umezaki, C. Tohda, Extracellular vimentin interacts with insulin-like growth factor 1 receptor to promote axonal growth, Sci. Rep. 5 (2015) 12055.

[52] D. Kozakov, D.R. Hall, B. Xia, K.A. Porter, D. Padhorny, C. Yueh, D. Beglov, S. Vajda, The ClusPro web server for protein-protein docking, Nat. Protoc. 12 (2017) 255–278.

[53] D. Schneidman-Duhovny, Y. Inbar, V. Polak, M. Shatsky, I. Halperin, H. Benyamini, A. Barzilai, O. Dror, N. Haspel, R. Nussinov, H.J. Wolfson, Taking geometry to its edge: fast unbound rigid (and hinge-bent) docking, Proteins 52 (2003) 107–112.

[54] R.A. Laskowski, PDBsum: summaries and analyses of PDB structures, Nucleic Acids Res. 29 (2001) 221–222.

[55] R.A. Laskowski, V.V. Chistyakov, J.M. Thornton, PDBsum more: new summaries and analyses of the known 3D structures of proteins and nucleic acids, Nucleic Acids Res. 33 (2005) D266–D268.

[56] K. Yugandhar, M.M. Gromiha, Protein-protein binding affinity prediction from amino acid sequence, Bioinformatics 30 (2014) 3583–3589.

[57] C. Montecucco, O. Rossetto, On the quaternary structure of taipoxin and textilotoxin: the advantage of being multiple, Toxicon 51 (2008) 1560–1562.

[58] A.K. Mukherjee, Phospholipase A_2-interacting weak neurotoxins from venom of monocled cobra *Naja kaouthia* display cell-specific cytotoxicity, Toxicon 51 (2008) 1538–1543.

[59] S.E. Gasanov, R.K. Dagda, E.D. Rael, Snake venom cytotoxins, phospholipase A_2s, and Zn^{2+}-dependent metalloproteinases: mechanisms of action and pharmacological relevance, Clin. Toxicol. 4 (2014) 1000181.

[60] A.H. Laustsen, Toxin synergism in snake venoms, Toxin Rev. 35 (2016) 165–170.

[61] R. Doley, R.M. Kini, Protein complexes in snake venom, Cell. Mol. Life Sci. 66 (2009) 2851–2871.

[62] A.K. Mukherjee, Non-covalent interaction of phospholipase A_2 (PLA_2) and kaouthiotoxin (KTX) from venom of *Naja kaouthia* exhibits marked synergism to potentiate their cytotoxicity on target cells, J. Venom Res. 1 (2010) 37–42.

[63] Y. Banerjee, J. Mizuguchi, S. Iwanaga, R.M. Kini, Hemextin AB complex, a unique anticoagulant protein complex from *Hemachatus haemachatus* (African Ringhals cobra) venom that inhibits clot initiation and factor VIIa activity, J. Biol. Chem. 280 (2005) 42601–42611.

[64] M. Cintra-Francischinelli, P. Pizzo, L. Rodrigues-Simioni, L.A. Ponce-Soto, O. Rossetto, B. Lomonte, J.M. Gutierrez, T. Pozzan, C. Montecucco, Calcium imaging of muscle cells treated with snake myotoxins reveals toxin synergism and presence of acceptors, Cell. Mol. Life Sci. 66 (2009) 1718–1728.

[65] A.K. Mukherjee, S.P. Mackessy, Pharmacological properties and pathophysiological significance of a Kunitz-type protease inhibitor (Rusvikunin-II) and its protein complex (Rusvikunin complex) purified from *Daboia russelii russelii* venom, Toxicon 89 (2014) 55–66.

[66] S. Gasanov, S. Kolusheva, B. Salakhutdinov, U. Beknazarov, T. Aripov, The mechanism of cobra venom phospholipase A_2 and cytotoxin synergistic action on phospholipids membrane structure, Dokl. Akad. Nauk UzSSR (1991) 44–46.

[67] A. Chaim-Matyas, G. Borkow, M. Ovadia, Synergism between cytotoxin P4 from the snake venom of *Naja nigricollis nigricollis* and various phospholipases, Comp. Biochem. Physiol. B: Biochem. Mol. Biol. 110 (1995) 83–89.

[68] J.B. Harris, M.J. Cullen, Muscle necrosis caused by snake venoms and toxins, Electron Microsc. Rev. 3 (1990) 183–211.

[69] G. Lambeau, J. Barhanin, M. Lazdunski, Identification of different receptor types for toxic phospholipases A_2 in rabbit skeletal muscle, FEBS Lett. 293 (1991) 29–33.

[70] G. Lambeau, P. Ancian, J.P. Nicolas, S.H. Beiboer, D. Moinier, H. Verheij, M. Lazdunski, Structural elements of secretory phospholipases A_2 involved in the binding to M-type receptors, J. Biol. Chem. 270 (1995) 5534–5540.

[71] T. Kostiza, J. Meier, Nerve growth factors from snake venoms: chemical properties, mode of action and biological significance, Toxicon 34 (1996) 787–806.

[72] R.H. Angeletti, Nerve growth factor from cobra venom, Proc. Natl. Acad. Sci. 65 (1970) 668–674.

[73] R. Levi-Montalcini, The nerve growth factor: thirty-five years later, Biosci. Rep. 7 (1987) 681–699.

[74] S.A. Mani, W. Guo, M.J. Liao, E.N. Eaton, A. Ayyanan, A.Y. Zhou, M. Brooks, F. Reinhard, C.C. Zhang, M. Shipitsin, L.L. Campbell, K. Polyak, C. Brisken, J. Yang, R.A. Weinberg, The epithelial-mesenchymal transition generates cells with properties of stem cells, Cell 133 (2008) 704–715.

[75] E. Boilard, S.G. Bourgoin, C. Bernatchez, M.E. Surette, Identification of an autoantigen on the surface of apoptotic human T cells as a new protein interacting with inflammatory group IIA phospholipase A_2, Blood 102 (2003) 2901–2909.

[76] L.K. Lee, K.J. Bryant, R. Bouveret, P.-W. Lei, A.P. Duff, S.J. Harrop, E.P. Huang, R.P. Harvey, M.H. Gelb, P.P. Gray, Selective inhibition of human group IIA secreted phospholipase A_2 (hGIIA) signaling reveals arachidonic acid metabolism is associated with colocalization of hGIIA to vimentin in rheumatoid synoviocytes, J. Biol. Chem. M112 (2013) 397893.

[77] E. Moisan, D. Girard, Cell surface expression of intermediate filament proteins vimentin and Lamin B1 in human neutrophil spontaneous apoptosis, J. Leukoc. Biol. 79 (2006) 489–498.

[78] N. Mor-Vaknin, A. Punturieri, K. Sitwala, D.M. Markovitz, Vimentin is secreted by activated macrophages, Nat. Cell Biol. 5 (2003) 59–63.

[79] J. Yang, L. Zou, Y. Yang, J. Yuan, Z. Hu, H. Liu, H. Peng, W. Shang, X. Zhang, J. Zhu, X. Rao, Superficial vimentin mediates DENV-2 infection of vascular endothelial cells, Sci. Rep. 6 (2016) 38372.

[80] A.E. Bryant, C.R. Bayer, J.D. Huntington, D.L. Stevens, Group A streptococcal myonecrosis: increased vimentin expression after skeletal-muscle injury mediates the binding of *Streptococcus pyogenes*, J. Infect. Dis. 193 (2006) 1685–1692.

[81] T.J. Podor, D. Singh, P. Chindemi, D.M. Foulon, R. McKelvie, J.I. Weitz, R. Austin, G. Boudreau, R. Davies, Vimentin exposed on activated platelets and platelet microparticles localizes vitronectin and plasminogen activator inhibitor complexes on their surface, J. Biol. Chem. 277 (2002) 7529–7539.

[82] D. Frescas, C.M. Roux, S. Aygun-Sunar, A.S. Gleiberman, P. Krasnov, O.V. Kurnasov, E. Strom, L.P. Virtuoso, M. Wrobel, A.L. Osterman, Senescent cells expose and secrete an oxidized form of membrane-bound vimentin as revealed by a natural polyreactive antibody, Proc. Natl. Acad. Sci. 201614661 (2017).

[83] A. Adolf, G. Leondaritis, A. Rohrbeck, B.J. Eickholt, I. Just, G. Ahnert-Hilger, M. Holtje, The intermediate filament protein vimentin is essential for axonotrophic effects of *Clostridium botulinum* C3 exoenzyme, J. Neurochem. 139 (2016) 234–244.

[84] J.J. Liang, C.Y. Yu, C.L. Liao, Y.L. Lin, Vimentin binding is critical for infection by the virulent strain of Japanese encephalitis virus, Cell. Microbiol. 13 (2011) 1358–1370.

[85] H. Herrmann, M. Häner, M. Brettel, S.A. Müller, K.N. Goldie, B. Fedtke, A. Lustig, W.W. Franke, U. Aebi, Structure and assembly properties of the intermediate filament protein vimentin: the role of its head, rod and tail domains, J. Mol. Biol. 264 (1996) 933–953.

[86] A. Rohrbeck, A. Schroder, S. Hagemann, A. Pich, M. Holtje, G. Ahnert-Hilger, I. Just, Vimentin mediates uptake of C3 exoenzyme, PLoS One 9 (2014) e101071.